13. TYRRHENIAN RISE – SITE 132

The Shipboard Scientific Party[1]

SITE DATA

Occupied: September 24-26, 1970.

Position: On a relatively smooth rise approximately 60 kilometers west and about 800 meters above the level of the central bathyal plain.
Latitude: 40° 15.70′N
Longitude: 11° 26.47′E

Water Depth: 2835 meters.

Cores Taken: Twenty-seven.

Total Penetration: 223 meters.

Deepest Unit Recovered: Solid gypsum rock of Upper Miocene (Messinian) age displaying undulating laminations characteristic of algal stromatolites.

MAIN RESULTS

A continuous sequence of Pleistocene and Pliocene fossiliferous pelagic ooze of a deep-water (bathyal) facies was found directly overlying Late Miocene evaporites which include barren pyritic, dolomitic, and gypsiferous marls, and indurated gypsum rock. The calcium sulfates are heavily recrystallized and partly calcitized, and the recovered gypsum laminites are interpreted to be a diagenetic replacement of former anhydrite stromatolites.

The contact between the inferred intertidal and supratidal evaporites and the pelagic ooze is marked by a thin layer of cross-bedded detrital sands with neritic species of benthic foraminifera and dwarfed specimens of a Messinian planktonic fauna. The boundary as found in Core 21 at 188 meters below the sea bed correlates with the uppermost surface of Reflector M. No transitional phase from shallow- to deep-water sedimentation has been found.

Thin beds of volcanic ash were found in the Quaternary strata. The Quaternary is also generally accompanied by greater amounts of terrigenous minerals than the older foraminiferal oozes of Pliocene age.

BACKGROUND

No clear conceptual picture exists today as to the origin and evolution of the Tyrrhenian Basin of the Mediterranean Sea. Some researchers, perhaps best represented by Glangeaud (1962), have suggested that the deep central depression is a fragment of "paleo-ocean" that possibly has existed as a deep-water trough since the Permian. Not convinced as to such permanence, other workers have envisioned the creation of new areas of young crust by the opening of sphenochasms and the drifting apart of continents following the break up of Pangaea (Carey, 1958; Vogt *et al.*, 1971). The proposed age of the extensional phases in the western Mediterranean, during which simatic crust was suspected to have been accreted, spans a broad range of time from the Lower Jurassic (Smith, 1971) to the late Eocene-Oligocene (Ryan *et al.*, 1971; Le Pichon *et al.*, 1971), and even into the Miocene (Argand, 1922; Stanley and Mutti, 1968).

There are still others who argue that the present bathyal areas of the Tyrrhenian Sea came into existence following the collapse of a craton (e.g., Merla, 1951; Klemme, 1958; Maxwell, 1959; Aubouin, 1965; Pannekoek, 1969; Van Bemmelen, 1969; Morelli, 1970; Heezen *et al.*, 1971). As to when the oceanization occurred, a recent paper of Selli and Fabbri (1971) reports on fossil assemblages found in "littoral" conglomerates recovered in dredge samples from the Stromboli and Oresi Canyons and the Baronie Seamount (Figure 1), and concludes that the foundering commenced as late as Middle Pliocene and proceeded at the tremendous rate of 1 to 1.1 mm per year.

Despite this wide range of opinion as to the geodynamic evolution of the Tyrrhenian Sea, a spirit pervaded the numerous dialogues of the Mediterranean Advisory Panel and its colleagues that a good number of these schemes were subject to direct testing through the drilling of a deep hole at some carefully selected location. Even if basement rocks were not obtainable themselves, it was believed that a cored sequence through the Neogene would elucidate the chronology of tectonic events, particularly those which would have accompanied the foundering of former shallow-water terrains. Furthermore, the recovery of an uninterrupted succession of sediments would allow the charting of the range distribution of key fossil assemblages, whose individual delineation in the total record was practically guaranteed to enhance the already carefully investigated stratotype sections in nearby outcrops on the surrounding borderlands.

Geologic Setting

The setting of the Tyrrhenian Basin (Figure 1) interior to the orogenic arc of the Tellian Atlas–the Sicilian, Calabrian, and Northern Apennines–is in some ways reminiscent of the so-called marginal basins of the Pacific Ocean (Karig, 1971). A northwestward dipping seismic zone descends to 450 kilometers beneath the Calabrian portion of the arc (Peterschmitt, 1956 and Caputo *et al.*, 1970). Evidence has been brought forth that seismic wave velocities near this zone are anomalously high, a result now thought to be characteristic of the islands arcs of the Pacific. Focal mechanism solutions of Ritsema (1969) and

[1]W. B. F. Ryan, Lamont-Doherty Geological Observatory; K. J. Hsü, Eidg. Technische Hochschule; M. B. Cita, Universita degli Studi di Milano; Paulian Dumitrica, Geological Institute, Bucharest; Jennifer Lort, University of Cambridge; Wolf Maync, Geological Consulting Service, Berne, Switzerland; W. D. Nesteroff, University of Paris; Guy Pautot, Centre Oceanologique de Bretagne; Herbert Stradner, Geologische Bundesanstalt, Vienna; and F. C. Wezel, Universita di Catania.

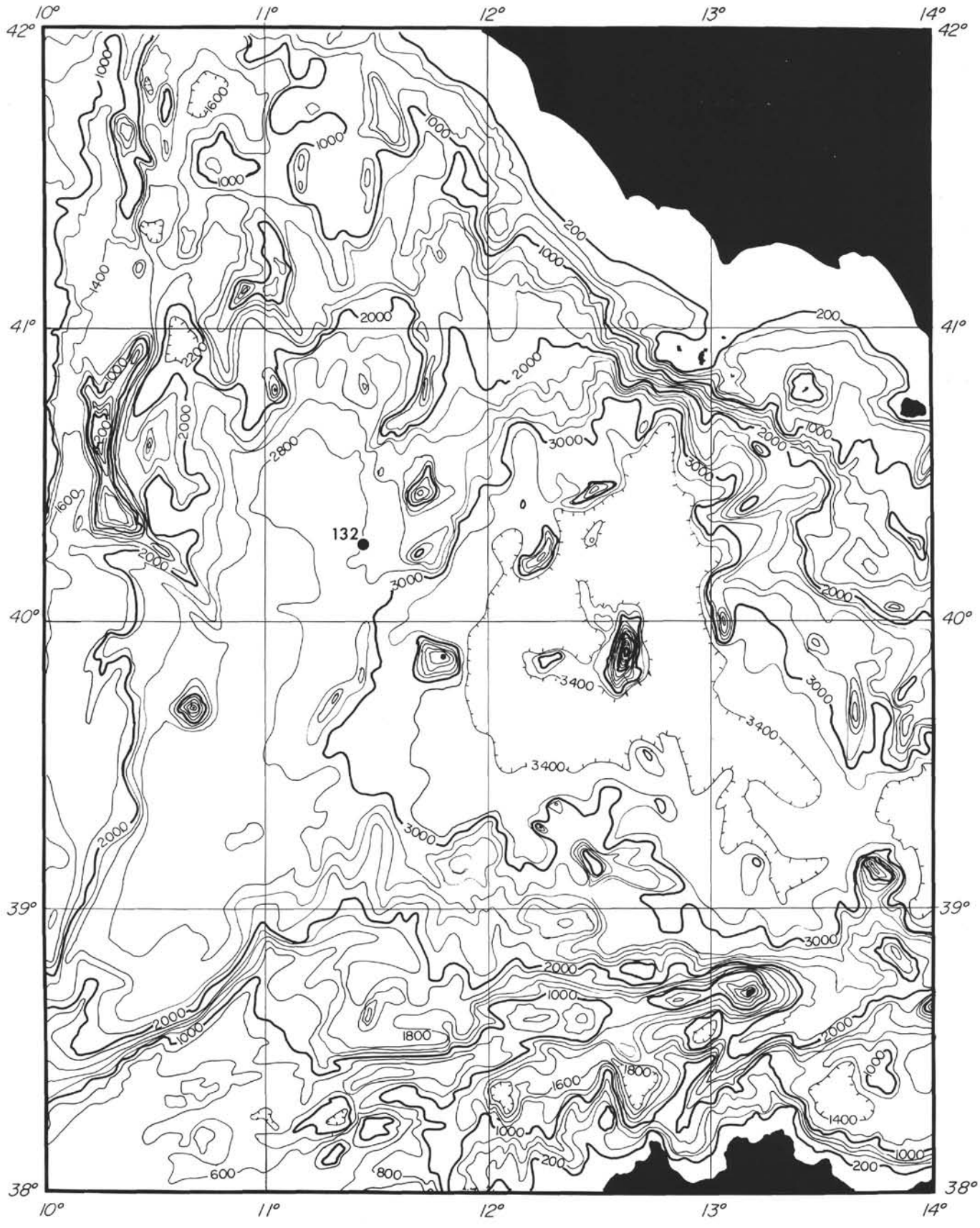

Figure 1. *Tyrrhenian Basin, contours in meters adapted from Chart 310 of the Defense Mapping Agency Hydrographic Center.*

Isacks and Molnar (1971) show *P* axes that plunge about 60 degrees toward the northwest and *B* axes that are nearly horizontal and parallel to the tectonic strike of the arc; these data concur with a downdip compressional stress in a northwestward-dipping lithospheric slab whose leading edge approximates a belt of both emerged and submerged volcanic cones situated at the northern terminus of the Cefalu, Gioia and Paola peri-Tyrrhenian basins of Selli (1970). Ratios of potash to silica in samples from the eruptives lie along discrete curves for volcanoes of equal height above the dipping seismic zone (Hatherton and Dickinson, 1969; Ninkovich and Hays, 1972). As is also the case for the Pacific marginal basins (McKenzie and Sclater, 1968) the heat flow within the Tyrrhenian Basin is markedly high throughout, with an average for twelve stations of 2.83 ± 1.07 μcal/cm^2 sec (Erickson, 1970). An area of uniformly high heat flow (3.38 ± 0.16) exists in the southeastern portion of the bathyal plain just inside the concave side of the Sicilian – Calabrian arc.

General Crustal Structure

The crustal structure as inferred from seismic refraction measurements (Ewing and Ewing, 1959; Moskalenko, 1965, 1967; and Fahlquist and Hersey, 1969) reveals a 7.1 km/sec layer at only a 6 km depth overlain by an interval with internal interfaces showing refracted arrivals of 4.0, 4.9 and 5.7 km/sec, all of which underlie a relatively thin veneer of low-velocity unconsolidated sediment. The 4 km/sec layer is considered by most workers to comprise consolidated sediments (Neprochov, 1968), and at a refraction station over the southern arm of the central deep bathyal plain this layer is less than 2.2 km thick if everything above the 7.1 km/sec layer is referred to as sedimentary. More than likely, however, the 5.7 km/sec velocity detected along reversed profiles represents basement rocks, and if this value is taken as an indication of the presence of "Layer 2" material, then the total thickness of the sedimentary unit is probably only on the order of 1.5 kilometers.

Sedimentary Layering

One can trace in continuous seismic profiles a ubiquitous subbottom reflecting horizon stretching beneath the sea floor almost the entire width of the Tyrrhenian Basin. In the highly detailed digitally processed profiles obtained in 1969 aboard the R/V *Marsili* during a cooperative program of the Consiglio Nazionale delle Richerche and the U.S. National Science Foundation, this horizon is clearly delineated by a sequence of three coherent echo phases (Figure 2). They can be followed along seismic line MS-1 from the subsurface of the Paola Basin off the coast of Calabria down beneath the central bathyal plain, out onto the lower flanks of a few protruding seamounts (e.g., Vavilov and Marsili) and on across a small elevated rise east of Sardinia (see Finetti *et al.*, 1970, and Chapter 17.2 of this volume).

Where the Marsili tracks cross those of the R/V *Robert D. Conrad* of the Lamont-Doherty Geological Observatory of Columbia University, the three-part series of reflectors coincides with a single very prominent highly reflective zone identified on the Lamont air gun records by Biscaye *et al* (1971) as Reflector M. At places where the aforementioned reflection profiles intersect the refraction stations, Reflector M corresponds to an interval with compressional-wave velocities of 3.92, 4.0 and 4.36 km/sec, probably signifying that the sediment in this interval is at least partly consolidated.

The superficial carpet of sediment above Reflector M is variable in thickness and acoustic reflectivity. In depressions of the bathyal plain, up to 1.2 seconds (two-way travel time) of horizontally stratified strata have been detected (e.g., see Plate 2 of Ryan *et al.*, 1969; and Figure 3 of Selli and Fabbri, 1971) although the average thickness is more like 0.7 second. The internal layering, as revealed in the continuous reflection profiles, generally abuts against protruding relief and is only slightly upwarped. Numerous graded sand-silt-clay beds are found in the upper 20 meters of the plain penetrated by piston cores (Norin, 1958; Ryan *et al.*, 1969) and demonstrate that coarse-grained sedimentary detritus is periodically carried to the central depression by turbidity currents.

Internal acoustic stratification is also present beneath the surfaces of the peri-Tyrrhenian slope basins, and bedding unconformities and discontinuities have frequently been recognized (Selli and Fabbri, 1971). The areas least affected by clastic sedimentation, or erosion and truncation, are the small broad rises within the central depression which crest above the upper surface of the ponded sediment of the bathyal plain. On these elevated portions of the basin floor, the airgun and sparker reflection records only show faint internal reflectivity, generally confined to a few discrete interfaces about a third of the way down in the section above Reflector M (see discussion in Chapter 17.2). Piston cores from the topographic highs are devoid of coarse-grained, detrital sand layers and contain carbonate-rich foraminifera and nannofossil oozes with intercalated thin beds of volcanic glass shards (tephra). Sedimentaion rates for these pelagic deposits range up to 6 cm/10^{3}y (W. Berggren, personal communication).

Site Selection

After much deliberation and welcomed outside advice, the Mediterranean Advisory Panel decided that the most expedient approach, in light of the reconnaissance nature of this first deep-sea drilling venture in the Tyrrhenian Basin, would be to drill a single hole as deep as the state-of-the-art technology permitted in an environment principally characterized by pelagic sedimentation and showing some promise of continuous uninterrupted sedimentation. It was anticipated that the recovery of a continuum of biostratigraphic and lithostratigraphic events (i.e., evolutionary changes, ecological adaptations, physio-chemical cycles of sedimentation, tephra falls, fluctuations in mineral input) would subsequently permit key reflecting interfaces to be identified and dated, thereafter allowing perhaps basin-wide extrapolations and correlations to be attempted on the basis of the regional coverage of the seismic reflection profiles.

Although no detailed site surveys were available, the newly obtained *Marsili* Flexotir traverses were shown to the site-selection panel by E.F.K. Zarudzki with the recommendation that a hole be drilled that would meet the above

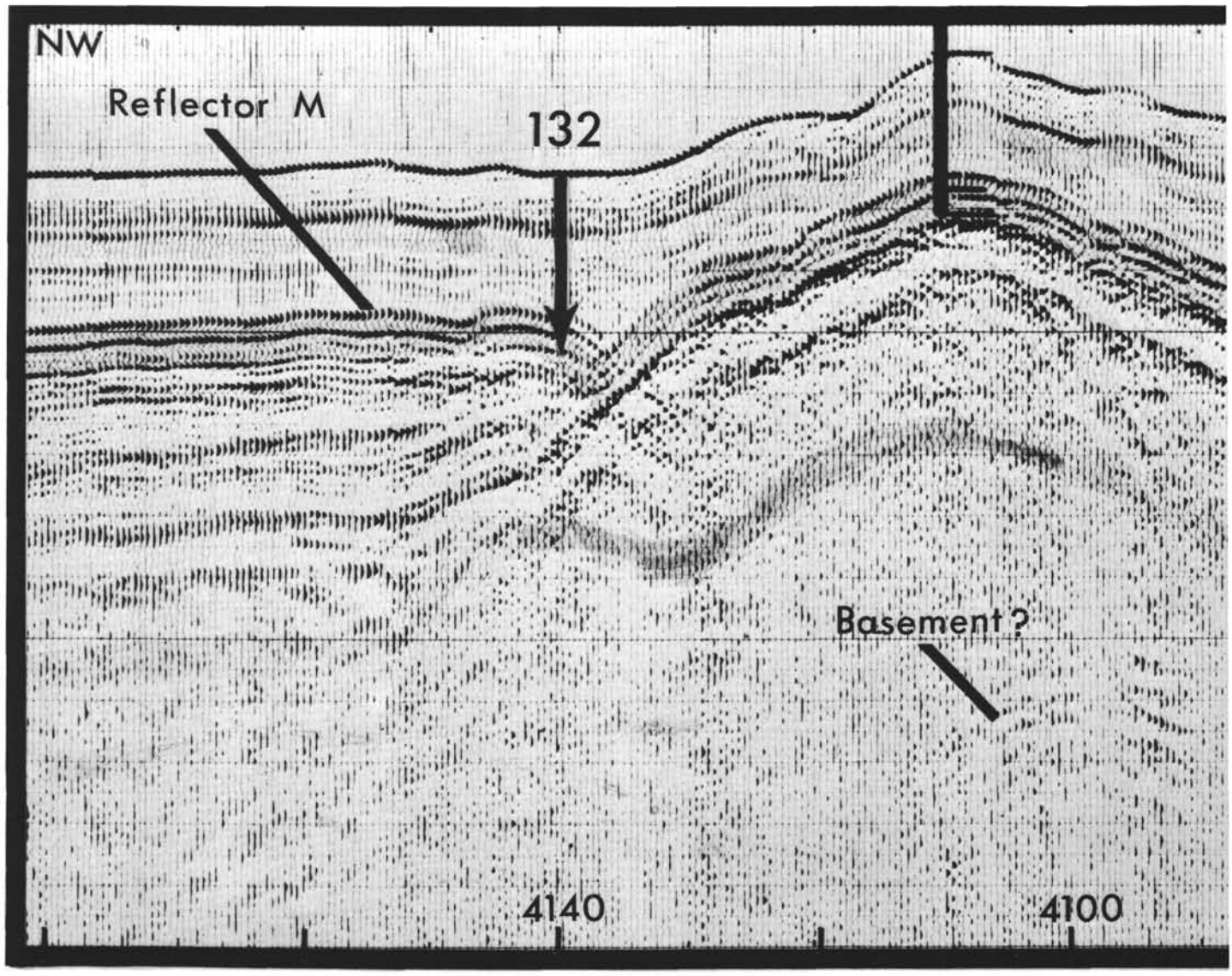

Figure 2. *A section of the digitally processed seismic reflection profile MS-1 of the R/V* Marsili *across the Tyrrhenian Rise (From Finetti* et al., *1970). The original site was targeted on the crest of a small knoll in the vicinity of Shot Point 4100. However the eventual location best projects onto the profile at the location of the arrow near Shot Point 4140. Note the continuity of Reflector M in a draped attitude above the subsurface relief. Vertical scale is in seconds (two-way travel time) and the vertical exaggeration is ≈ 6.5:1.*

criteria at a location to the west of the central bathyal plain (see Figure 1) in the vicinity of Shot Point 4100 of profile MS-1 (see Figure 2). This choice was enthusiastically received by paleontologists eager to have good fossiliferous material in cores from the central Mediterranean Sea close to Neogene stratotype sections.

At the proposed drilling location the echo sequences of the M-Reflectors are very coherent and form a regionally smooth surface beneath approximately 0.25 second of a uniformly thick sediment. Discrete internal reflecting interfaces could be recognized above Horizon M, particularly in the upper 0.1 second, and these could be traced laterally across almost the entire basin, lending great support to the promise of future extrapolations. The target itself was situated on the crest of an isolated swell of gentle relief some 150 meters above the surface of the surrounding rise, thus minimizing the chances of intercalations of unwanted resedimented materials.

Principal Objectives

From a technical point of view, the goal was to core continuously from the first contact with the sea bed down to, into, and hopefully through, the M-Reflectors. Beneath the knoll at a subbottom depth of some 0.95 second on the MS-1 profile at Shot Point 4100, one can observe crescent-shaped echo sequences and a general texture of noncoherence that seems to resemble the character of acoustic basement in other ocean basins (see, for instance, Ewing and Ewing, 1971). Surmising that this level might indeed be basement in light of the shallow depth of the 5.9

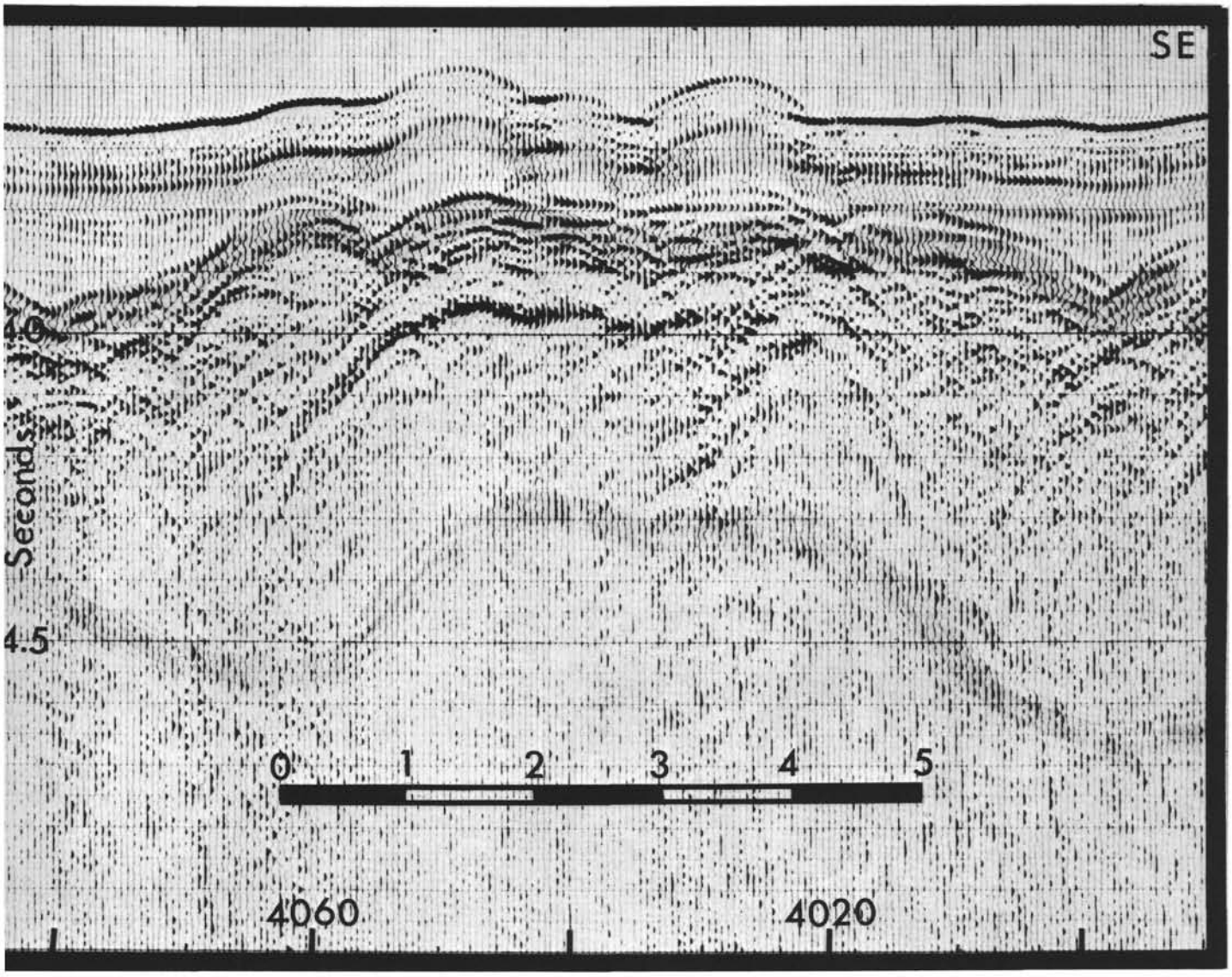

igure 2. *(Continued)*

km/sec refracting interace on the available refraction profiles, the plan was to penetrate the drill hole as deep as possible so as to hopefully reach *in situ* bedrock.

The scientific goals included recovery of an intact record of the Pleistocene and Pliocene in a deep-water setting, the identification of the nature of the physical contact between the materials which make up the M-Reflectors and the overlying more transparent strata, the age of this contact and the knowledge of whether or not it represents a discontinuity, the lithology of the M-Reflectors and earlier sediment, and the properties of the acoustic basement.

Based on the experience of previous drilling in the Valencia Trough and in the Balearic and Ionian basins at Sites 122, 124 and 125 respectively, we were particularly curious to see if the M-Reflectors would correspond to the same Upper Miocene evaporite formation as had been encountered elsewhere, and to learn what kind of evaporite facies might be present at a topographic setting well above the deepest part of the Tyrrhenian Sea.

Strategy

Contrary to otherwise excellent site planning by the advisory panel, the chief scientists found themselves on board the *Glomar Challenger* with merely a polaroid photo of part of the *Marsili* MS-1 profile and a single latitude and longitude of the designated target. Knowing, at least, that the profile commenced in the southeastern corner of the basin and crossed the Marsili and Vavilov seamounts in a straight line transverse, we chose to postpone the drilling of this site until the *Challenger*'s return from the eastern Mediterranean through the Strait of Messina. By doing this, we could then set a track ourselves which would cause no deviation and subsequent loss of time but would take us down the *Marsili* profile to the drilling target. We inferred that as we crossed the central bathyal plain the two tracks would converge and that we would pay careful attention to the onboard seismic airgun recording for similarities to the MS-1 profile until arrival at the designated coordinate. If we recognized a setting similar to that on the polaroid copy,

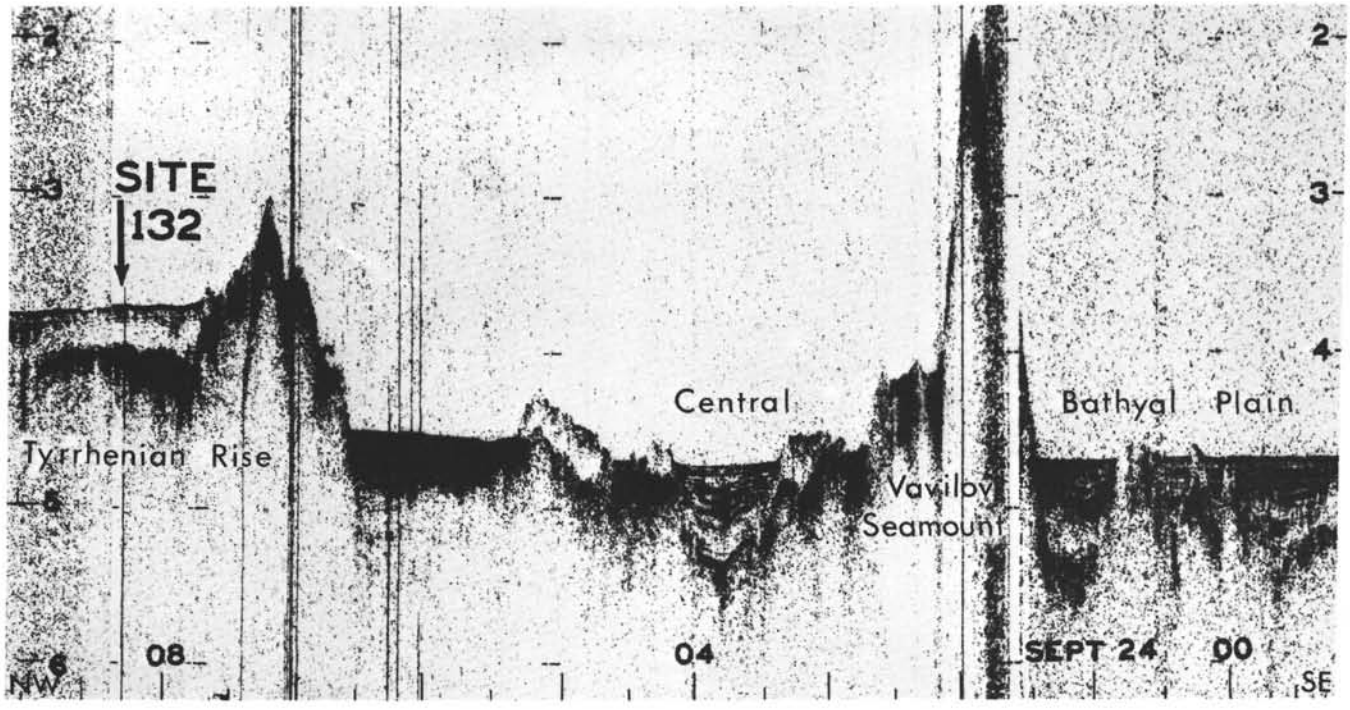

Figure 3. *Reflection profile of the* Glomar Challenger *across the central bathyal plain of the Tyrrhenian Basin and up, on, and across the Tyrrhenian Rise and Site 132. Reflector M appears as a broad interval of markedly high reflectivity in this record made with an airgun sound source, and this horizon can be traced across most of the basin beneath a level of acoustic transparency. Vertical scale is in seconds (two-way travel time), and the vertical exaggeration is 28:1.*

we would drop a marker buoy, come on station, and commence drilling.

Challenger Site Approach

Heading on a course of about 296 degrees the *Glomar Challenger* crossed the Vavilov Seamount at 0150 hours on September 24, 1970 (see Figure 3). Some five hours later we found ourselves ascending a relatively steep escarpment of a basement ridge which took us from the bathyal plain up to the Tyrrhenian Rise and on across the drill site (Figure 4). Now that we were near that part of the *Marsili* track for which we had a record, a certain degree of familiarity began to be noted in the sea bed morphology. The smooth surface of the rise was reached at 0745 hours with an initial depth reading of 1460 tau. Faint subbottom echo sequences were visible on the 12 kHz fathogram and Reflector M was very bold and easy to identify on the airgun profile. The sea bed leveled and then, as it began to rise again across a slight swell, a free-floating marker buoy was ejected at 0816 hours and the vessel immediately slowed to 4 knots to retrieve the streamed geophysical sensors. At 0837 hours with the gear secured, the vessel swung around to the right and returned to the buoy, arriving and stopping there at 0855 hours. The acoustic positioning beacon was dropped to the sea bed at 0900 hours on the flank of the swell at a PDR depth of 2813 meters (corrected for sound velocity) only about 40 meters above the surrounding rise. Satellite fixes obtained while drilling during the next two days placed the eventual hole about 2.7 km to the SSW of the *Marsili* line opposite Shot Point 4110 (Figure 5). As discussed in Chapter 17.2, the water-depth equivalent setting of the drill site best correlates with Shot Point 4140.

OPERATIONS

The *Glomar Challenger* stayed on location for two days, from 0900 hours on September 24 to 1010 hours on September 26th. A continuous section of Pleistocene and Pliocene pelagic oozes was cored, and the hole was reluctantly terminated at 223 meters below bottom in an Upper Miocene evaporite formation. The core inventory is given in Table 1 and the drilling rates are graphically presented in Figure 6.

The drilling crews probably established a new DSDP record in the rate of core recovery. In the first 24-hour period, a total of twenty-two core barrels were hauled on deck, with more than 90 percent recovery.

The first nine cores were cut mostly with the circulation shut off except as indicated in Figure 6. Cores 9 to 20 were cut with occasional brief periods of circulation. The last cores were taken with full circulation, using one pump while strokes increased gradually from 15 SPM to 50 SPM. The bit weight also increased steadily from 5,000 to 12,000 pounds for the first nine cores, and from 12,000 to 30,000 pounds for the last cores.

The penetration rate showed two well-defined changes in the upper unconsolidated sediment section. The first occurred at 36 meters below bottom with a decrease of from 2 to about 1 meter/minute commencing with the cutting of Core 5 at a level equivalent to the shallowest of several intermediate subbottom echo sequences. The second, amounting to a further decrease to 0.5

TABLE 1
Core Inventory – Site 132, Tyrrhenian Rise

Core	No. Sections	Date	Time	Cored[a] Interval (m)	Cored (m)	Recovered (m)	Subbottom Penetration (m) Top	Subbottom Penetration (m) Bottom	Lithology	Age
1	7	9/24	1545	2845-2854	9	9.2	0	9	Marl oozes, tephra	Quaternary
2	4	9/24	1645	2854-2863	9	5.2	9	18	Marl oozes, tephra	Quaternary
3	4	9/24	1740	2863-2872	9	5.4	18	27	Marl oozes, tephra	Quaternary
4	6	9/24	1840	2872-2881	9	8.0	27	36	Marl oozes, tephra, sapropel	Quaternary
5	3	9/24	1950	2881-2890	9	4.6	36	45	Marl oozes, tephra	Quaternary
6	7	9/24	2050	2890-2899	9	9.3	45	54	Marl oozes, tephra	Quaternary
7	7	9/24	2150	2899-2908	9	9.4	54	63	Foraminiferal oozes	U. Pliocene
8	6	9/24	2245	2908-2917	9	9.1	63	72	Foraminiferal oozes	U. Pliocene
9	6	9/24	2350	2917-2926	9	9.1	72	81	Foraminiferal oozes	U. Pliocene
10	7	9/25	0115	2926-2935	9	9.2	81	90	Foraminiferal oozes	U. Pliocene
11	6	9/25	0230	2935-2944	9	9.2	90	99	Foraminiferal oozes	U. Pliocene
12	7	9/25	0350	2944-2953	9	9.2	99	108	Foraminiferal oozes	U. Pliocene
13	7	9/25	0500	2953-2962	9	9.3	108	117	Foraminiferal oozes	U. Pliocene
14	3	9/25	0605	2962-2971	9	2.6	117	126	Foraminiferal oozes	U. Pliocene
15	6	9/25	0725	2971-2980	9	9.1	126	135	Foraminiferal oozes	L. Pliocene
16	7	9/25	0835	2980-2989	9	9.3	135	144	Foraminiferal oozes	L. Pliocene
17	7	9/25	0945	2989-2998	9	9.3	144	153	Foraminiferal oozes	L. Pliocene
18	7	9/25	1055	2998-3007	9	9.2	153	162	Foraminiferal oozes	L. Pliocene
19	4	9/25	1205	3007-3016	9	6.1	162	171	Foraminiferal oozes	L. Pliocene
20	4	9/25	1330	3016-3025	9	5.1	171	180	Reddish foraminiferal ooze	L. Pliocene
21	2	9/25	1435	3025-3034	9	2.6	180	189	Red ooze, pyritic and dolomitic marl	L. Pliocene/ U. Miocene
22	1	9/25	1600	3034-3036	2	1.0	189	191	Evaporite	U. Miocene
23	1	9/25	1730	3036-3043	7	1.0	191	198	Evaporite	U. Miocene
24	0	9/25	1845	3043-3052	9	Tr.	198	207	Evaporite	U. Miocene
25	2	9/26	2105	3052-3059	7	2.5	207	214	Evaporite	barren
26	1	9/26	0030	3059-3065	6	1.5	214	220	Evaporite	U. Miocene
27	2	9/26	0315	3065-3068	3	2.4	220	223	Evaporite	U. Miocene
Total Cored					223	168.3				
% Recovered						75.5%				

[a]Drill pipe measurement from derrick floor.

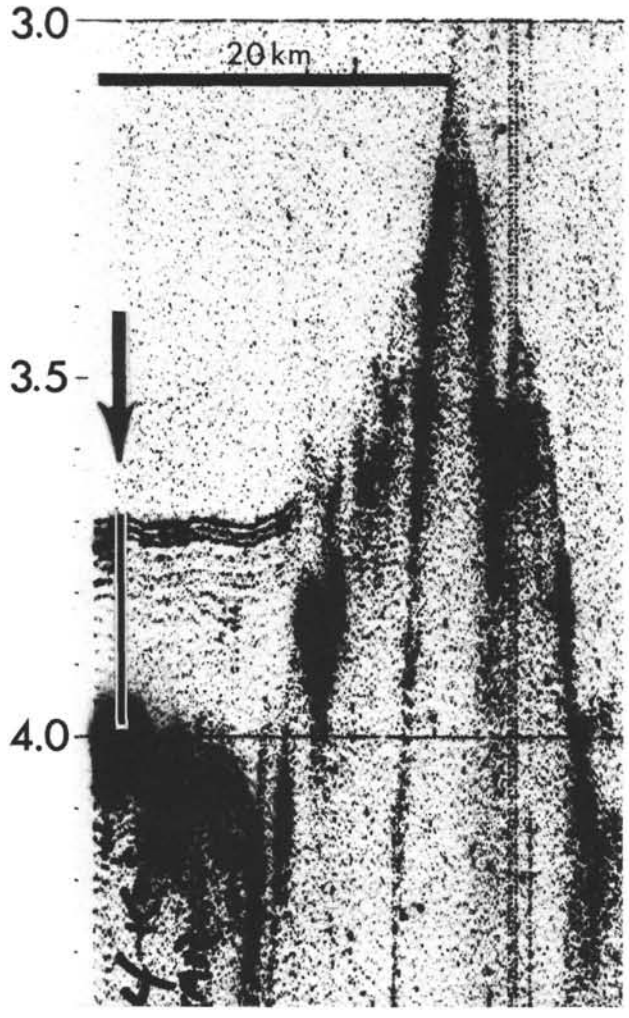

Figure 4. *Enlargement of the* Challenger *reflection profile across the Tyrrhenian Rise. Note some apparent acoustic stratification near the site (arrow) within the first 0.1 seconds of two-way travel time, and also the presence of Reflector M in pockets on the flanks of the protruding basement ridge. Vertical exaggeration of this expanded record is ≈ 55.1.*

meters/minute, was noticed at 80 meters below bottom and correlates with the inferred level of the most prominent of the intermediate reflectors. From then on the drilling was remarkably steady and uniform down to the abrupt contact with Horizon M at 188 meters which was reached while cutting Core 21. Not only was the penetration rate greatly hindered here but the drill stem experienced erratic torquing and shaking.

Beginning with the cutting of Core 22 a new core catcher was inserted which was especially designed for the recovery of hard rocks, and the next five cores sampled predominantly lithified evaporites. Cores 22 and 23 had poor recovery, whereas Core 24, which showed a rapid easy penetration, came up empty. Apparently soft sediments (perhaps sands?) were washed away during this coring attempt as we were required to keep a high pump pressure to prevent intercalated firm or hard material from jamming the core barrel.

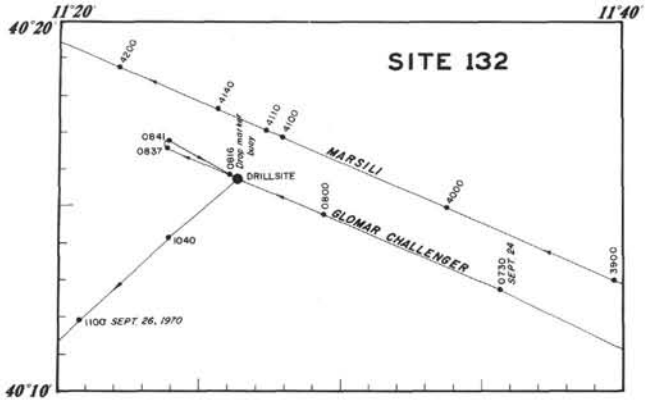

Figure 5. *Details of the* Challenger *site approach. The eventual site lies about 2.7 km SSW of the* Marsili *track opposite Shot Point 4110. The best correlation of the* Challenger *profile at its intersection with the drill hole to the* Marsili *profile (See Figure 2) is at Shot Point 4140.*

The drilling rate slowed practically to a halt when solid gypsum rock of a nodular and laminated texture was encountered in Core 27 at 220 meters below bottom. With a forecast of up to 0.5 seconds (two way reflection time) more of strongly reflective strata before any expectation of breaking through into preevaporite sediment (which at the going rate of a few meters an hour would amount to hundreds of hours more of drilling), it was reluctantly decided to terminate this hole at 223 meters so as to have time left on the leg for one more site in the western Mediterranean.

One of the problems encountered in the operations at this site was to ensure full recovery for a continuously cored section. A tungsten-carbide chip-bit (Hycalog SSFD 3 WC) was chosen. On the whole, our effort was satisfactory. However, less than perfect results were obtained during the recovery of Cores 2, 3, 5, and 14. The different reasons for these partial recoveries were analysed and reported in the shipboard narrative. Full recovery is difficult where the sediments are stiff enough to require partial or full circulation. No full recovery was achieved after Core 18, or below 171 meters below bottom, even though care and caution had been exercised.

BIOSTRATIGRAPHY

The primary objective, to obtain a continuous section of pelagic sediments of Pleistocene and Pliocene age, was successfully met, as was the objective to recover the Miocene/Pliocene boundary as a contact between evaporites and open marine oozes. The hole was unfortunately terminated before reaching preevaporite sediments because of hard drilling in the evaporites.

Recovery was generally excellent for the pelagic oozes (Cores 1 through 20) and rather poor for the evaporites (Cores 21 through 27). Mechanical disturbances of bedding structures were very limited, and only Core 5 from the Pleistocene succession was considered unsuitable for detailed paleontological investigations.

The Pliocene/Pleistocene boundary falls in Core 8, at about 70 meters below bottom; the Miocene/Pliocene/Pleistocene boundary falls in Section 2 of Core 21, some

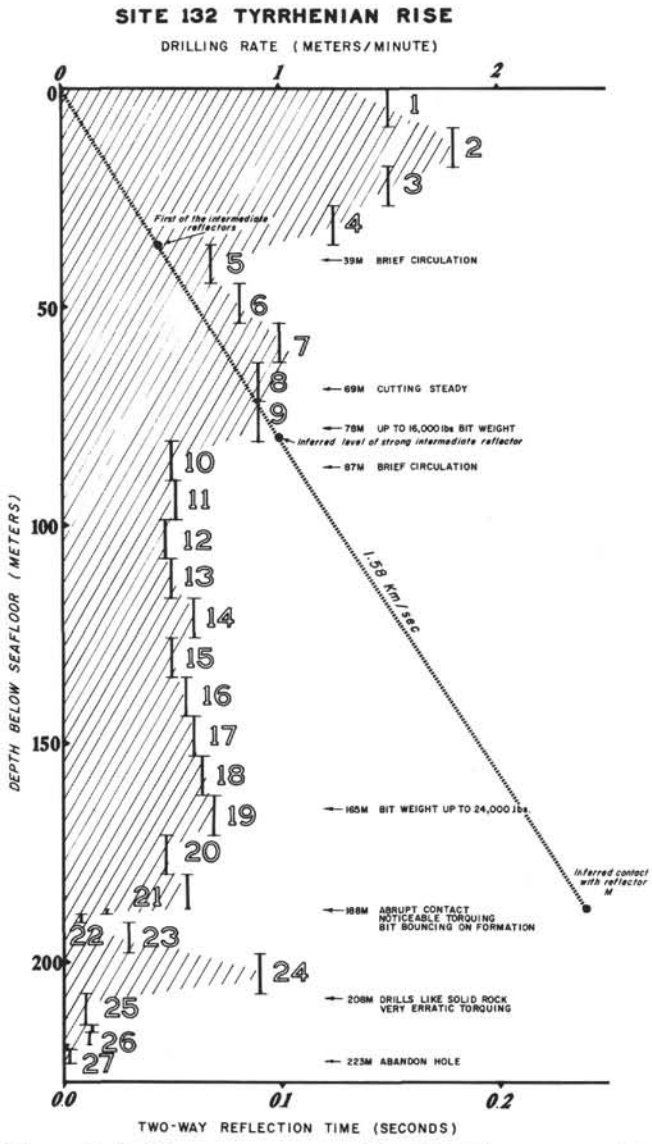

Figure 6. *Drilling rate curve for Site 132. The contact with the upper surface of Reflector M is well shown at 188 meters below bottom and was preserved in Section 2 of Core 21. Note in particular, the very uniform drilling rates through the Pliocene pelagic oozes of Cores 10 to 21 with some slight indication of compaction with depth.*

183 meters below bottom and 113 meters below the Pliocene/Pleistocene boundary.[2]

The best represented fossil groups are foraminifera (predominantly planktonic) and calcareous nannofossils. Pteropods are also present and often abundant in the topmost part of the section. Ostracods, fish remains, pelecypods and holothurian sclerites are minor components of the faunal assemblages. Siliceous microfossils are practically absent, with the exception of some siliceous spicules mainly in the Pleistocene section. Benthonic foraminifera are limited in number in most of the samples (see appropriate section of this chapter). Usually they represent 1 per cent or less of the sand-sized fraction of the sediment, which consists entirely of foraminiferal shells and other fossil debris. Only in the layers rich in volcanic glass is the sand-size fraction not entirely organogenic. Benthonic foraminifera are practically absent in the lowermost Pliocene beds (*Sphaeroidinellopsis* Acme-Zone).

Calcareous micro- and nannofossils are much scarcer in the late Miocene than in the Pliocene and Pleistocene. However, the topmost part of the Messinian consists of pyritic marls which contain a few dwarfed planktonic and benthonic foraminifera and thus permit an age determination. Both nannofossils and foraminifera are also present in small amounts in the sandy layers intercalated in the evaporitic section.

The Pliocene-Pleistocene pelagic section of Site 132 has been studied in some detail as reported in Chapters 46 and 47. We want to acknowledge here the careful work and the interest demonstrated towards our research by a number of scientists who worked with us on many of the cores.[3]

The Miocene/Pliocene Boundary (M.B.C.)

The Miocene/Pliocene boundary is contained in Section 2 of Core 21, where a sharp break in the sedimentary record is clearly visible. Pale gray pyritic marls, overlying the evaporites and poor in both micro- and nannofossils, are directly overlain by a varicolored pseudo-breccia with dark red and brown hues. These colors indicate an oxidizing environment strongly different from the reducing environment of the underlying pyritic marls. The varicolored material above the contact is a stiff, compacted nanno-foram ooze which yields abundant micro- and nannofossils that indicate an earliest Pliocene age.

A digression is necessary here in order to discuss the evidence for the above statement since the Miocene/Pliocene boundary and its definition constitute a unique problem. Reference is made to Cita (1970, p. 296-298) where the Miocene/Pliocene boundary is discussed in terms of problems involved in reference sections and world wide zonations.

Uncertainties concerning the location of this boundary are apparent in the published reports of the DSDP, and the best chronological datum is probably that given by Berggren (1971).

[2] Core 21 recovered only two sections. By DSDP convention, the boundary in Section 2 is placed 3 meters down from where the cutting of the core started, thus at 183 meters. However, a marked change in drilling rate and torquing was not noted until near the end of the coring interval at 188 meters below bottom, and this latter measurement is probably the best approximation of the *in situ* depth of the actual lithologic contact.

[3] Dr. W. H. Benson, Smithsonian Institution, Washington, D.C., Dr. R. Ciampo, Institute of Paleontology, University of Naples, Dr. N. Ciaranfi, Institute of Geology, University of Bari, Ms. J. Flood, Dr. J. Lawrence, and Dr. T. Saito, Lamont-Doherty Geological Observatory of Columbia University, Palisades, N.Y., Dr. A. Longinelli, Laboratory of Nuclear Geology, University of Pisa, Dr. M. Moncharmont Zei, Institute of Paleontology, University of Naples, and Dr. G. Scorziello, Institute of Paleontology, University of Naples.

Historically, the Pliocene was first defined in Italy. Two stages, the Tabianian in the Northern Apennines and the Zanclean in Sicily, have been proposed for the lowermost Pliocene. Only the former has been stratotypified. However, the faunal assemblages of the latter (the so-called Trubi marls) are well known, and according to Blow (1969), the base of the Trubi marls belongs to his Zone N.18.

In Sicily, there are several outcrop sections where the Trubi marls can be seen to rest directly above units assigned to the Late Miocene evaporite epoch. The microfauna of our Core 21 is very similar to that of the lowermost part of these Trubi marls, where a level very rich in *Sphaeroidinellopsis* spp. has been noted. In fact, the thickness of this interval of abundant *Sphaeroidinellopsis* spp. in the outcrops is quite comparable to that in the lowermost part of the pelagic section cored at Site 132 and, based primarily on this evidence, we have assigned this unit to the *Sphaeroidinellopsis* Acme-zone.

In terms of other foraminiferal zones, the boundary between the evaporites and the overlying pelagic ooze would be located within, or close to, the base of Zone N.18 of Blow's zonal scheme. Specimens referable to primitive *Sphaeroidinella*, with supplementary apertures, have been found in Sample 132-21-1 (60-62 cm), (see Plate 6, Figure 5, Chapter 47). Consequently, the N.18/N.19 zonal boundary falls within the *Sphaeroidinellopsis* Acme-zone, as it occurs according to Blow (1969), within the lower part of the Trubi marls. Also, Bizon and Bizon (1968) found primitive *Sphaeroidinella* to occur in the *Sphaeroidinellopsis* Acme-zone of the basal Pliocene in Greece.

The occurrence of *Globorotalia* cf. *plesiotumida* in Samples 132-22-1, 0-2 cm and 132-26, CC has been noted. *G. plesiotumida* has been recorded in the Messinian of Italy (see Catalano and Sprovieri, 1969, 1971; Colalongo, 1970) and is considered as a zonal marker.

Zone N.17 is documented by the microfauna in Cores 22 and 26 (evaporitic sequence); Zone N.18 and the Zone N.18/Zone N.19 boundary (?) in Core 21.

The lowermost beds of the pelagic oozes overlying the sedimentary break belong to the *Ceratolithus tricorniculatus* Zone, the same zone that is also recorded by Martini (1971) in the Trubi marls at Buonfornello, Sicily. The underlying pyritic marls of the evaporite unit are assigned to the *Discoaster quinqueramus* Zone, which immediately underlies the *C. tricorniculatus* Zone in Martini and Worsley's (1971) standard zonation.

Paleoenvironment (M.B.C.)

Quaternary

During Quaternary time, numerous subaerial volcanoes were active, in the area surrounding the Tyrrhenian Sea, and several of them were apparently of the explosive type as documented by the many discrete tephra layers found in Cores 1 through 7 of Site 132.

Reference is made to Chapter 46 where the Quaternary record of Site 132 is analyzed in some detail. There, the reader will find a faunal climatic curve, which indicates that important climatic fluctuations with marked cold intervals are limited to about the upper half of the Pleistocene, while the lower half is characterized by smaller fluctuations without marked cold episodes.

Pliocene

The paleoenvironmental conditions during Pliocene time were very favorable to the ecological adaptations of calcareous zoo- and phytoplankton, as documented by the abundance and diversity of both fossil groups. Sedimentation was purely pelagic, i.e., biogenic, with only a very minor terrigenous influx. No evidence was found for any significant volcanic activity during early Pliocene times. The rate of sedimentation is remarkably uniform (Figure 7). We consider this section ideally suited for detailed biostratigraphic investigations.

Evidence of climatic change was found especially in the upper Pliocene. Six distinct climatic episodes have been distinguished and can be correlated with changes recorded in the Ionian Basin.

A gradual variation in some sedimentary characters is observed in the lowermost part of the Pliocene section penetrated in the Tyrrhenian Basin. The hues, which are dominantly whitish to pale gray in most of the overlying interval, are reddish from about 172 meters to about 183 meters below bottom (Section 1 of Core 20 to Section 2 of Core 21). The red hues are observed near the Miocene/Pliocene contact previously discussed and possibly are related to the occurrence of oxidized iron compounds derived from nearby emergent areas.

The suddenness of the change from pyritic marls to the oxygenated Pliocene ooze and the pelagic aspect of the earliest Pliocene deposits has long been recognized in Sicily, but has not been satisfactorily explained so far. Recently, evidence has been presented by Benson and Sylvester-Bradley (1971) that early Pliocene sediments of the Mediterranean basins contain a cosmopolitan (psychrospheric) fauna of ostracods characteristic of deep, cold ocean bottom conditions. As reported in Chapter 36.1 of this volume, identical species of ostracods have now been found in the cores from Site 132.

It is worthwhile mentioning that the lowermost Pliocene sediments are very rich in representatives of the genus *Sphaeroidinellopsis*, which is the ancestor of the living genus *Sphaeroidinella*, a planktonic foraminifer with one of the deepest living habitats. Species of *Sphaeroidinellopsis* have tests that are particularly resistant to solution effects at depths approaching the carbonate compensation level, and a positive correlation has been noted for some time between depth habitat and resistance to solution (see, for example, the discussion by Cita, 1971). It is significant that shallow-water benthonic foraminifera, which normally should be expected in a transgressive deposit, are absent in the lowermost Pliocene oozes. In fact, the earliest Pliocene strata are practically devoid of any bottom-dwelling forms.

There seem therefore, to be abundant data from a variety of sources to suggest that for the time period represented by the pelagic oozes of Cores 1 to 21, the Tyrrhenian Sea was not only deep, but was well ventilated with oxygen and nutrients and supported a flourishing open marine fauna.

As to the precise depth of the Tyrrhenian Rise, we found firm evidence of slight dissolution of foraminiferal tests in Core 132-19, of early Pliocene age. Benson (1972),

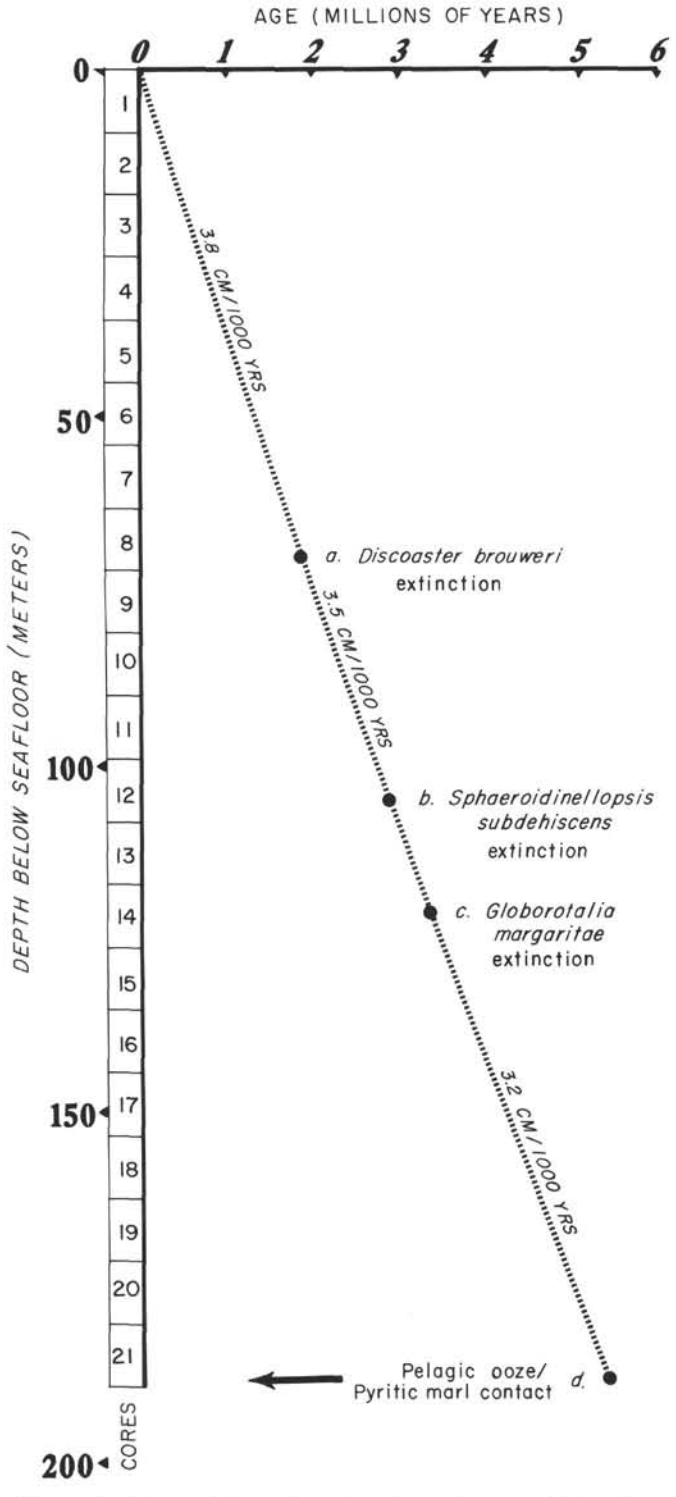

Figure 7. *Interpolated rates of sediment accumulation for Hole 132 on the Tyrrhenian Rise. The age assignments for the four data points have been determined from an interpreted sequence of magnetic reversals obtained from paleomagnetic measurements on the drill cores (See Chapters 19 and 47). The pelagic ooze – pyritic marl contact in Core 21 has been placed at 188 meters below bottom where a marked drilling break was observed, and this lithologic contact corresponds to the Pliocene/Miocene boundary at ≈ 5.4 million years B.P.*

Chapter 36.2 believes that the psychrospheric ostracods present in the Pliocene and lowermost Pleistocene strata of Hole 132 were likely to have once dwelled on sea beds with water depths ranging from 1000 to 1500 meters and with bottom water temperatures as cold as 4°C to 6°C.

Miocene

The most interesting finding at Site 132 concerning the paleoenvironment during the periods of evaporite deposition is that an open marine fauna, though restricted both in number of taxa and specimens, was supported intermittently for brief periods of time. This indicates that between cycles of the inferred desiccation and formation of evaporites, there was periodic communication with the Atlantic Ocean, during which favorable environmental conditions were established. However, the vast part of the evaporite formation is completely barren of autochthonous fossils other than filaments of blue-green algae in stromatolite laminae.

Rates of Sedimentation

Rather precise rates of sedimentation can be calculated for the Pleistocene and Pliocene sequence because paleontological datum levels could be recognized which have been correlated to the paleomagnetic reversal time scale (Hays et al, 1969; Foster and Opdyke, 1970). Figure 7 shows a graph of age versus depth in the sediment column for three biohorizons which have been identified in the cores at, or near, reversal boundaries (see Chapter 47.2). They are as follows:

a) The extinction level of *Discoaster brouweri* in Section 5 of Core 8 at 70 meters below bottom, which occurs in the Olduvai event of the Matuyama epoch at ≈1.85 my.

b) The extinction level of *Sphaeroidinellopsis subdehiscens*, between Sections 4 and 5 of Core 12 at 105 meters, located in the Kaena event of the Gilbert epoch at ≈2.90 my

c) The extinction level of *Globorotalia margaritae* found just above the core catcher of Core 14 at 121.5 meters, which lies at the Gauss/Gilbert epoch boundary, dated at 3.32 my.

In addition, we have used the lithologic change from pelagic ooze to pyritic marl in Section 2 of Core 21, which from the paleomagnetic data of Chapter 19 has an extrapolated age of ≈ 5.4 my. This level has been assigned to 183 meters below bottom according to DSDP convention, but most likely corresponds to the drilling break recognized at 188 meters.

Average sedimentation rates are 3.8 cm/10^3y for the Pleistocene, 3.5 cm/10^3y for the Upper Pliocene back to 3.32 my, and 3.2 cm/10^3y for the Lower Pliocene. The volcanic component is considered most significant for the greater values observed in the Upper Pliocene and Pleistocene. These rates are all slightly higher than those calculated for the Pliocene and Pleistocene recovered at Site 125 on the Mediterranean Ridge where there are considerably less ash and other volcanic components due to the greater distance of this site from appropriate sources. However, at both sites the sedimentation rate has been practically constant during the last 5 my; this is in agreement with our interpretation of a continuing pelagic environment.

Lacking a reliable level for the base of the evaporite strata, no calculations of the sedimentation rate have been made for the upper Miocene.

Planktonic Foraminifera (M.B.C.)

Planktonic foraminifera are abundant, well preserved, and diversified in the pelagic sediments of Cores 1 through 21, while they are rare in the lower cores (21 through 27) which penetrated the evaporite sequence.

Quaternary

Reference is made to Chapter 46. A range chart is attached to that report, as well as some twenty photographic plates illustrating most of the foraminiferal species recorded.

As at other Mediterranean drilling sites, the range of *Globorotalia truncatulinoides* is restricted, while *Globigerina pachyderma* is present throughout the section, with frequency a function of climate.

Pliocene

As observed at other Mediterranean drilling sites, the Pliocene/Pleistocene boundary appears very gradational in terms of planktonic foraminifera. The reader is referred to Chapter 47 for a discussion of the Pliocene biostratigraphy and chronostratigraphy. Plates 1 through 5 in that chapter illustrate significant planktonic foraminifera as well as the species used as markers in the newly presented zonation. Some comments on the taxonomy and distribution of selected species can be found in the biostratigraphy section of Chapter 7.

The Pliocene section recovered at Site 132 is the most complete from the Mediterranean sites, and is the only section where all six of the foraminiferal zones could be recognized. Table 2 shows the distribution of various species of planktonic foraminifera at 86 levels investigated in detail from the Pliocene cores. It is worthwhile mentioning here that no overlap was seen between *Globorotalia margaritae* (121.5 m below bottom) and the first occurrence of *G. crassaformis* (103.5 m below bottom). In view of the calculated sedimentation rate of 3.5 cm/10^3y, this interval corresponds to approximately 0.5 my, which represents about 1/7th of the duration of the entire Pliocene.

Miocene

The occurrence of a limited number of planktonic foraminifera in the late Miocene (Messinian) sequence penetrated in the lower part of Site 132 has already been discussed in the section of this chapter concerning the Miocene/Pliocene boundary. The fossiliferous intervals are as follows: Core 21, Section 2, intervals sampled at 80-82 cm, 90-92cm, 106-108 cm, 21 CC, Core 22, Section 1, 0-2 cm, 22 CC; Core 25 CC; Core 26 CC.

The richest assemblage was found in the Core Catcher of Core 26, and includes:

Globigerina bulbosa, G. bulloides, G. microstoma, G. multiloba, G. cf. *nepenthes, Globigerinita glutinata, Globigerinoides obliquus, G. obliquus extremus, G.* cf. *trilobus, Globorotalia acostaensis, G. plesiotumida, Globoquardrina dehiscens, Orbulina universa, Sphaeroidinellopsis seminulina, S. subdehiscens.*

Also, a single specimen of *Globotruncana* was found in the sand fraction, which is very rich in clastic grains including quartz, mica, and gypsum fragments.

Benthonic Foraminifera (W.M.)

The benthonic foraminiferal fauna (Table 3), though rare, is quite varied and diverse and includes both shallow-water littoral species in the Upper Miocene evaporites, and exclusively deep-water species in the overlying pelagic oozes of Pliocene and Quaternary age.

An Upper Miocene age for the evaporitic sequence is indicated by the occurrence of *Globorotalia plesiotumida* Blow and Banner which appears in a dark gypsiferous clay in land outcrops on the Messinian type section below the varicolored pseudo-breccia in Sample 21-2, 80-84 cm where also the characteristic benthonic association with *Bolivinoides miocenicus* Gianotti, *Bolivina antiqua* d'Orb., *Bolivina scalprata miocenica* MacFadyen, and *Bolivina scalprata retiformis* Cush. was found, mixed with shallow-water forms such as *Ammonia beccarii* (Linn.) and *Elphidium macellum* (Fichtel and Moll).

Nannofossils (H.S.)

The pelagic oozes of Cores 1 through 21 are very rich in well-preserved nannofossils.

Quaternary

The base of the Quaternary is defined by the extinction level of *Discoaster brouweri*, located between 125 and 150 cm in Section 5 of Core 8 at a subbottom depth of ≈70 meters. Three nannofossil zones are recognized within the Quaternary. The *Emiliania huxleyi* Zone, with a thickness of about 21 meters, occurs from the sea floor down to the level of Sample 132-3-1, 78 cm. The boundary between the next lower zone (*Gephyrocapsa oceanica* Zone) and the subjacent *Pseudoemiliania lacunosa* Zone unfortunately cannot be precisely discerned since the latter taxon apparently has an extended range in the Tyrrhenian Basin all the way through the *Gephyrocapsa oceanica* occurrences.

Since *Discoaster perplexus* and *Oolithothus antillarum* are absent, only the highest occurrence of *Reticulofenestra pseudoumbilica* marks a horizon between the upper glacial and the lower pre-glacial Quaternary, as at Sites 127 and 128 in the Hellenic Trench. These large coccoliths which, according to the standard nannoplankton range chart, are though to have become extinct during the Lower Pliocene, are common in the lower levels of the Quaternary of the Mediterranean. Their uppermost occurrence at Site 132 was found in Sample 132-4-6, 133 cm. The occurrence of large specimens of *Braarudosphaera bigelowi* in the earliest part of the Quaternary, from 132-7-3, 11 cm down to 132-8-4, 30 cm, is remarkable.

The age-diagnostic quaternary nannofossil assemblages in selected samples are shown below (H. S.):

Samples: 13-132-1-0, 2 cm; 132-1-0-20 cm; 132-1-4, 110 cm; 132-1, CC; 132-2-116 cm; 132-2-3, 15 cm; 132-2-3, 140 cm; 132-2, CC; 132-3-1, 78 cm:

Braarudosphaera bigelowi
Coccolithus pelagicus

Cyclococcolithus leptoporus
Discolithina macorpora
Emiliania huxley
Gephyrocapsa oceanica
Helicosphaera carteri
Pontosphaera japonica
Pontosphaera scutellum
Rhabdosphaera stylifera
Scyphosphaera apsteini
Syracosphaera pulchra
Sphenolithus abies
Age: Upper Quaternary to Recent
Zone: *Emiliania huxleyi* (NN 21)

Samples: 13-132-3-3, 9 cm; 132-3, CC; 132-4-1, 134 cm; 132-4-3, 140 cm:
Braarudosphaera bigelowi
Coccolithus annulus
Coccolithus pelagicus
Cyclococcolithus leptoporus
Discolithina macropora
Gephyrocapsa oceanica
Helicosphaera carteri
Pontosphaera multipora
Pontosphaera scutellum
Pseudoemiliania lacunosa
Rhabdosphaera stylifera
Scyphosphaera apsteini
Syracosphaera pulchra
Thoracosphaera imperforata
Age: Upper (glacial) Quaternary
Zone: *Gephyrocapsa oceanica* (NN 20)

Samples: 13-132-4-6, 133 cm; 132-5-1, 30 cm; 132-5-2, 80 cm; 132-5, CC; 132-6-1, 60 cm; 132-6-4, 10 cm; 132-6, CC; 132-7-1, 40 cm:
Braarudosphaera bigelowi
Coccolithus pelagicus
Cyclococcolithus leptoporus
Discolithina macropora
Gephyrocapsa oceanica
Helicosphaera carteri
Pontosphaera japonica
Pontosphaera scutellum
Pseudoemiliania lacunosa
Retilucofenestra pseudoumbilica
Rhabdosphaera stylifera
Scapholithus fossilis
Scyphosphaera apsteini
Sphenolithus abies
Syracosphaera pulchra
Age: Lower ("pre-glacial") Quaternary
Zone: *Pseudoemiliania lacunosa* (NN 19)

Samples: 13-132-7-3, 11 cm; 132-7, CC; 132-8-8, 27 cm; 132-8-2, 145 cm; 132-8-4, 30 cm; 132-8-5, 125 cm:
Braarudosphaera bigelowi (large specimens in 7, CC!)
Ceratolithus cristatus
Coccolithus pelagicus
Cyclococcolithus leptoporus
Discolithina macropora
Gephyrocapsa oceanica
Helicosphaera carteri
Pontosphaera japonica
Pontosphaera scutellum
Pseudoemiliania lacunosa
Reticulofenestra pseudoumbilica
Scyphosphaera apsteini
Scyphosphaera intermedia
Syracosphaera pulchra
Rhabdosphaera stylifera
Age: Lower Quaternary
Zone: *Pseudoemiliania lacunosa* (NN 19)

Pliocene and Miocene

The highest Pliocene nannofossil zone, the *Discoaster brouweri* Zone (NN 18), extends from Sample 132-8-5, 150 cm to Sample 132-10-4, 75 cm, over a distance of approximately 18 meters.

It was very fortunate to find the next lower zone, the *Discoaster pentaradiatus* Zone (NN 17) with the routine fifty centimeter sampling interval since it comprises only about one meter of sediment between 125 centimeters in Section 4, and 75 centimeters in Section 5, of Core 10. This zone has also been recognized at other locations as being very short, and with some further closer sampling, it may be possible to refine its exact duration at Site 132. Sample 132-20-4, 75 cm contains only rare specimens of *Discoaster brouweri*, and in Sample 132-10-5, 125 cm is located the last occurrence of *Discoaster surculus.*

The *Discoaster surculus* Zone (NN 16) was continuously cored from the extinction level of this species down to 132-12-4, 125 cm. It contains very abundant and excellently preserved discoasters. The highest occurrence of *Reticulofenestra pseudoumbilica*, which marks the NN 15/NN 16 boundary, was found in Sample 132-12, CC. The *Reticulofenestra pseudoumbilica* Zone (NN 15) extends from Sample 132-12, CC to Sample 132-14-3. Its boundary with the underlying *Discoaster asymmetricus* Zone (NN 14), which is marked by the last occurrence of *Ceratolithus tricorniculatus*, seems to lie in the gap between Cores 14 and 15, and corresponds to the extinction level of *Globorotalia margaritae* at the Gauss/Gilbert epoch boundary. This magnetic reversal horizon, dated at 3.32 my, has been widely used throughout the Leg 13 volume to separate the lower from the upper Pliocene. *Discoaster asymmetricus* is found to be very conspicuous at this site, ranging from 132-15-1, 63 cm up to 132-12-3, 25 cm.

The subjacent *Ceratolithus rugosus* Zone (NN 13) extends to the base of Core 16, the lower boundary being defined by the first appearance of this taxon. Although the base of the *Ceratolithus rugosus* Zone has been considered by Martini (1971) as equivalent to the base of the Pliocene in Pacific Ocean drill cores, we have discovered at several Mediterranean sites that considerably more pelagic sediment exists below this zone and the nannofossil assemblages are characterized there by occurrences of *Ceratolithus tricorniculatus.* In fact, we are able to extend an entire NN 12 Zone from Core 16, CC to the basal contact of pelagic ooze above the pyritic marls of Section 2, Core 21, an observation which is further discussed in Chapter 42. The samples from above this sharp break in the sedimentary record contain *Ceratolithus tricorniculatus*,

TABLE 2
Range Distribution of Planktonic Foraminifera in the Pliocene Sediment Interval of Hole 132 – Tyrrhenian Rise

Legend: ● Present; X c.f.

PLANKTONIC FORAMINIFERA – *Globorotalia*

Depth Below Sea Floor (m)	Recovery (m)	Core Number	Section Number	Sample Interval (cm from top)	*acostaensis*	*aemiliana*	*bononiensis*	*crassaformis*	*crassaformis viola*	*crassula*	*dutertrei*	*humerosa*	*inflata*	*margaritae evoluta*	*margaritae margaritae*	*margaritae primitiva*	*obesa*	*puncticulata*	*cf. puncticulata*	*scitula*	*scitula ventriosa*	*plesiotumida*	*cf. tosaensis*
69	8	8	5	40-42													●			●			
				97-99									●				●			●			
			6	40-42									●				●			●			
72			CC	CC									●										
72	9	9	1	35	●						●		●				●			●			
			2	35									●							●			
			3	35	●					X●							●			●			●
			4	35				●	●	X●										●			●
			5	35	●															●			
			6	35																●			
81			CC	CC	●			●	●	●			●							●			●
87	9	10	1	35	●					X●							●		●	●			●
			2	35	●			●									●		●				
			3	35				●									●		●				
			4	35															●	●			
			5	35	●			●	●										●	●			●
			6	35				●			●						●		●				
90			CC	CC		●		●	●	●							●			●			
90	9	11	1	35		●				X●							●	●	●	●			
			2	35		●	●			X●									●	●			
			3	35			●			X●							●	●					
			4	35	●		●										●		●				
			5	35	●		●			X●							●		●				
			6	35			●										●		●				
99			CC	CC	●	●			●	X●													

PLANKTONIC FORAMINIFERA – *Globigerina*

Depth Below Sea Floor (m)	Recovery (m)	Core Number	Section Number	Sample Interval (cm from top)	*apertura*	*bulbosa*	*bulloides*	*eggeri*	*falconensis*	*foliata*	*microstoma*	*pachyderma*	*praedigitata*	*quinqueloba*	*cf. nephenthes*
69	8	8	5	40-42		●	●	●	●				●	●	
				97-99				●				●		●	
			6	40-42		●	●	●	●					●	
72			CC	CC		●	●		●			●		●	
72	9	9	1	35		●						●		●	
			2	35			●	●	●		●	●			
			3	35			●		●			●		●	
			4	35		●	●				●	●		●	
			5	35			●		●			●		●	
			6	35	●		●		●			●	●		
81			CC	CC	●	●	●		●			●	●		
87	9	10	1	35	●		●		●		●	●		●	
			2	35					●			●	●	●	
			3	35	●		●	●	●			●	●	●	
			4	35	●	●	●	●	●		●		●	●	
			5	35		●		●					●		
			6	35		●	●		●		●		●	●	
90			CC	CC	●	●	●				●		●	●	
90	9	11	1	35	●	●	●							●	
			2	35			●							●	
			3	35	●	●	●		●		●	●		●	
			4	35	●		●				●	●	●	●	
			5	35	●		●				●				
			6	35	●	●	●		●		●			●	
99			CC	CC	●	●	●				●			●	

PLANKTONIC FORAMINIFERA – *Globigerinoides*

Depth Below Sea Floor (m)	Recovery (m)	Core Number	Section Number	Sample Interval (cm from top)	*bollii*	*conglobatus*	*elongatus*	*cf. fistulosus*	*helicinus*	*obliquus extremus*	*pyramidalis*	*quadrilobatus*	*ruber*	*sacculifer*	*trilobus*
69	8	8	5	40-42		●	●				●		●		●
				97-99			●	●			●	●	●	●	
			6	40-42			●				●		●		
72			CC	CC			●				●		●		●
72	9	9	1	35	●		●		●		●	●	●		
			2	35	●		●		●				●		
			3	35	●		●		●				●		
			4	35	●		●				●	●			
			5	35	●		●								
			6	35	●		●		●		●		●		
81			CC	CC			●		●		●	●	●	●	
87	9	10	1	35	●		●		●		●				
			2	35			●	●		●		●	●	●	●
			3	35			●			●	●	●	●	●	
			4	35			●						●		
			5	35			●		●	●	●		●		
			6	35			●			●			●	●	●
90			CC	CC			●			●	●		●		●
90	9	11	1	35			●				●		●	●	●
			2	35		●	●		●	●		●	●	●	●
			3	35			●					●	●		
			4	35	●					●			●		●
			5	35			●			●		●	●	●	●
			6	35					●	●		●	●	●	
99			CC	CC						●					

PLANKTONIC FORAMINIFERA – Other Genera

Depth Below Sea Floor (m)	Recovery (m)	Core Number	Section Number	Sample Interval (cm from top)	*Globigerinita glutinata*	*Globigerinita uvula*	*Globoquadrina altispira*	*Hastigerina siphonifera*	*Orbulina bilobata*	*Orbulina suturalis*	*Orbulina universa*	*Sphaeroidinella dehiscens*	*Sphaeroidinellopsis subdehiscens*	*Sphaeroidinellopsis seminulina*	Zones	Age and Stage
69	8	8	5	40-42	●	●		●			●				*Globorotalia truncatulinoides* Total-range-zone	Pleistocene (Calabrian)
				97-99	●			●			●					
			6	40-42	●	●		●			●				*Globorotalia inflata* Interval-zone	UPPER PLIOCENE (PIACENZIAN)
72			CC	CC	●	●		●			●					
72	9	9	1	35	●	●		●			●					
			2	35	●			●			●					
			3	35	●			●			●					
			4	35	●			●			●					
			5	35	●			●			●					
			6	35	●	●		●	●		●					
81			CC	CC	●			●	●		●					
87	9	10	1	35	●			●			●					
			2	35	●	●		●			●				*Globigerinoides obliquus extremus* Interval-zone	
			3	35	●	●		●	●		●					
			4	35	●			●			●					
			5	35	●			●			●					
			6	35	●			●			●					
90			CC	CC	●			●	●		●					
90	9	11	1	35	●	●		●			●					
			2	35				●			●					
			3	35	●			●			●					
			4	35	●	●		●								
			5	35	●			●								
			6	35	●	●		●			●					
99			CC	CC	●	●		●								

99	9	12	1	35	
			2	35	
			3	35	
			4	35	
			5	35	
			6	35	
108			CC	CC	
108	9	13	1	35	
			2	35	
			3	35	
			4	35	
			5	35	
			6	35	
117			CC	CC	
117	4,5	14	1	115	
			2	35	
			3	115	
126			CC	CC	
126	9	15	1	35	
			2	35	
			3	35	
			4	35	
			5	40	
			6	35	
135			CC	CC	
135	9	16	1	35	
			2	40	
			3	35	
			4	35	
			5	35	
			6	115	
144			CC	CC	
144	9	17	1	35	
			2	35	
			3	35	
			4	35	
			5	35	
			6	35	
153			CC	CC	

TABLE 2 – *Continued*

typical specimens of which are found regularly from Sample 132-21-2, 37 cm to Sample 132-15, CC. According to the range charts of Martini (1971), *Ceratolithus tricorniculatus* can be expected up to levels equivalent to the top of Core 15, where it is noted as very rare, and seems to diminish slowly toward the upper boundary of the *Discoaster asymmetricus* Zone (NN 14).

The entire *Ceratolithus tricorniculatus* Zone can be placed in the Pliocene since the presence of *Discoaster quinqueramus* (last occurrence) defines its base and was noted only in the pyritic marls of Section 2, Core 21. However, because no ceratoliths were found below this contact[4] it is possible that some depositional hiatus is represented by the sharp discordant facies contact and that either part of Zone NN 12 might be missing, or perhaps, more likely, the upper part of the subjacent *Discoaster quinqueramus* Zone was truncated by erosional processes.

The pyritic marls of Core 21 are clearly Miocene in age because of diagnostic occurrences of *Discoaster bollii, D. variabilis*, and *D. challengeri. Discoaster bollii*, generally has its range in the NN 9 and NN 10 nannoplankton zones, but does not contradict an age assignment into the Upper Miocene even if the presence of *Discoaster quinqueramus* in two specimens is not convincingly proved.

The nannofossils indicate continuous sedimentation throughout the interval of pelagic ooze from the sea bed down to Core 21. If a hiatus is present, it is between the ooze and the underlying evaporites and not within the overlying Pliocene and Pleistocene sequences.

Another interesting result is the placing of the *Ceratolithus tricorniculatus* Zone (NN 12) within the Lower Pliocene and not in the Upper Miocene as it is assigned by Martini (1971). The Miocene/Pliocene boundary in Europe occurs somewhere below the *Sphaeroidinella* datum, and in the Mediterranean region generally coincides with a change in sedimentation from restricted conditions associated with the "crises of salinity" to an open marine environment conducive to well-developed pelagic organisms.

In our cores a similar situation is found; the *Sphaeroidinella* datum is approximately one core section above the pelagic ooze/pyritic marl contact of Core 21, at a level (188 meters) considerably below the first occurrence of *Ceratolithus rugosus* (Core 15, CC at 144 meters). The cross-correlation of nannofossil zones to foraminiferal biohorizons proposed here has been supported in a recent publication of Berggren (1971) and is discussed at greater length in Chapter 47 of this volume.

The age-diagnostic Pliocene and Miocene assemblages in selected samples are shown below (H.S.):

Samples: 132-8-5, 150 cm; 132-8-6, 40 cm; 132-8-6, 70 cm; 132-8, CC; 132-9-1, 25 cm; 132-9-3, 125 cm; 132-9, CC; 132-10-1, 125 cm; 132-10, 75 cm; 132-10-1, 125 cm; 132-10-2, 25 cm; 132-10-2, 75 cm; 132-10-2, 125 cm; 132-10-3, 75 cm; 132-10-3, 125 cm; 132-10-4, 25 cm; 132-10-4, 75 cm:

Braarudosphaera bigelowi
Coccolithus pelagicus
Cyclococcolithus leptoporus
Discoaster brouweri
Lithostromation perdurum
Pontosphaera scutellum
Pseudoemiliania lacunosa
Scyphosphaera apsteini
Scyphosphaera pulcherrima
Syracosphaera pulchra

Age: Upper Pliocene
Zone: *Discoaster brouweri* (NN 18)

Samples: 132-10-4, 125 cm; 132-10-5, 25 cm; 132-10-5, 75 cm:

Same assemblage as above with abundant *Discoaster pentaradiatus*

Age: Upper Pliocene
Zone: *Discoaster pentaradiatus* (NN 17)

Samples: 132-10-5, 125 cm; 132-10-6, 25 cm; 132-10, CC; 132-11-1, 125 cm; 132-11-3, 125 cm; 132-11, CC; 132-12-1, 25 cm; 132-12-3, 25 cm; 132-12-4, 125 cm:

Braarudosphaera bigelowi
Ceratolithus rugosus
Coccolithus pelagicus
Cyclococcolithus leptoporus
Discoaster asymmetricus
Discoaster brouweri
Discoaster pentaradiatus
Discoaster surculus
Helicosphaera carteri
Lithostromation perdurum
Pontosphaera japonica
Pontosphaera scutellum
Scyphosphaera apsteini
Scyphosphaera intermedia
Syracosphaera pulchra

Age: Upper Pliocene
Zone: *Discoaster surculus* (NN 16)

Samples: 13-132-12, CC; 132-13-1, 75 cm; 132-13-3, 75 cm; 132-13-4, 25 cm; 132-13, CC; 132-14-1, 125 cm; 132-14-3, 75 cm:

Ceratolithus rogusus
Coccolithus pelagicus
Cyclococcolithus leptoporus
Discoaster asymmetricus
Discoaster brouweri
Discoaster pentaradiatus
Discoaster surculus
Discolithina macorpora
Helicosphaera carteri
Lithostromation perdurum
Pontosphaera japonica
Pontosphaera scutellum
Pseudoemiliania lacunosa (132-13, CC)
Reticulofenestra pseudoumbilica
Scyphosphaera apsteini
Scyphosphaera intermedia

[4] In Pacific Ocean sequences the species of *Ceratolithus tricorniculatus* has its first appearance well down in the subjacent *Discoaster quinqueramus* Zone (NN 11).

TABLE 3
Range Distribution of Benthonic Foraminifera in Hole 132 – Tyrrhenian Rise

Age	Depth Below Sea Floor (m)	Core	*Cibicides ungerianus-pseudoungerianus*	*Pyrgo depressa* (d'Orb.)	*Dentalina inornata* d'Orb.	*Lagena acuticosta* Reuss	*Lagena bradyana* Forn.	*Marginulina obesa* Cush.	*Bolivina pseudoplicata* Herr. All. & Earl.	*Pleurostomella alternans* Schwager	*Cassidulina carinata* Silv.	*Nodophtalmidium* cf. *tibia* (J. & P.)	*Pyrgo serrata* (Bailey)	*Articulina tubulosa* (seg.)	*Lagena* cf. *staphyllaria inermis* Buchner	*Bulimina aculeata basispinosa* Ted. & Zanm.	*Bulimina* cf. *costata* d'Orb.	*Cassidulina subglobosa* Brady	*Karreriella bradyi* (Cush.)	*Gyroidina* cf. *laevigata* d'Orb.	*Cyclogyra carinata* (Costa)	*Hopkinsina bononiensis* (Forn.)	*Pullenia bulloides* (d'Orb.)	*Bolivina* cf. *punctata* d'Orb.	*Robulus* cf. *orbicularis* (d'Orb.)	*Bulimina marginata* d'Orb.	*Eggerella bradyi* (Cush.)	*Gyroidina* cf. *soldanii* (d'Orb.)	*Spiroloculina* cf. *tenuiseptata-tenuis*	*Dentalina filiformis* (d'Orb.)	*Siphonodosaria monilis* (Silv.)	*Sigmoilina schlumbergeri* (Silv.)	*Pyrgo* cf. *oblonga* (d'Orb.)	*Vaginulinopsis sublegumen* Parr	*Bolivina alata* Seg.	*Siphonodosaria consobrina* (d'Orb.)	*Eponides umbonatus* (Reuss)	*Lagena longitrostris* (Seg.)	*Lagena orbignyana* (Seg.)	*Siphonina reticulata* (Czjzek)	*Cibicides* cf. *boueanus* (d'Orb.)	*Chilostomella oolina* Schwager	*Spiroloculina excavata* d'Orb.	*Bulimina ovata* d'Orb.	*Eponides* cf. *tenera* (Brady)	*Bolivina subspinescens* Cush.	*Eponides umbonatus stellatus* (Silv.)	*Pullenia quadriloba* (Reuss)	*Pullenia* cf. *salisburyi* Stew.
PLEISTOCENE	Sea Floor 2845 m																																																
	0-9	1	■	■	■	■	■	■	■	■	■	■																																						
	9-18	2	■									■	■	■	■	■	■	■																																		
	18-27	3	■				■			■	■	■	■	■			■		■	■		■																												
	27-36	4	■	■						■	■	■		■					■		■		■	■																										
	36-45	5	■						■	■		■		■					■		■				■	■	■																						
	45-54	6	■				■		■	■		■		■	■												■	■	■																				
	54-63	7	■	■	■					■		■		■				■			■								■	■																		
	63-72	8	■						■	■	■							■	■		■										■	■																
UPPER PLIOCENE	72-81	9	■	■						■											■												■															
	81090	10	■	■			■			■									■										■				■														
	90-99	11	■	■	■					■									■																												
	99-108	12	■		■		■			■									■		■			■							■	■															
	108-117	13	■	■			■			■									■														■														
	117-126	14	■	■															■																													
LOWER PLIOCENE	126-135	15	■																■														■														
	135-144	16	■																■																													
	144-153	17	■				■			■									■														■														
	153-162	18	■							■									■														■														
	162-171	19	■							■									■														■														
	171-180	20	■							■									■																													
	180-189	21	■				■																																									
Messinian (Upper Miocene) Evaporite Section–Cores 21 (part) through 27; No benthonic foraminifera found.																																															

TABLE 3 – *Continued*

Age	Depth Below Sea Floor (m)	Core	*Dentalina* cf. *inflexa* Reuss	*Planulina wuellerstorfi* (Schwager)	*Bigenerina nodosaria* d'Orb.	*Cibicides bradyi* (Trauth)	*Lagena* cf. *apiculata* (Reuss)	*Marginulina crebricosta* Seg.	*Lagena ardasii* (Seg.)	*Orthomorphina challengeriana* (Thalm.)	*Orthomorphina* cf. *tenuicostata* (Costa)	*Eponides* cf. *schreibersii* (d'Orb.)	*Cibicides robertsonianus* (Brady)	*Nonion* cf. *depressulum* (Walk. & Jac.)	*Orthomorphina* cf. *jedlitschkai* (Thalm.)	*Dentalina leguminiformis* (Batsch)	*Lagena laevis* (Montagu)	*Fissurina wiesneri* Barker	*Laticarinina pauperata* (P. & J.)	*Martinottiella communis* (d'Orb.)	*Glandulina laevigata* d'Orb.	*Angulogerina angulosa* (Will.)	*Neoconorbina terquemi-orbicularis*	*Ellipsoidina ellipsoides* Seg.	*Chrysalogonium obliquatum* (Batsch)	*Pullenia quinqueloba* (Reuss)	*Anomalina helicina* (Costa)	*Lagena gracillima* (Seg.)	*Lagena quadricostulata* Reuss	*Marginulina* cf. *glabra* d'Orb.	*Uvigerina pygmaea-mediterranea*	*Bolivina* cf. *catanensis* Seg.	*Bolivinoides miocenicus* Gianotti	*Bolivina antiqua* d'Orb.	*Bolivina* cf. *cistina?* Cush.	*Bolivina scalprata miocenica* MacFadyen	*Bolivina scalprata retiformis* Cush.	*Bolivina* cf. *usensis* Conato	*Bulimina* cf. *exilis* Brady	*Uvigerina canariensis* d'Orb.	*Trifarina bradyi* Cush.	*Discorbis globularis* (d'Orb.)	*Asterigerina planorbis* (d'Orb.)	*Ammonia beccarii* (Linn.)	*Elphidium macellum* (F. & M.)	*Cibicides lobatulus* (Walk. & Jac.)	*Nonion padanum* Perconig	*Gyroidina neosoldanii* Brotzen	*Hanzawaia boueana* (d'Orb.)
PLEISTOCENE	Sea Floor 2845 m																																																
	0-9	1	■																																														
	9-18	2	■																																														
	18-27	3	■																																														
	27-36	4	■																																														
	36-45	5	■																																														
	45-54	6	■																																														
	54-63	7	■																																														
	63-72	8	■																																														
UPPER PLIOCENE	72-81	9	■	■	■																																												
	81-90	10	■		■	■	■	■	■					■																																			
	90-99	11	■			■				■	■	■	■	■	■																																		
	99-108	12	■		■	■					■	■	■			■																																	
	108-117	13	■			■	■					■	■	■	■				■	■																														
	117-126	14	■			■	■					■	■	■							■	■	■																										
LOWER PLIOCENE	126-135	15	■			■	■					■	■	■			■	■			■			■	■																								
	135-144	16	■			■						■	■	■			■		■		■					■																							
	144-153	17	■			■	■					■	■	■							■						■																					
	153-162	18	■			■	■					■	■	■							■							■	■	■	■																	
	162-171	19	■			■	■					■	■				■				■								■	■	■	■																
	171-180	20	■			■																										■																	
	180-189	21	■																														■	■	■	■	■	■	■	■	■	■	■	■	■	■	■	■	■

Messinian (Upper Miocene) Evaporite Section – Cores 21 (part) through 27; No benthonic foraminifera found.

Scyphosphaera pulcherrima
Scyphosphaera recurvata
Sphenolithus abies
Syracosphaera pulchra
Thoracosphaera imperforata
Trochoaster deflandrei
Age: Lower part of Upper Pliocene
Zone: *Reticulofenestra pseudoumbilica* (NN 15)

Samples: 13-132-14, CC; 132-15-1, 63 cm:
Ceratolithus rugosus
Ceratolithus tricorniculatus
Coccolithus pelagicus
Cyclococcolithus leptoporus
Discoaster asymmetricus
Discoaster brouweri
Discoaster challengeri
Discoaster pentaradiatus
Discoaster surculus
Helicosphaera carteri
Lithostromation perdurum
Pontosphaera scutellum
Reticulofenestra pseudoumbilica
Scyphosphaera apsteini
Sphenolithus abies
Age: Lower Pliocene
Zone: *Discoaster asymmetricus* (NN 14)

Samples: 13-132-15-3, 75 cm; 132-15, CC; 132-16-1, 125 cm; 132-16-4, 125 cm; 132-16, CC:
Ceratolithus rugosus
Coccolithus pelagicus
Cyclococcolithus leptoporus
Discoaster brouweri
Discoaster challengeri
Discoaster pentaradiatus
Discoaster surculus
Discoaster variabilis
Discolithina macropora
Helicosphaera carteri
Lithostromation perdurum
Pontosphaera multipora
Pontosphaera scutellum
Reticulofenestra pseudoumbilica
Rhabdosphaera stylifera
Scyphosphaera apsteini
Scyphosphaera pulcherrima
Scyphosphaera recurvata
Sphenolithus abies
Thoracosphaera imperforata
Age: Lower Pliocene
Zone: *Ceratolithus rugosus* (NN 13)

Samples: 13-132-17-1, 75 cm; 132-17-3, 25 cm; 132-17, CC; 132-18-1, 75 cm; 132-18-3, 25 cm; 132-18-5, 25 cm; 132-18, CC; 132-19-1, 25 cm; 132-19-1, 125 cm; 132-19-4, 25 cm; 132-19, CC; 132-20-1, 130 cm; 132-20-4, 80 cm; 132-20, CC; 132-21-2, 5 cm; 132-21-2, 33 cm; 132-21-2, 37 cm:
Ceratolithus tricorniculatus
Coccolithus pelagicus
Cyclococcolithus leptoporus
Discoaster brouweri
Discoaster challengeri
Discoaster pentaradiatus
Discoaster surculus
Discoaster variabilis
Helicosphaera carteri
Pontosphaera japonica
Pontosphaera scutellum
Scyphosphaera apsteini
Scyphosphaera intermedia
Scyphosphaera recurvata
Sphenolithus abies
Thoracosphaera imperforata
Age: Lower Pliocene
Zone: *Ceratolithus tricorniculatus* (NN 12)

Samples: 13-132-21-2, 70 cm; 132-21-2, 76 cm; 132-21-2, 93 cm:
Coccolithus cf. *pelagicus*
Discoaster bollii
Discoaster challengeri
Discoaster phyllodus
Discoaster quinqueramus (?)
Discoaster surculus
Discoaster variabilis
Pontosphaera multipora
Sphenolithus abies
Age: Upper Miocene
Zone: *Discoaster quinqueramus* (NN 11)

Sample 13-132-21, CC:
Same assemblage with Pliocene downhole contaminants.
Cores 132-22 to 24:
Only rare nondiagnostic coccoliths and downhole contaminants of younger sediments were registered.

LITHOSTRATIGRAPHY

Three major lithologic units are recognized at Site 132, (Table 4). The first two units comprise the fossiliferous pelagic oozes of Pliocene and Pleistocene age which lie above Horizon M, and the third includes sedimentary sequences of evaporitic origin which are correlated to the M-Reflectors and were deposited during the late Miocene "crisis of salinity." The contact between the pelagic oozes and evaporites is remarkably sharp and occurs within a one-millimeter-thick interval at 74 cm in Section 2 of Core 21 at a subbottom depth of 183 meters.[5]

The layer of pelagic ooze has been somewhat arbitrarily subdivided into two separate units in recognition of a noticeable change in both the carbonate content and amount of volcanic contribution with depth. Unit 1, from the sea floor to 50 meters below bottom, consists of

[5] Only two sections (1.5 meters length each) were recovered for the coring interval 21 from 180 to 189 meters below bottom. Because the actual *in situ* depth of the recovered material is unknown, DSDP convention arbitrarily assigns Sections 1 and 2 of this core a depth to the top of the interval of 180 to 183 meters. However, the notable drilling break to which the contact is correlated actually occurred at 188 meters just before the cutting of the core was completed.

TABLE 4
Lithologic Units of Site 132

Unit	Lithology	Age
1	Foraminiferal marl oozes with discrete layers of volcanic ash (tephra) and sands	Pleistocene
----50 m----		
2	Foraminiferal oozes with only scattered occurrence of volcanic ash	Pre-glacial Pleistocene and Pliocene
~183 m[a]		
3	Evaporites including pyritic marls, gypsiferous and dolomitic sands, dolomitic marls, chert, terrestrial soils, and massive recrystallized gypsum	Upper Miocene
223 m		

[a]188 meters in situ according to footnote 5

foraminiferal marl ooze with a highly variable content of calcium carbonate (Figure 8), but generally less than 50 per cent, intercalated with discrete tephra layers. Unit 2, which extends down to the evaporites, has more uniform carbonate values (for the most part above 50%) and contains glass shards only as a minor constituent mixed with fossiliferous components.

Unit 1 – Marl Oozes with Intercalations of Ash and Sands

Plastic marl oozes with ash and sand intercalations were recovered from the sea floor down to 50 meters. They belong to the *Globorotalia truncatulinoides* Total-range-zone and are Quaternary in age.

The sediments of Unit 1 often have a relatively high fine-grained terrigenous fraction, sometimes up to 70 per cent. They are olive to olive gray in color with some red, brown, and black beds. They are mainly composed of quartz and clay minerals together with nannoplankton and relatively few foraminifera. They are well bedded, highly burrowed and display hydrotroilite spots.

Ash beds are intercalated at several intervals, particularly in the uppermost part of the Quaternary. A few ash layers are also present at the base of the unit. They are composed of clear volcanic glass shards (30-70%) with an index of refraction of less than 1.55.

Sometimes fragments of brown, acicular glass were also observed (e.g., Core 6, Section 4). The median thickness of the volcanic tephra layers is 3 to 5 cm; the maximum thickness observed is 20 cm in Section 3 of Core 1. Here, this thick ash layer shows graded bedding, which is not apparent in other cases. The volcanic glass is generally mixed with quartz, pyrite, biotite, hornblende, and sometimes with a small fraction of nannoplankton.

Other intercalations are represented by foraminiferal and terrigenous sand layers. The latter are composed of 50 per cent quartz, 15 per cent calcite, 5 per cent hornblende, 8 per cent chlorite, 3 per cent plagioclase and biotite, and 20 per cent pelagic constituents (estimates from smear slides).

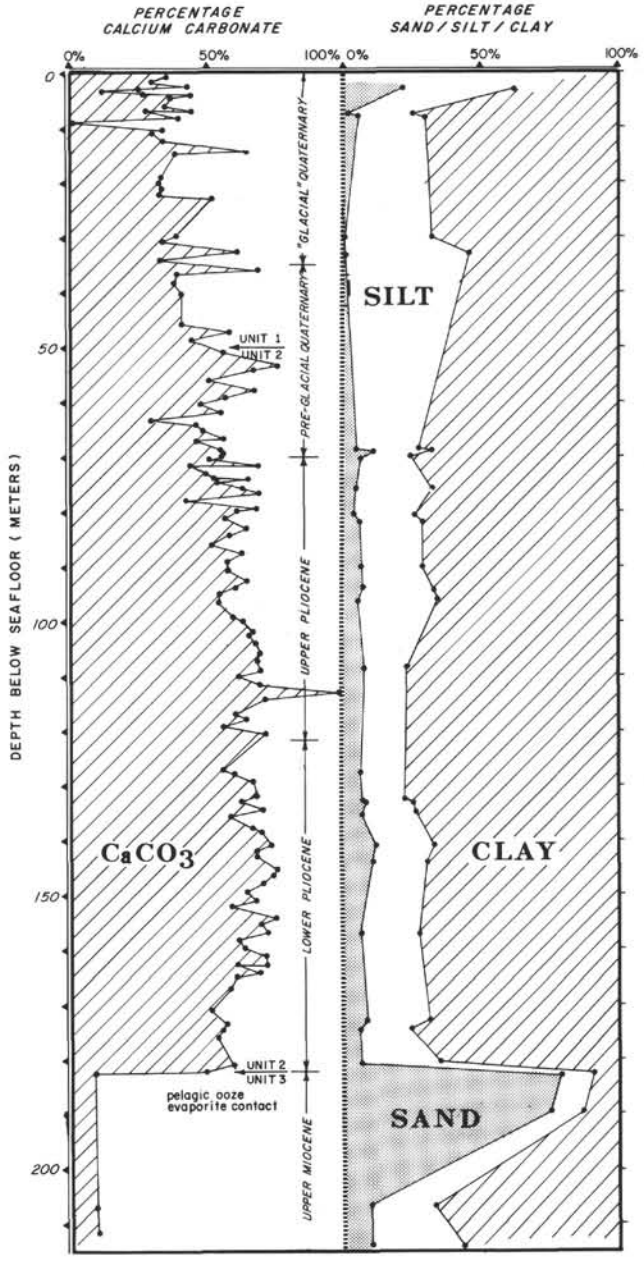

Figure 8. *Variations in the carbonate content and percentage abundance of sand, silt, and clay down the continuously cored section of Hole 132. Note the abrupt change at the Miocene/Pliocene boundary with pelagic oozes above and evaporites below.*

These sand layers are megascopically devoid of internal sedimentary structures (gradation, lamination, etc.) and may have been reworked by gentle bottom current activity. Layers of pyritic marl oozes with foraminifera were also observed in Unit 1. The average mineralogic composition of these pyritic sediments is: 20 to 40 per cent pyrite, 10 per cent muscovite, 5 per cent quartz, 30 to 40 per cent nannofossils and 5 ro 30 per cent foraminifera. In Core 2, Section 1, 107 cm, there is a darker layer with a high content of organic material which contains 35 per cent clear volcanic glass shards ($n < 1.55$).

Unit 2 – Foraminiferal Oozes

Foraminiferal oozes were drilled between 50 and 183 meters. They are Pliocene in age and very similar to the Trubi marls of southern Italy. The upper boundary with Unit 1 is somewhat arbitrary and is gradational. The lower boundary is found in Section 2 of Core 21 and is discontinuous on the evaporitic series.

From the lithologic point of view, the main characteristics that distinguish this unit from Unit 1 are: (a) a higher $CaCO_3$ content (50-60%); (b) the presence of abundant visible planktonic foraminifera (about 10%); (c) the lack of terrigenous intercalations (only a thin silt lamina in Core 9, Section 6) and therefore the absence of stratification; (d) the presence of abundant and randomly distributed spots, streaks, pockets and bands of hydrotroilite; (e) a general light olive gray color with occasional transitional color variations in brown, yellowish brown, greenish gray, etc.; and (f) heavy burrowing.

The lithologic uniformity also corresponds to a homogeneous mineralogy. The numerous smear slides analyzed have shown a constant amount (50-60%) of pelagic constituents, mainly nannofossils with 5 to 10 per cent tests of foraminifera, and rare *Braarudosphaera*. The coarse fraction of the terrigenous material is composed of very small lamellae of muscovite and very fine angular quartz. On the whole, the unit displays little lithologic change from top to bottom, except that planktonic foraminifera are slightly more abundant in the lower horizons.

The sediments of Unit 2 are interpreted as pelagic deposits in an environment isolated from significant terrigenous input. The bottom 10 meters above the contact with the evaporitic series are hematite or limonite-goethite stained in various hues of red and brown. Just above the contact, the section contains a 25-centimeter-thick layer of a pseudobrecciated marl ooze. Streaks of multicolored sediments crisscross and interfinger with each other along very irregular and often diffuse contacts. Unlike a true breccia, there are no clearly visible isolated homogeneous fragments. The stiffness of the sediment seems to rule out mechanical brecciation during the drilling operations, and the gross overall appearance of carefully scraped surfaces suggests some sort of post-depositional diagenic alternation and selective staining, perhaps (?) by solutions of brine percolating up from the immediately subjacent evaporite layer. The lower contact of the pseudobreccia with subjacent pyritic marls and sands is very sharp (Figure 9) and has an appearance of an erosional surface with truncated sandy laminae.

Unit 3 – Evaporite Series

Dark gray marl oozes and dolomitic marls with abundant gypsum crystals and pyrite along with intercalated thick layers of solid gypsum were drilled between the contact at 183 meters and the bottom of the hole at 223 meters. The contact with the overlying pelagic ooze truncates sand laminae in the subjacent pyritic marls. Rather than to postulate a major stratigraphic gap at the contact, we prefer instead to interpret the bedding structures as an indication of a sudden change in the sedimentary conditions rather than as a major unconformity.

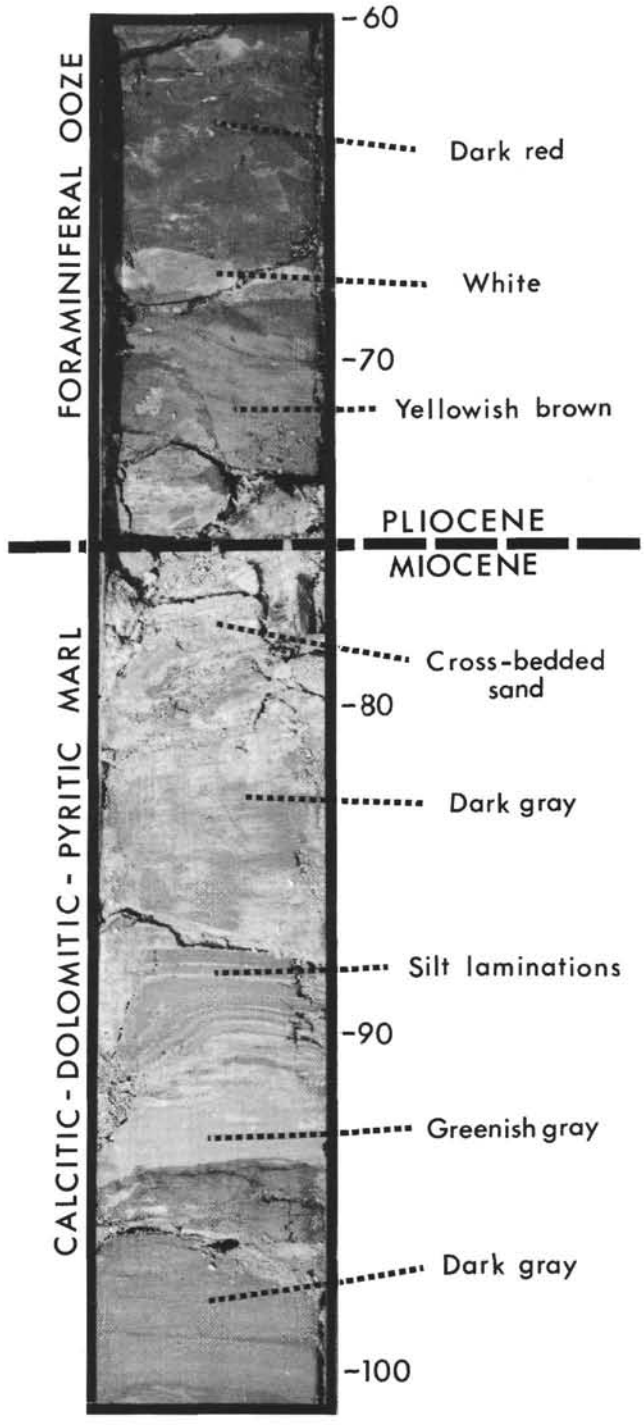

Figure 9. *Photograph of the visual facies boundary in Section 2 of Core 21, separating the Pliocene pelagic oozes (here a pseudo-breccia) above from pyritic marls of the Late Miocene evaporite series below. Note the evidence of erosion and winnowing in the cross-bedded sands and silts at the contact, itself.*

The upper part of the evaporitic series (Cores 21 and 22, 182-191 m) comprises interbedded sands and marls containing micritic calcite and very fine-grained anhedral dolomite. The very top is a 25-centimeter-thick bed of silty and sandy clay displaying cross-laminations (see Figure 9).

Below, the marls contain layers of coarse clayey quartzose sand with rounded fragments of gypsum and shallow-water, neritic species of foraminifera.

The interbedded marls are composed of fine quartz, clay minerals, and calcite, in addition to the small amounts of anhedral dolomite (see Chapter 21). The clay minerals are illite, mixed-layer clays, montmorillonite, chlorite and kaolinite. The fauna comprises nannofossils, benthonic foraminifera and a poor assemblage of planktonic foraminifera. The oozes are practically gypsum free in their upper part, but gypsum in the form of isolated selenite crystals of "swallow-tail" shape becomes more and more abundant down the hole. At 190.1 meters the drilling recovered the first bed of solid, bedded gypsum, 12 cm thick. Below this horizon, dark reddish brown marls are crosscut with selenite crystals.

The next Core, 23 (191-198 m), recovered a light gray, laminated, plastic to semi-indurated sediment. X-ray analysis showed gypsum with traces of quartz. A single cobble-sized piece of white saccharoidal gypsum with finely laminated "balatino" bedding structures was found in the core along with a 4-centimeter-thick fragment of black chert.

Fifteen meters below, the first section of Core 25 (207-214 m) consists of a light gray plastic dolomitic marl with closely spaced (5 to 10 cm) intercalations of millimeter-thick beds of crystalline gypsum. Isolated crystals of selenite occur throughout the bulk of the ooze. The sediment comprises quartz, feldspar, the same clay minerals as in Cores 21 and 22, and both calcite and dolomite. Scattered foraminifera are still present but nannofossils are absent.

The second sections of Cores 25 and 26 (214-220 m) are composed of interbedded plastic beds and thick layers of solid gypsum. All display a large variety of colors: yellow, brown, red, green, black, etc., and are well bedded to laminated. The plastic beds comprise mainly gypsum with small or trace amounts of quartz, calcite or dolomite (10 to 12% of carbonates). The fauna from intercalated marl oozes comprises a rich assemblage of planktonic foraminifera but no nannofossils. Between 60 to 85 cm in Section 2 of Core 25, we observed a bright, blood-red arkosic arenite which is completely barren of microfossils and is very rich in pollen and spores. The distinctive color comes from a finely disseminated hematite powder, indicative of highly oxidizing conditions in contrast to the gray dolomitic marls with abundant dark organic matter and pyrite. It is quite possible that the red layer represents a terrestrial soil deposited during a brief past exposure of the sea bed—a situation analogous to interpretations of the Arenazzolo Formation of the Gesso Solfifera series of Sicily (Ogniben, 1957).

The growth of the indurated gypsum rock in Cores 25 and 26 has involved considerable brecciation (Figure 10). The crystallization observed in Core 26 is clearly post-depositional and is believed to be a secondary replacement of primary anhydrite, with the deformation linked to volume changes which accompany this diagenetic transition.

The parallel laminations at 130 cm in Section 1 of Core 26 are highly reminiscent of the banded laminites found in Core 8 of Hole 124, except that here at the Tyrrhenian site, the crystal plates are gypsiferous instead of anhydritic. The light-colored layers, typified in Figures 10 C and 10 D appear to have been former dolomitic or calcitic partings.

When viewed in thin section cut parallel to the split face of the rock cores, the light bands lie just above thin streaks (films?) of very dark organic matter which does not seem to have suffered much diagenesis. The organic matter ranges from yellow brown to black in color and is optically similar to filaments of present-day algal mats of the intertidal zone of the Persian Gulf (Kinsman, 1966; Shearman and Fuller, 1969) and of the Red Sea (G. Friedman, personal communication). A dark gray color permeates the secondary brecciated gypsum rock of Core 26, accentuating the considerable abundance of organic constituent.

In Core 27, the gypsum rock takes on an orange and reddish brown color reflecting the presence of iron oxides in the detrital partings. Very well-preserved wavy stramatolites occur at 111 cm in Section 2 of this core and are illustrated in Figure 11A. Here much of the original anhydrite has been diagenetically altered to coarsely crystalline calcite. Where solution and metamorphism have been particularly effective, suture boundaries (stylolites) can be recognized and these often cut across the primary bedding structures as shown in Figure 11B. Traces of hematite, goethite, and limonite, characteristic of the aforementioned red arkosic arenite, are invariably present in the most severely altered units, suggesting to us a reflux leaching action by local groundwater, perhaps in an exposed supratidal flat environment (sabkha) as envisioned by Shearman (1966).

PHYSICAL PROPERTIES

Because of the induration of the evaporitic facies of Cores 22 to 27, it was only possible to make meaningful physical property measurements on the first 21 core barrels at Site 132. These cores include the foraminiferal marls and oozes of Lithologic Units 1 and 2 with occasional interbedded tephra and sand horizons.

Penetrometer Readings

Penetrometer readings are the highest in the beds of low bulk density and high water content. At the top of the hole, in Cores 1 to 5 above a depth of 45 meters, the measurements vary widely between 11×10^{-1} mm and 328×10^{-1} mm which was made in Core 21 at 183 meters depth. Laminated marls present in Cores 15, 16, and 17 display small-scale variation in penetrometer readings. The homogeneity of the marl oozes in Cores 10, 11, and 12 is reflected by constant readings in the range 40 to 80×10^{-1} mm, and is also supported by consistent gamma counts.

Densities

Bulk densities fall in the range 1.40 to 1.89 gm/cc, which are a little lower than the corresponding GRAPE values, which lie between 1.50 and 1.77 gm/cc. The trend follows a general increase with depth up to 160 meters, and then decreases from 1.89 to 1.68 gm/cc in the subjacent nannofossil oozes of lithology similar to those above. The decrease may be a result of drilling disturbance, as those sediments occurring in Cores 19, 20 and 21 comprise

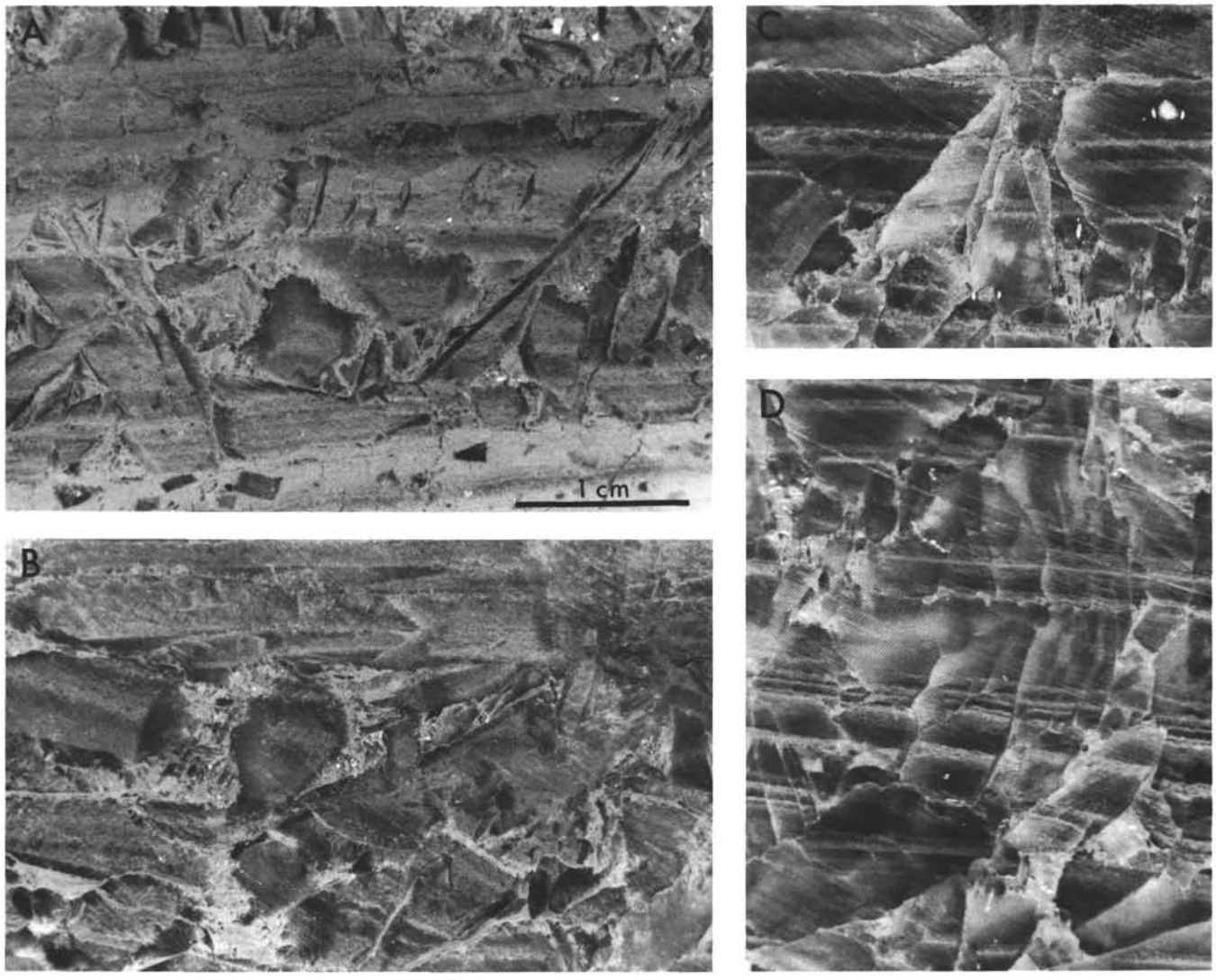

Figure 10. *Evidence of post-depositional diagenesis leading to volume changes and subsequent brecciation in the transition from former laminated anhydrite and dolomite to secondary gypsum. A and B are from 96 to 99 cm and 101 to 104 cm in Section 2 of Core 25, respectively. C and D are from 128 to 133 cm in Section 1 of Core 26.*

mottled textures. Densities calculated from core section weights correspond fairly closely with the GRAPE values; they are generally less than that determined from laboratory determinations, but the greatest discrepancy is only 0.1 gm/cc. Grain densities vary between 2.43 and 2.96 gm/cc. There are, however, several cases of unreasonably high computed densities. This may be due to poor data, or, alternatively, may be explained by localized lithification within the cores. For example, the value of 3.08 gm/cc in Core 3-2 may have been measured on a pyrite nodule; in Core 4, Section 6 and Core 6, Section 3, values of 3.04 and 3.08 gm/cc may be related to the unusual composition of the sand and ash layers. In Core 5, Section 1, the value of 4.39 gm/cc is obviously too high to be real; in Cores 9, Section 6 and Core 19, Section 1, values of 3.06 and 3.02 gm/cc may be correlated to the high calcium carbonate content of a practically pure nannofossil ooze.

Porosity and Water Content

An inverse correlation can be made between porosity and water content and bulk densities. Water content varies between 52.9 and 28.3 per cent, and porosity between 74.8 and 51.4 per cent; maximum values occur at the top of the hole and decrease steadily downwards. Only in disturbed cores are the values extraordinarily high. There is a marked decrease toward 81 meters depth, where values are 28.3 and 52.4 per cent respectively; although, the values remain fairly constant below that depth.

Natural Gamma Radiation

Natural gamma readings reveal systematic trends. Counting rates at the top of the hole are noticeably higher than those at the bottom in the same lithological unit of nannofossil oozes. They range in general between 2500 and

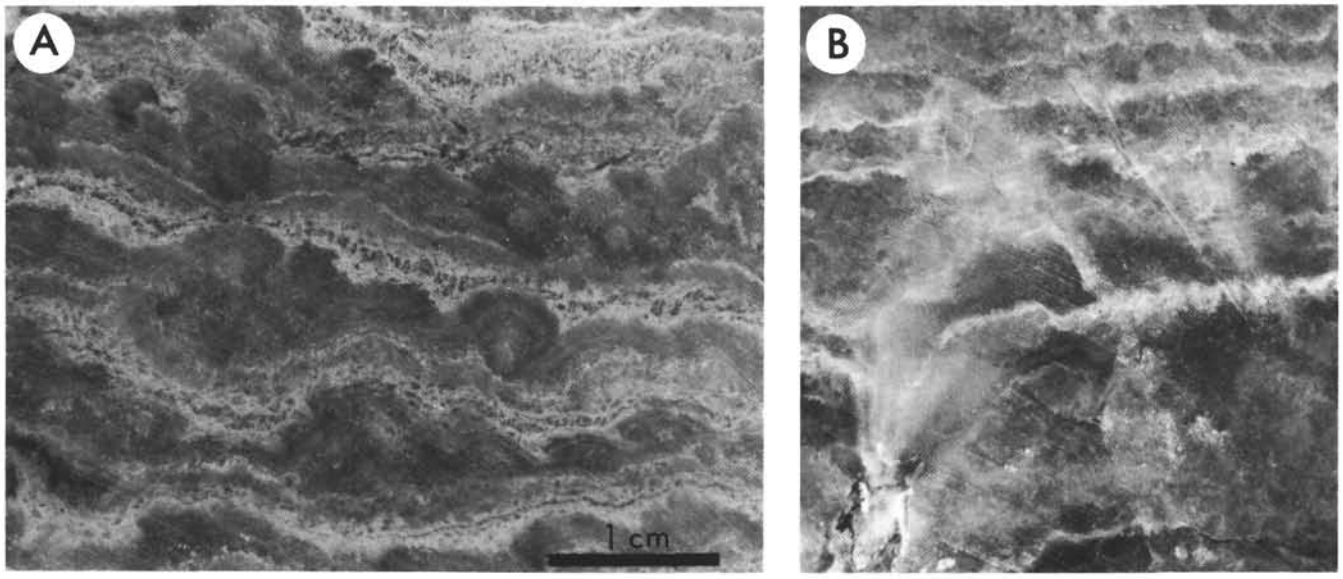

Figure 11. *Illustrations of stramotolite-like wavy laminations and cross-cutting styolites. Both rock units shown here have undergone extensive solution, recrystallization, and replacement including some calcitization of former anhydrite spherules and nodules at the left in Core 27, Section 2, 111 to 114 cm. Sample at right is from Core 27, Section 1, 124-127 cm.*

3000 counts in Cores 1 to 3, 2500 and 3400 counts in Cores 6 to 10, 2000 and 2500 counts in Cores 11 to 15 and reach a minimum of 1900 to 2400 counts in lower cores.

Within these units, variations occur between lithologies with different values of calcium carbonate content, easily recognizeable, for example, in Cores 1, 2 and 3. The oozes are multicolored in shades of gray, brown and yellow, and it appears that the yellow oozes are poorer in radioactive constituents than the darker clays. Also, area of hydrotroilite spotting seem to give low counts. Core 10, between 81 and 90 meters, shows a sequence of multicolored nannofossil oozes and hydrotroilite spotted laminated marl oozes over which the variation can be traced. A typical sequence of values for a color change from dark gray to spotted to brownish yellow clays, as in Sections 3 and 4 of Core 10, is 3150 to 2300 to 2350 counts. Cores 6 to 20 show similar trends.

There are specific horizons at which the level of radiation increases. Extremely high counts of over 6000 occur in Core 1, Section 3 and Core 5, Section 4, which can be correlated with tephra horizons. Coarse-grained sands, containing volcanic glass and quartz fragments also produce high count rates of 3600 in Core 1. The following typical count rates are provided to show how lithologies may be distinguished. Values in Core 1, Section 2 are 2600 counts in nannofossil oozes, 3000 counts in a dark gray sapropelitic ooze, 2800 counts in impure oozes, and 4100 counts in consolidated fine sand or arenite.

All counts greater than 4000 may be correlated with layers of ash or sapropel. In Core 3, Section 4, however, an anomalously high count of 4800 corresponds to a bed of "stiffer, darker clay," of which several occur throughout the hole. Values over these lithologies range from 3000 to 4800 counts in the upper part of the hole, and from 2300 to 2600 counts in the lower part. They apparently contain a greater proportion of radioactive constituents along with an increased carbon content. There seems to be a reduction in the count level to just above 2000 over basal pyritic and dolomitic marls, the massive gypsum rocks and the recrystallized anhydritic laminites.

DISCUSSION AND CONCLUSIONS

Since drilling operation had to be abandoned with unacceptably slow penetration rates in the evaporites long before we were able to reach acoustic basement, no information is yet available on the composition or nature of the crustal rocks at the site. Fortunately, however, just one month prior to the spudding in of Site 132, R/V *Atlantis II* of the Woods Hole Oceanographic Institution was able to successfully dredge an outcrop of the basement layer some 75 km to the east of the targeted drilling location on an exposed escarpment of the De Marchi Mountain (Heezen *et al.*, 1971). There, at five locations along what has been interpreted to be a tilted fault block, metamorphic rocks including crystalline schists, phyllites, and marbles were recovered in association with sedimentary rocks showing signs of considerable deformation and fracturing. Some undeformed fossiliferous limestone was brought up in a few of the hauls, but as of the time of writing this chapter we do not yet know the diagnostic ages of the faunal assemblages.

The schists are of low to medium metamorphic grade, and according to Heezen *et al.* (1971), this metamorphism implies a former moderately deep burial of materials making up a continent-like terrain which they identify as a

fragment of Tyrrhenides.[6] The authors believe that the outcropping of the metamorphic rock on the sea bed implies a former period of subaerial erosion prior to the foundering of the crustal ridges and the creation of a deep basin floor.

Analogies can perhaps be made here to the finding of other metamorphic suites beneath the floor of the Alboran Sea at Site 121 and near the eastern edge of the Balearic Abyssal Plain at Site 134.

Comments on the Age of Foundering

Though drilling results in the Tyrrhenian Basin add little to our understanding of the processes of emplacement of these metamorphic basement terrains, the recovery of the overlying sedimentary blanket of pelagic oozes and evaporites does allow us to place some new constraints on the timing of the supposed foundering and permits us to examine a mechanism for their shallow subbottom exposure.

Many researchers place the age of the creation of a deep Tyrrhenian Basin sometime in the Neogene (Norin, 1958; Sègre, 1958; Kuenen, 1959; Stanley and Mutti, 1968; de Booy, 1969, Pannekoek, 1969; Drooger and Meulenkamp, 1969; Heezen *et al.*, 1971; Selli and Fabbri, 1971). Schemes for the evolution of the bathyal areas involves subsidence, extension, or a combination of these two.[7]

On the basis of Site 132, it is clear that Reflector M in the Tyrrhenian Basin corresponds to the top of the Late Miocene evaporite series that was found at all the other western and eastern Mediterranean sites, and that this formation is capped on the Tyrrhenian Rise by a blanket of pelagic oozes deposited in a deep basin environment not too different from that which exists today.

The digitally processed Flexotir reflection profile MS-1 of Finetti *et al.* (1970) documents a lateral continuity of Reflector M beneath most of the east-to-west track across the deep-water part of the basin (i.e., from Shot Point 0 to Shot Point 4200 inclusive, with only small gaps near the crests of Vavilov and Marsili Seamounts). The regional extent and the conformably draped appearance of the acoustic horizon beneath the central bathyal plain (particularly in the general vicinity of Shot Point 2500) can be used to support an argument that the basin configuration of this part of the central Mediterranean was already in existence at the time the evaporites were deposited. Compressional wave velocities on the recovered gypsum reported in Chapter 18 match the 5.0 km/sec layer determined by the refraction measurements of Moskalenko (1966) and support the interpretation that the thickness of this evaporite layer approaches 1 km throughout the region of the bathyal plain. In fact, around the drill site, at Shot Point 4140 (Figure 2), more than 0.5 second of strongly reflective strata can be clearly identified below Reflector M, which, with an average interval velocity of only 4 km/sec, might account for another kilometer of evaporites beneath the Tyrrhenian Rise as well.

The facies of the recovered evaporites (in particular the gypsum laminites with a wavy banding, characteristic of algal stromatolites) and the supposed terrestrial arkosic arenite, reflect a shallow-water intertidal and supratidal depositional environment during parts of the Late Miocene. In the seismic profiles, the evaporite layer is transgressive over the flanks of protruding basement ridges and seems to be either very thin or absent only on the crests of the high peaks. The change in relative spacing and the acoustic character of the reflecting interfaces from the depressions to the highs can be interpreted to imply that even much of the local subbottom relief predates the evaporite epoch, with different facies (i.e. carbonates vs sulfates) being on either side of a depressed shoreline.[8]

Contrary to the aforementioned models of crustal foundering, we looked for but found no evidence at Horizon M in Core 21 of any kind of a transgressive deposit indicating a passage from shallow water to deep water on which to date the development of the present day Tyrrhenian Basin.

From the several lines of evidence presented in Chapters 30, 36, 43, and 47, we believe we can reasonably conclude that the deep-water character of the Pliocene and Pleistocene pelagic oozes originates from an abrupt flooding of a formerly desiccated deep basin through the establishment of a permanent opening by way of a deep passage to the Atlantic Ocean about 5.4 my ago, rather than from vertical tectonic subsidence.[9]

We would choose to place the post-orogenic collapse and extension of the basin tentatively either in Serravallian (after Drooger and Meulenkamp, 1969) or Tortonian time, prior to the "crises of salinity" during the Messinian which then led to a partial drying up of already existing Mediterranean basins.

It is important, however, to mention that our conclusions are not in agreement with the hypothesis recently put forth by Selli and Fabbri (1971). They believe that the present Tyrrhenian is essentially of Middle Pliocene age and has resulted from foundering about 4 my ago, corresponding to what they believe to be a recognizable and extensive transgression; it "may very well be the youngest deep sea of the world" (Selli and Fabbri, op. cit. p. 104).

Their conclusions are reached from geological evidence obtained during dredging in the Stromboli and Orosei Canyons–the former only some 50 km from the drilling site. Dredge No. 48, at a water depth of 2200 meters, yielded a conglomerate of vesicular basalt, sandstone, and

[6] Tyrrhenides is a term for an ancient landmass that is inferred to have occupied the present site of the Tyrrhenian Sea, and to have shed detritus of a "sialic" composition eastward into the Apennine geosyncline before its subsidence sometime in the Neogene. (See for instance, de Booy, 1969). The islands of Sardinia, Corsica and Elba are considered to be remnant fragments of this craton (Sègre, 1958).

[7] See discussion by Van Bemmelen, Ritsema, Collette and Schuiling; in the Symposium on the problem of oceanization of the western Mediterranean (1969), for a most interesting debate on this particular point.

[8] The reader is referred to Chapter 43 for a more thorough discussion of the patterns of facies distribution to be expected during the formation of an evaporite layer.

[9] This is not to discredit isostatic adjustments resulting from the removal and addition of the water layers (see Le Pichon *et al.*, 1971).

clayey marls of inferred Lower Pliocene age (with *Globorotalia puncticulata*). The matrix includes littoral and shallow-water mollusks thought to be indicative of a Middle or Upper Pliocene age. Quoting Selli and Fabbri (1971, p. 109), "...Another argillaceous-marly sample, dredged at contact with the conglomerate, contains a rich Foraminifera fauna with *Globigerina decoraperta, G. druryi, G. falconensis, Globigerinoides obliquus* (*Globogerina pachyderma* and *Globorotalia inflata* are absent), *Siphotextularia affinis, Stainforthia concava*, etc. It pertains to the upper part of the *Globorotalia cassaformis zone*, i.e. uppermost part of Middle Pliocene. Therefore, this is the age of the conglomerate and also the age of the transgression."

We cannot concur with such a conclusion. In fact, none of the taxa mentioned, nor their assemblage, can be considered characteristic of the age inferred by Selli and Fabbri (1971). According to the well known monograph of Blow (1969), *Globigerina decoraperta* ranges from Zone N.14 (which is Serravallian in age) to Zone N.21 (latest Pliocene); *Globigerina druryi* ranges from Zone N.11 to N.14; *Globigerina falconensis* ranges from Zone N.7 (Burdigalian) to Zone N.22 (Quaternary). All these species have been recorded in the type Tortonian of Italy (see Cita, Premoli Silva and Rossi, 1965). In fact, if we accept the limited range given by Blow (*op. cit.*) for *Globigerina druryi*, a Pliocene age should be excluded.

The continuously cored section at Site 132 passes through the level referred to as the upper part of the Middle Pliocene by Selli and Fabbri[10] (after the disappearance of *Globorotalia puncticulata*, within the range of *G. crassaformis*, and prior to the first occurrence of *G. inflata*) without any interruption in the sedimentary sequence. This interval corresponds to Cores 10, 11, and 12 which we reexamined carefully for evidence of a hiatus or unconformity. There is no apparent lithologic change within the sequence of pelagic oozes (see Chapter 47.1).

As to the geophysical evidence for a major transgression at that time, Selli and Fabbri (1971) point to a number of widespread angular unconformities observed in their high-resolution sparker profiles near the two canyons they have surveyed. Their Y-Y horizon, which they refer to as the Lower Messinian "gessoso solfifera" formation near the Stromboli Canyon, would be identified by us as Reflector M (see Figure 31B in Ryan *et al.*, 1971), as would their horizon X-X near the Oresi Canyon. We would most likely interpret the conglomerate obtained by dredging as a detrital bed associated with the Messinian shallow-water evaporite series (i.e., fanglomerate after Hardie and Eugster, 1971) as we have for the cobbles and pebbles of a similar position recovered at Site 133 on the Western Sardinia Slope (see Chapter 14). We do not accept the recovered faunal assemblage as indicative of a post-upper Miocene age. Perhaps the unroofing of the metamorphic rocks dredged by the *Atlantis II* could also have occurred during the periods of desiccation when vast tracts of the sea bed, particularly the basement ridges, were subaerially exposed and subject to extensive erosion.

[10] Those authors have employed the Pliocene zonation of Cati *et al.*, 1968.

Hiatuses and unconformities in the subsurface of the basin have been recognized in many seismic reflection profiles obtained in areas where bottom currents are active at present or have been in the past, and in no way by themselves do they demand strandline transgressions to account for their development. In fact, much of Leg 11 of the Deep Sea Drilling Project has been spent investigating the widespread occurrence of such seismic horizons in the deep basin of the North Atlantic Ocean (Ewing and Hollister, 1972).

We would think that the unreasonably high inferred foundering rate of 1100 meters per million years would alone rule out a regional origin to the supposed transgression, and leave other explanations involving current winnowing and non-deposition at least as more attractive alternate explanations.

Sedimentary Record of the Pliocene and Pleistocene

The recovery of a continuous cored section has permitted us to examine at quite close intervals the development of sediment deposition from the abrupt termination of the evaporite epoch to the present. The results of these investigations are reported in detail with more complete documentation in Chapters 46 and 47, of this volume.

We have noted that the Lower Pliocene sequence reflects uniform pelagic deposition accompanied by deep-water psychrosphaeric benthic faunas (see Chapter 37). The highest and most uniform carbonate contents are found there along with the greatest abundance of foraminiferal tests per gram of sediment. Volcanic contributions only become important in the Quaternary, and major explosive eruptions on the mainland of Italy have left thick layers of coarse glassy tephra. Though speculative, the appearance of the andesitic ash in the cores at this time might reflect a progression of the northward dipping lithosphere beneath the Calabrian Arc (Caputo *et al.*, 1970) to a sufficient depth to generate calc-alkaline vulcanism above the seismic zone.

Sapropels, *sensu stricto*, are not found in the Tyrrhenian cores as they were in the sequences recovered from the eastern Mediterranean basins. However, we have noted in Chapter 46 that at levels in the Site 132 cores, which were deposited synchronously with the bottom stagnation to the east, there is an extra abundance of pyrite. This, and the development of a brief anomalous faunal assemblage, lead us to believe that the water mass stratification which induces the oxygen depletion in the deep Ionian and Levantine basins also makes its presence felt in the central Mediterranean.

REFERENCES

Argand, E., 1922. La tectonique de l'Asie. *Congr. Géol. Intern., Compt. Rend.*, **13**e, *Bruxelles*, 1922, p. 171.

Aubouin, J., 1965. Geosynclines. **In** *Developments in Geotectonics.* Elsevier, Amsterdam, **1**, 335p.

Benson, R. H.. Ostracods as indicators of threshold depth in the Mediterranean during the Pliocene. **In** *The Mediterranean Sea: A natural sedimentation laboratory.* Stanley, D. J. (Ed.). Allen Press (in press).

Benson, R. H. and Sylvester-Bradley, P. C., 1971. Deep-sea ostracods and the transformation of ocean to sea in the

Tethys. **In** Paleoecologie Ostracodes – Pau, 1970. Oertli, H. J. (Ed.), *Bull. Gentre Rec. Pau-SNPA.* **5** (suppl), 63.

Berggren, W. A., 1971. Multiple phylogenetic zonations of the Cenozoic based on planktonic Foraminifera. *Proc. II Plankt. Conference, Rome.* **1**, 41.

Biscaye, P., Ryan, W. B. F. and Wezel, F., 1971. Age and nature of the Pan-Mediterranean subbottom Reflector M. **In** *The Mediterranean Sea: A natural sedimentation laboratory.* D. J. Stanley (Ed.). Allen Press (in press).

Bizon, G. and Bizon, J. J., 1968. Microfaunes Planctoniques Du Paléogène Supérieur Et Néogène Marins En Grece Occidentale. *Giorn. Geol.* **35**, 313.

Blow, W. H., 1969. Late Middle Eocene to Recent planktonic foraminiferal biostratigraphy. *Proc. I. Intern. Conference Plankt. Microf.* Brill (Ed.). **1**, 199.

de Booy, T., 1969. Repeated disappearance of continental crust during the geological development of the Western Mediterranean area. *Trans. Koninkl. Ned. Geol. Mijnbouwk. Genootl.* **26**, 79.

Caputo, M., Panza, G. F. and Postpischl, D., 1970. Deep structure of the Mediterranean basin. *J. Geophys. Res.* **75**, 4914.

Carey, S. W., 1958. *A Tectonic Approach to Continental Drift.* University of Tasmania, Hobart, 251p.

Catalano, R. and Sprovieri R., 1969. Stratigrafia e micropaleontologia dell'intervallo tricolaceo del Torrente Rossi (Enna). *Atti Acc. Gioenia Sc. Nat., Catania.* (ser. 7), **1**, 513.

———, 1971. Biostratigrafic di alcune serie saheliane (Messiniano inferiore) in Sicilia. *Proc. Second Plankt. Conference, Roma.* **1**, 211.

Cati, F. *et al.*, 1968. Biostratigrafia del Neogene Mediterraneao basata sui foraminiferi planctonici. *Boll. Soc. Geol. Ital.* **87**, 491.

Cita, M. B., 1971. Paleoenvironmental aspects of DSDP Lega I-IV. *Proc. Second Plankt. Conference, Roma.* **I**, 251.

Cita, M. B., Premoli Silva, I. and Rossi, R., 1965. Foraminiferi planctonici del tortoniano-tipo. *Riv. Ital. Paleont.* **71** (1), 217.

Cita, M. B., Nigrini, C. and Gartner, S., 1970. Biostratigraphy. **In** Peterson, M. N. A., Edgar, N. T. *et al.*, 1970. *Initial Reports of the Deep Sea Drilling Project, Volume II.* Washington (U.S. Government Printing Office).

Colalongo, M. L., 1970. Appunti biostratigrafici sul Messiniano. *Giorn. Geol.* (ser. 2), **36**(2), 515.

Drooger, C. W. and Meulenkamp, J. E., 1969. Stratigraphic marginal notes to the Symposium on Oceanization of the Western Mediterranean Sea. *Trans. Koninkl. Ned. Geol. Mijnbouwk, Genootl.* **26**, 149.

Erickson, A. J., 1970. The measurement and interpretation of heat flow in the Mediterranean and Black Seas. Ph.D. Thesis, Massachusetts Institute of Technology and the Woods Hole Oceanographic Institution.

Ewing, J. and Ewing, M., 1959. Seismic refraction measurements in the Atlantic Ocean basins, in the Mediterranean Sea, on the Mid-Atlantic Ridge, and in the Norwegian Sea. *Bull. Geol. Soc. Am.* **70**, 291.

———, 1971. Seismic reflection. **In** *The Sea.* Part I (A. E. Maxwell, Ed.) John Wiley and Sons. **4**, 1.

Ewing, J. and Hollister, C. D., 1972. Regional aspects of deep sea drilling in the western North Atlantic: **In** Hollister, C. D., Ewing, J. I. *et al.* 1972. *Initial Reports of the Deep Sea Drilling Project, Volume XI.* Washington (U.S. Government Printing Office). 951.

Fahlquist, D. A. and Hersey, J. B., 1969. Seismic refraction measurements in the western Mediterranean Sea. *Bull. Instit. Oceanogr. Monaco, 67.* **1386**, 1.

Finetti, I., Morelli, C. and Zarudzki, E., 1970. Reflection seismic study of the Tyrrhenian Sea. *Boll. di Geofisica Teorica ed applicata.* **XII** (48), 311.

Foster, J. H. and Opdyke, N. D., 1970. Upper Miocene to Recent magnetic stratigraphy in deep-sea sediments. *J. Geophys. Res.* **75**, 4465.

Glangeaud, L., 1962. "Paleogeographie dynamique de la Mediterranée et de ses bordures. Le rôle des phases Ponto-Plio-Quaternaires," **In** Océanographie Géologique et Géophysique de la Mediterranée occidentale, *Colloques Internationaux C.N.R.S.*, Villefranche, 125.

Hardie, L. A. and Eugster, H. P., 1971. The depositional environment of marine evaporites: a case for shallow, clastic accumulation. *Sedimentology.* **16**, 187.

Hatherton, T. and Dickinson, W. R., 1969. The relationship between andesitic volcanism and seismicity in Indonesia, the Lesser Antilles, and other island arcs. *J. Geophys. Res.* **74**, 5301.

Hays, J. D., Saito, T., Opdyke, N. D. and Burckle, L. H., 1969. Pliocene-Pleistocene sediments of the Equatorial Pacific. Their paleomagnetic, biostratigraphic and climatic record. *Bull. Geol. Soc. Am.* **80**, 1481.

Heezen, B. C., Gray, C., Sègre, A. G. and Zarudzki, E. F. K., 1971. Evidence of foundered continental crust beneath the central Tyrrhenian Sea. *Nature.* **229** (5283), 327.

Isacks, B. and Molnar, P., 1971. Distribution of stresses in the descending lithosphere from a global survey of focal-mechanism solutions of mantle earthquakes. *Rev. of Geophys. and Space Physics.* **9**, 103.

Karig, D. E., 1971. Structural history of the Mariana Island Arc System. *Bull. Geol. Soc. Am.* **82**, 323.

Kinsman, D. J. J., 1966. Gypsum and anhydrite of Recent age, Trucial Coast, Persian Gulf. **In** *Second symposium on salt, Northern Ohio Geol. Soc.*, Cleveland, Ohio. **1**, 302.

Klemme, H. D., 1958. Regional geology of circum-Mediterranean Region. *Bull. Am. Assoc. Petrol. Geol.* **42**, 477.

Kuenen, Ph. H., 1959. Age d'un bassin Mediterranéen. **In** *La topographie et la Géologie des Profondeurs Océaniques, Colloques Internationaux C.M.R.S.*, Nice-Villefranche. p. 157.

Le Pichon, X., Pautot, G. J., Auzende, J. M. and Olivet, J. L., 1971. La Mediterranée occidentale depuis l'Oligocène: schema d'evolution. *Earth and Planet. Science Letters.* **13**, 145.

Martini, E., 1971. Standard Tertiary and Quaternary calcareous nannoplankton zonation. *Proc. Second Plankt. Conference, Roma.* **II**, 739.

Martini, E. and Worsley, T., 1971. Standard Neogene Calcareous Nannoplankton zonation. *Nature.* **225** (5229), 289.

Maxwell, J.C., 1959. Turbidite, tectonic and gravity transport: northern Apennine Mountains, Italy. *Bull. Am. Assoc. Petrol. Geol.* **40**, 2701.

McKenzie, D. and Sclater, J. C., 1968. Heat flow inside the Island Arcs of the northwestern Pacific. *Geophys. Res.* **73**, 3173.

Merla, G., 1951. Geologia dell'Apennino settintrionale. *Boll. Sco. Geol. Ital.* **70**, 95.

Morelli, C., 1970. Physiography, gravity, and magnetism of the Tyrrhenian Sea. *Boll. di Geofisica Teorica ed Appl.* **12** (48), 275.

Moskalenko, V. N., 1965. "Study of the sedimentary series of the Mediterranean Sea by seismic methods. **In** *Basic Features of the Geological Structure of the Hydrological Regime and Biology of the Mediterranean Sea*. L. M. Fomin, (Ed.), Moscow, 224p.

_____, 1966. New data on the structure of the sedimentary strata and basement in the Levant Sea. *Oceanologiya* **6**, 828.

_____, 1967. Structure of the sedimentary series in the Tyrrhenian Sea by seismic methods. *Izvestia Akad. Nauk (SSSR)*. Ser. Geol. 6, 49.

Neprochnov, Yu. P., 1968. Structure of the earth's crust of epi-continental seas: Caspian, Black and Mediterranean. *Earth Sch.* **5**, 1037.

Ninkovich, C. D. and Hays, J. D. (1972). Tectonic setting of Mediterranean volcanoes. *Acta of the International Scientific Congress on the Volcanoe of Thera.* Athens, Greece, Sept. 15-23, 1969. (in press).

Norin, E., 1958· The sediments of the central Tyrrhenian Sea. **In** *Rept. Swed. Deep-Sea Exped.* **8** (1), 1.

Ogniben, L., 1957. Petrografia della Serie Solfifera Siciliana e considerzioni geologiche relative. *Mem. Descrit. Carla. Geol. Ital.* **33**, 275p.

Pannekoek, A. H., 1969. Uplift and subsidence in and around the western Mediterranean since the Oligocene; a review. *Trans. Koninkl. Ned. Geol. Mijnbouwk. Genootl.* **26**, 53.

Peterschmitt, 1956. Quelques données nouvelles sur les seismes profonds de la mer Tyrrhenièn̈ne. *Ann. Geofis.*, **9**, 305.

Ritsema, A. R., 1969. Seismic data of the western Mediterranean and the problem of oceanization. *Verhandelingen Kon. Ned. Geol. Mijnbouwk. Gen.* **26**,105.

_____, 1970. On the origin of the western Mediterranean Sea basins. *Tectonophysics.* 10, 609.

Ryan, W. B. F., Workum, F., Jr. and Hersey, J. B., 1965. Sediments on the Tyrrhenian Abyssal Plain. *Bull. Geol. Soc. Am.* **76**, 1261.

Ryan, W. B. F., Stanley, D. J., Hersey, J. B., Fahlquist, D. A. and Allan, T. D., 1971. The tectonics and geology of the Mediterranean Sea. **In** *The Sea*, A. Maxwell (Ed.), John Wiley and Sons, Intersci., New York. **4**, 387.

Ségre, A. G., 1958. *Geol. Resch.* **47**, 195.

Selli, R., 1970. Cenni morfologici generali sul Mar Tirreno (Crociera C.S.T. 1968), **In** Selli, R. (Ed.), Ricerche geologiche preliminari nel Mar Tirreno. *Giornale di Geologia*, **37** (I), 4.

Selli, R. and Fabbri, A., 1971. Tyrrhenian: a Pliocene deep sea. *Accad. Naz. Lincei, Rend. Cl. Sc. Fisl. Mat., Nat.* **50** (5), 104.

Shearman, D. J., 1966. Origin of marine evaporites by diagenesis, *Inst. of Mining and Metallurgy Trans.* Sec. B. **75**, 208.

Shearman, D. J. and Fuller, J. G., 1969. Anhydrite diagenesis, calcitration, and organic laminites, Winnipegosis Formation, Middle Devonian, Saskatchewan, *Bull. Can. Petrol. Geol.* **17** (4), 496.

Smith, A. G., 1971. Alpine deformation and the oceanic areas of the Tethys, Mediterranean, and Atlantic. *Bull. Geol. Soc. Am.* **82**, 2039.

Stanley, D. J., and Mutti, E., 1968. Sedimentological evidence of an emerged land mass in the Ligurian Seas during the Paleogene. *Nature.* **218**, 32.

Van Bemmelen, R. W., 1969. The origin of the western Mediterranean arean area (an illustration of the progress of oceanization). *Trans. Koninkl. Ned. Geol.-Mijnbouwk. Genootl.* **26**, 13.

Vogt, P. R., Higgs, R. H. and Johnson, G. L., 1971. Hypotheses on the origin of the Mediterranean basin: Magnetic data. *J. Geophys. Res.* **76**, 3207.

Site Summary 132

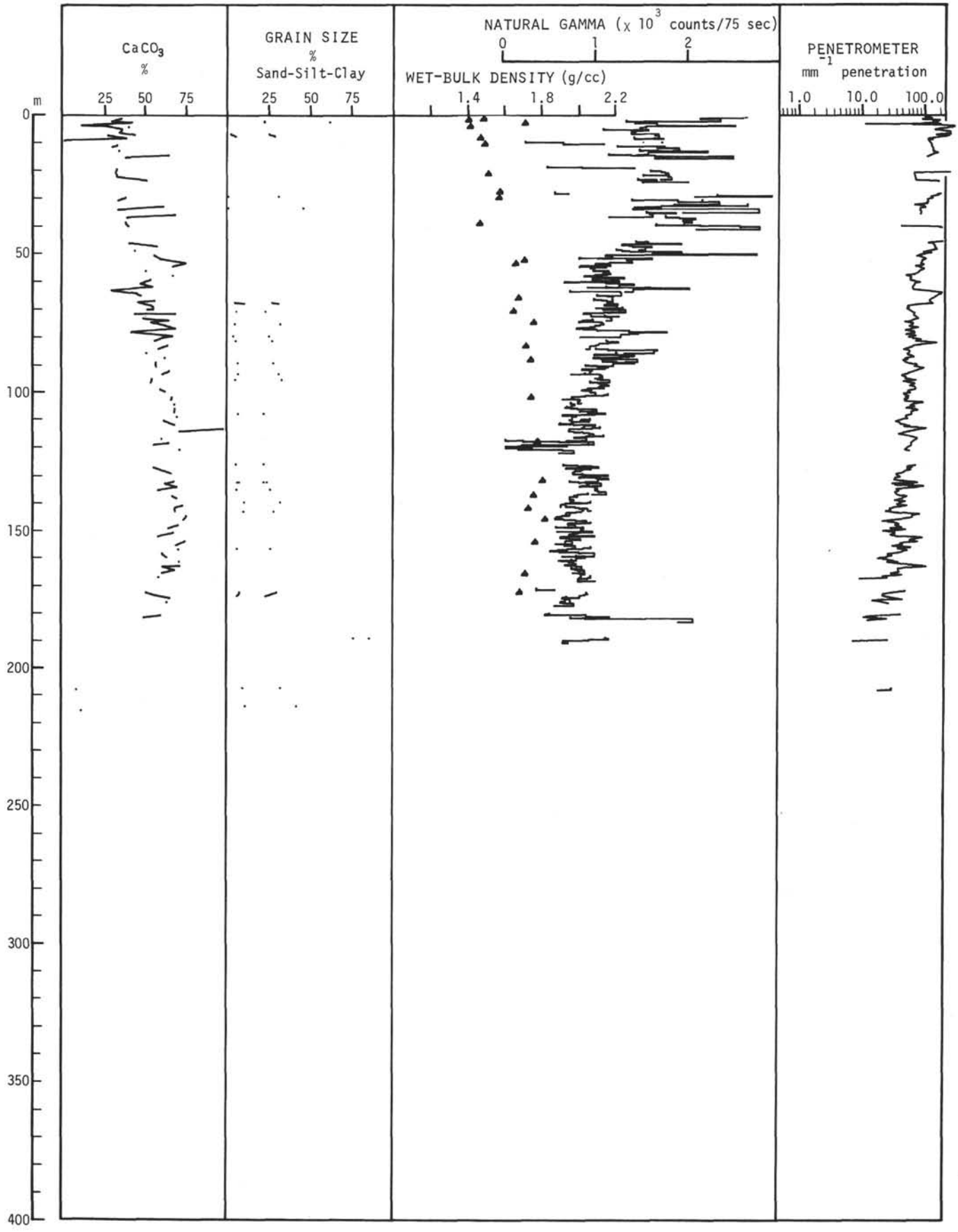

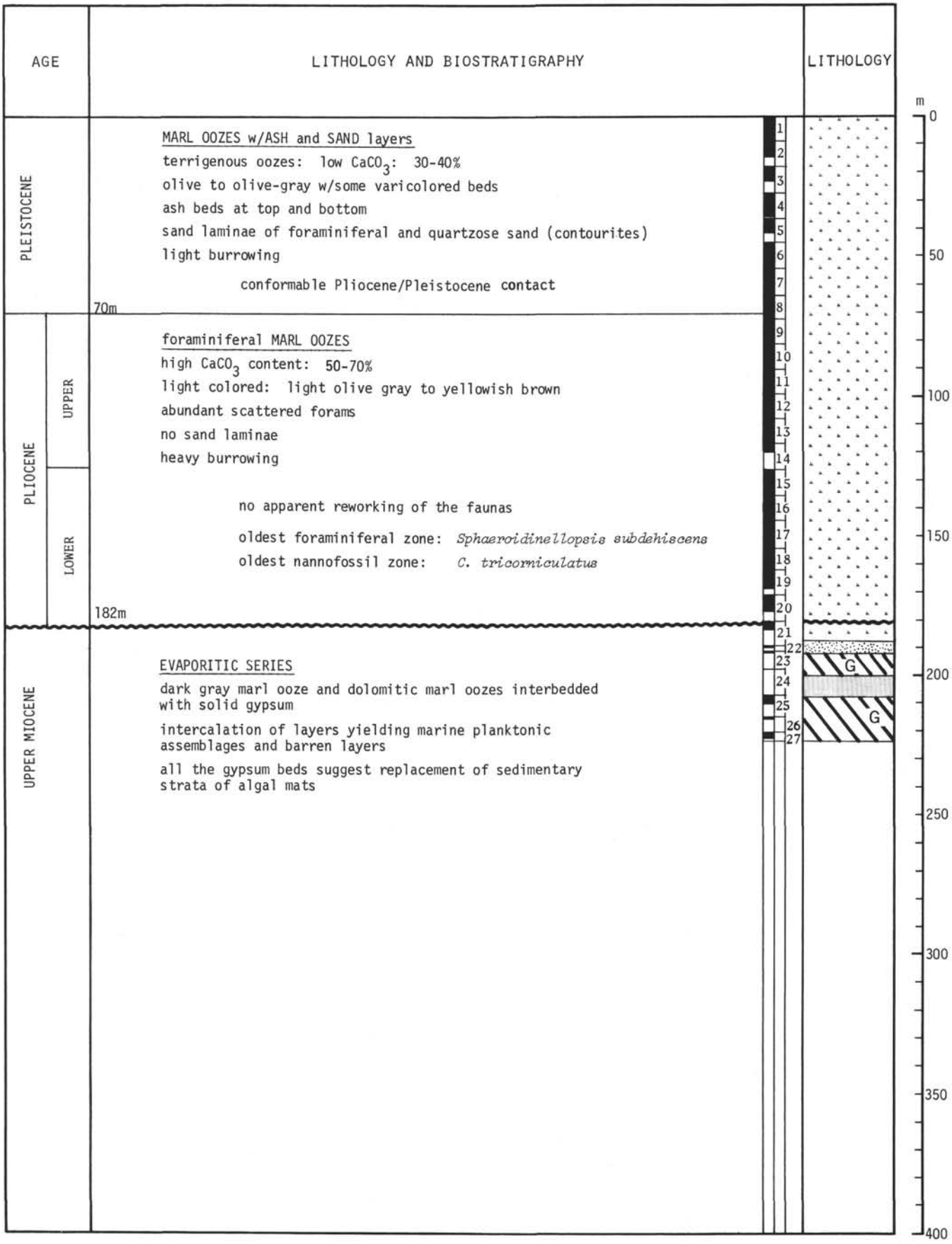
AGE
LITHOLOGY AND BIOSTRATIGRAPHY
LITHOLOGY
m
PLEISTOCENE
MARL OOZES w/ASH and SAND layers
terrigenous oozes: low $CaCO_3$: 30-40%
olive to olive-gray w/some varicolored beds
ash beds at top and bottom
sand laminae of foraminiferal and quartzose sand (contourites)
light burrowing
conformable Pliocene/Pleistocene contact
70m
PLIOCENE
UPPER
foraminiferal MARL OOZES
high $CaCO_3$ content: 50-70%
light colored: light olive gray to yellowish brown
abundant scattered forams
no sand laminae
heavy burrowing
LOWER
no apparent reworking of the faunas
oldest foraminiferal zone: Sphaeroidinellopsis subdehiscens
oldest nannofossil zone: C. tricorniculatus
182m
UPPER MIOCENE
EVAPORITIC SERIES
dark gray marl ooze and dolomitic marl oozes interbedded with solid gypsum
intercalation of layers yielding marine planktonic assemblages and barren layers
all the gypsum beds suggest replacement of sedimentary strata of algal mats
1
2
3
4
5
6
7
8
9
10
11
12
13
14
15
16
17
18
19
20
21
22
23
24
25
26
27
G
G
0
50
100
150
200
250
300
350
400

SITE 132 CORE 1 Cored Interval 0-9 m

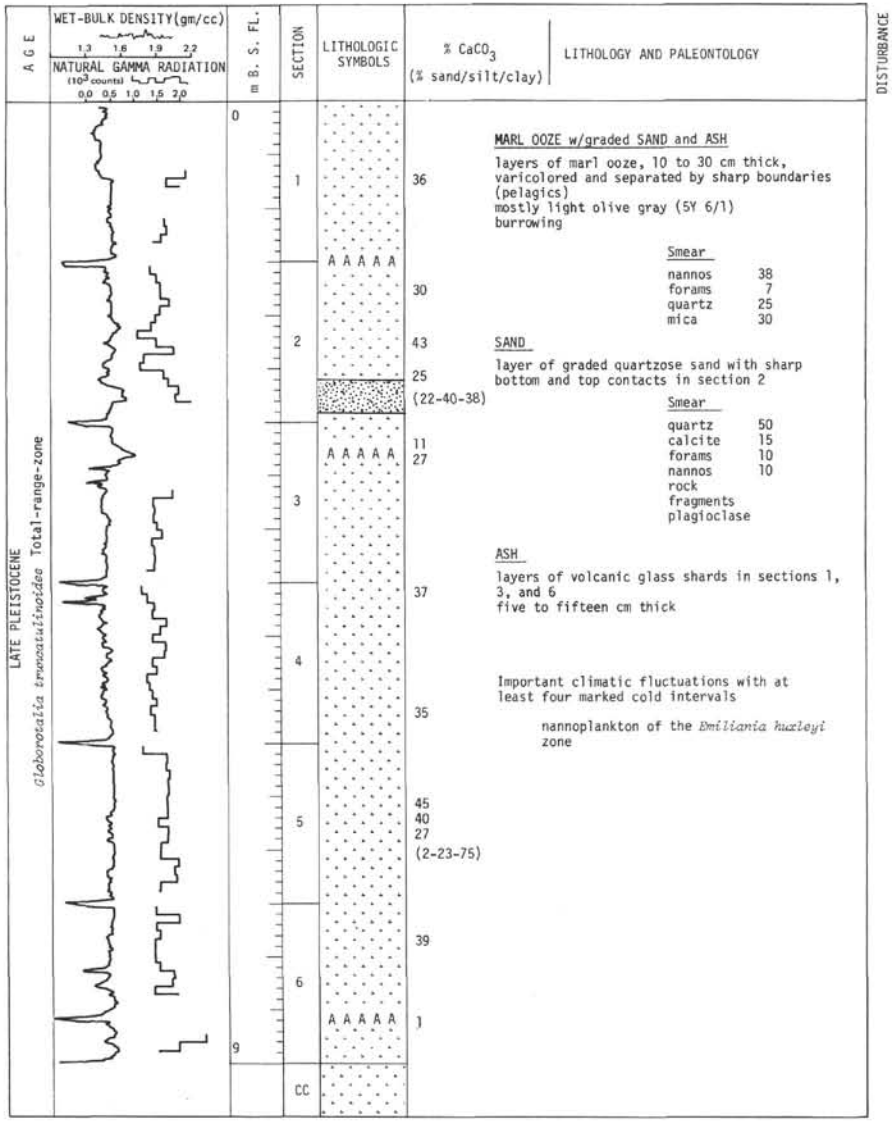

SITE 132 CORE 2 Cored Interval 9-18 m

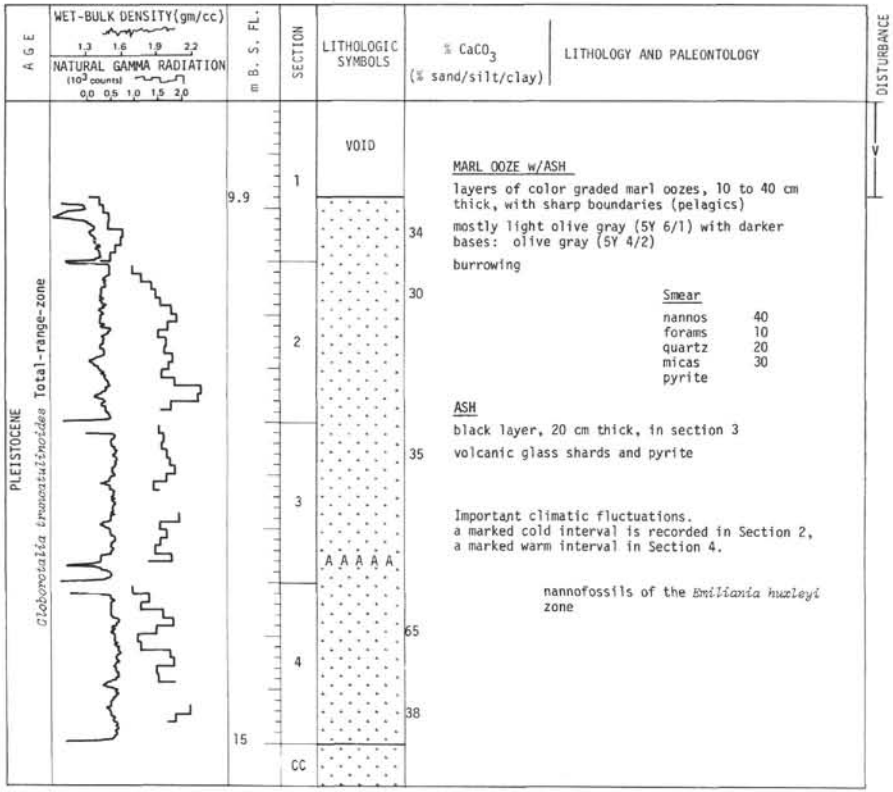

SITE 132 CORE 3 Cored Interval 18-27 m

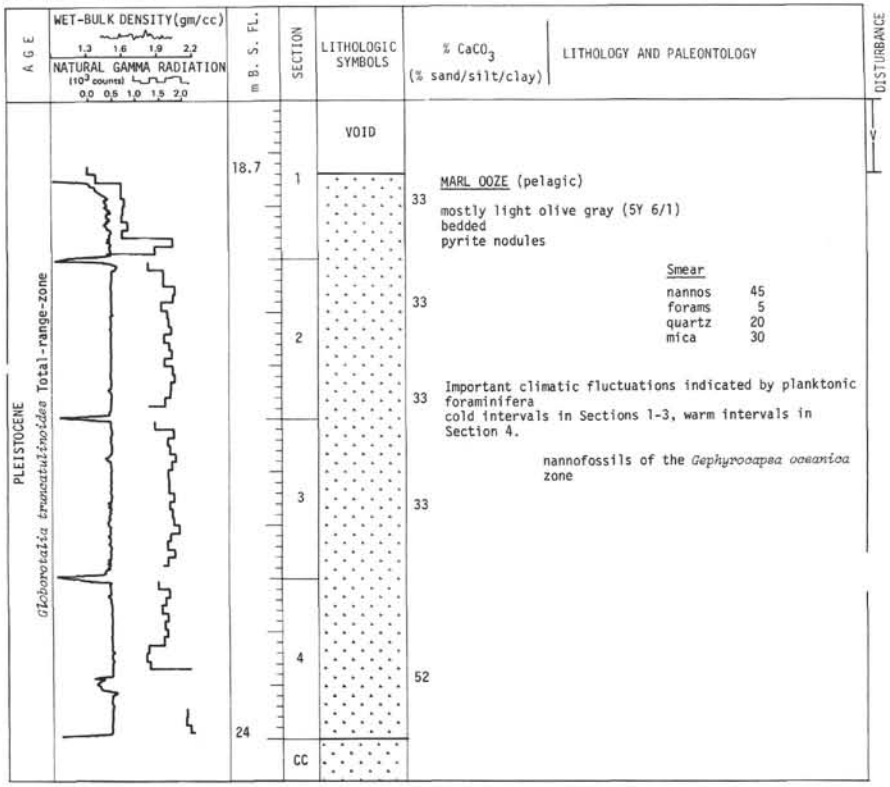

SITE 132 CORE 4 Cored Interval 27-36 m

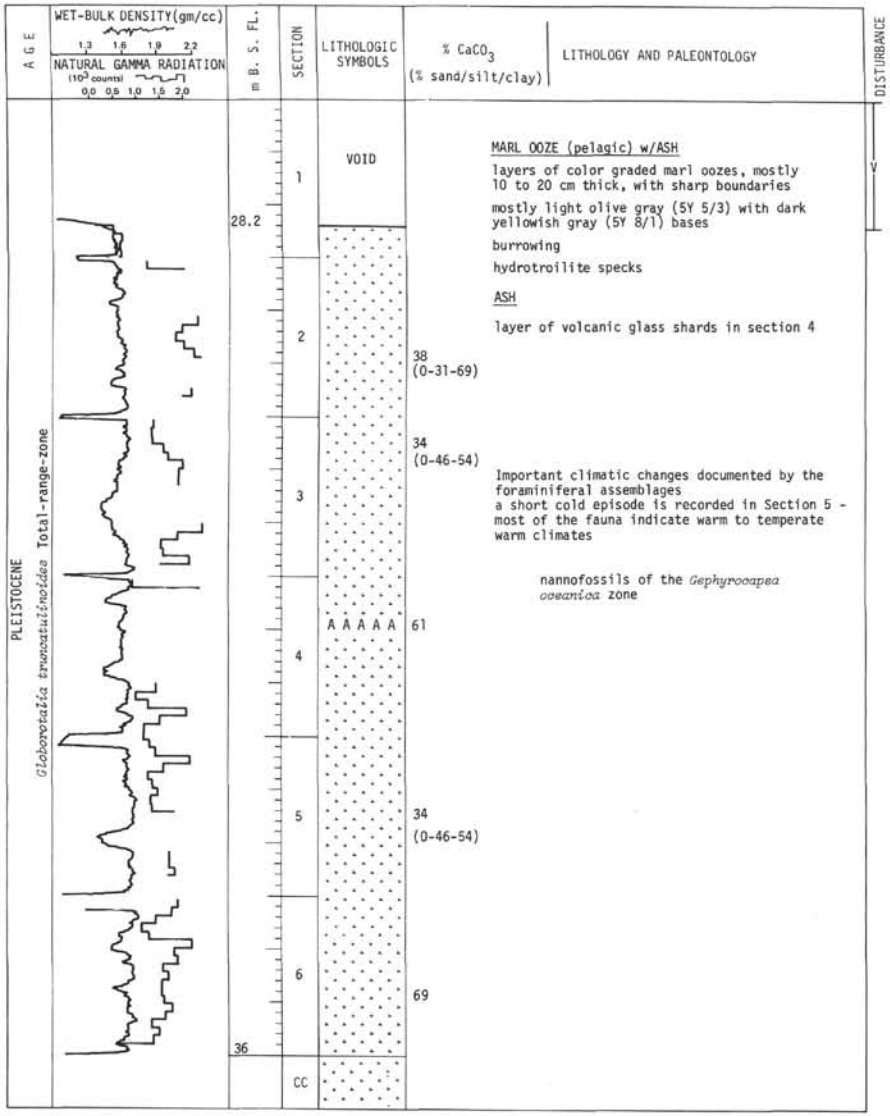

SITE 132 CORE 5 Cored Interval 36-45 m

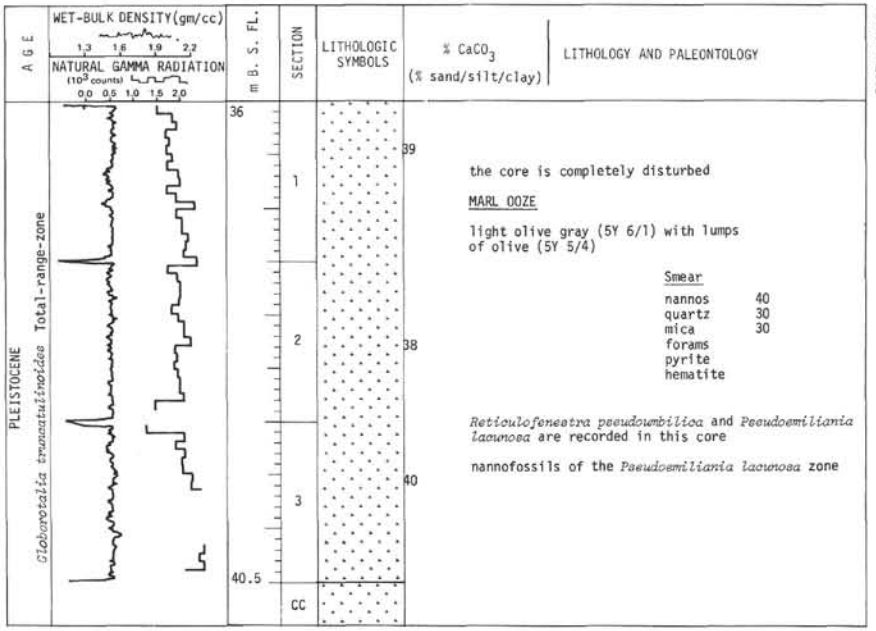

SITE 132 CORE 6 Cored Interval 45-54 m

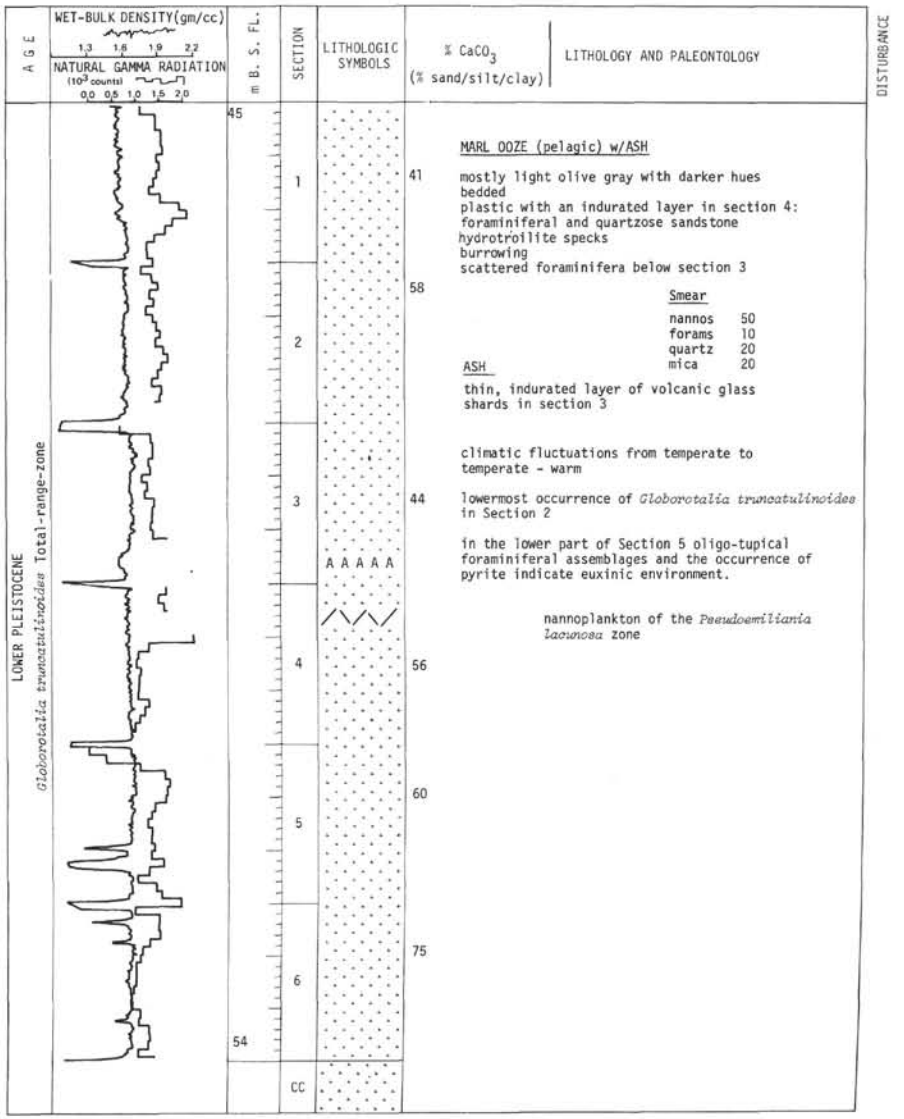

SITE 132 CORE 7 Cored Interval 54-63 m

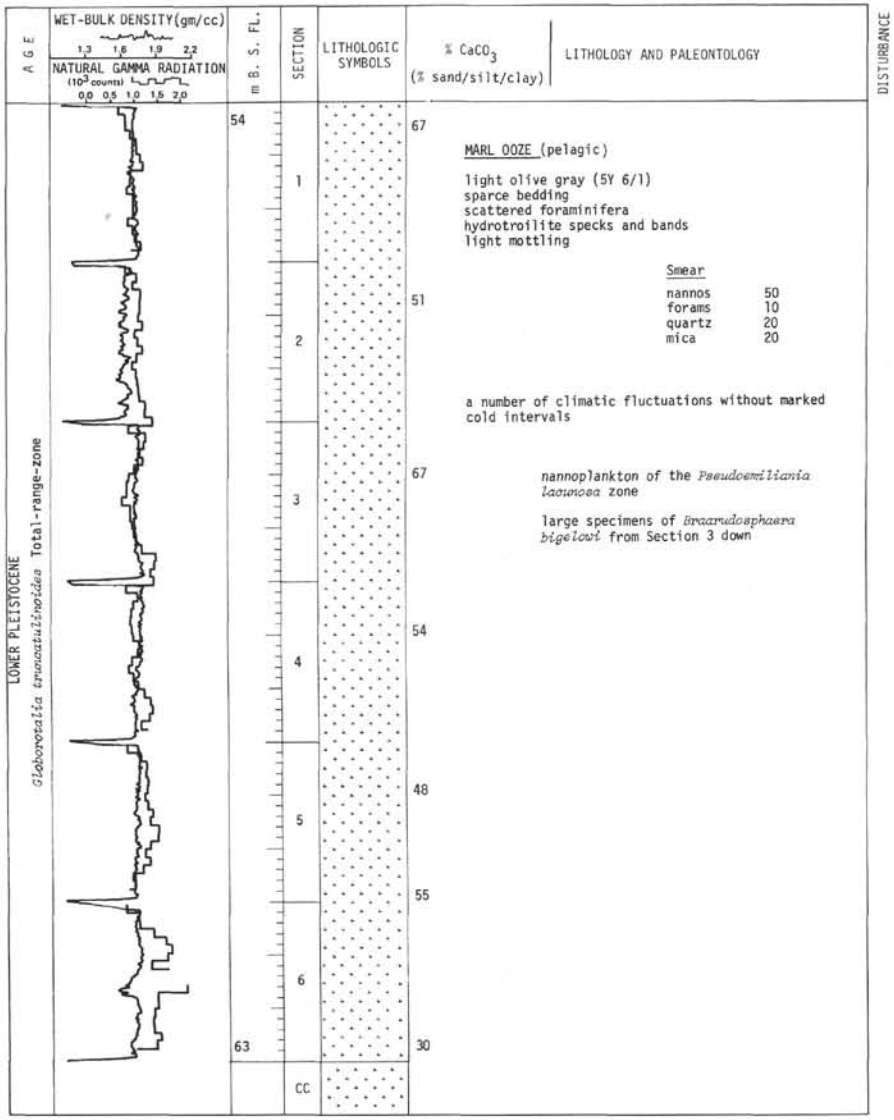

SITE 132 CORE 8 Cored Interval 63-72 m

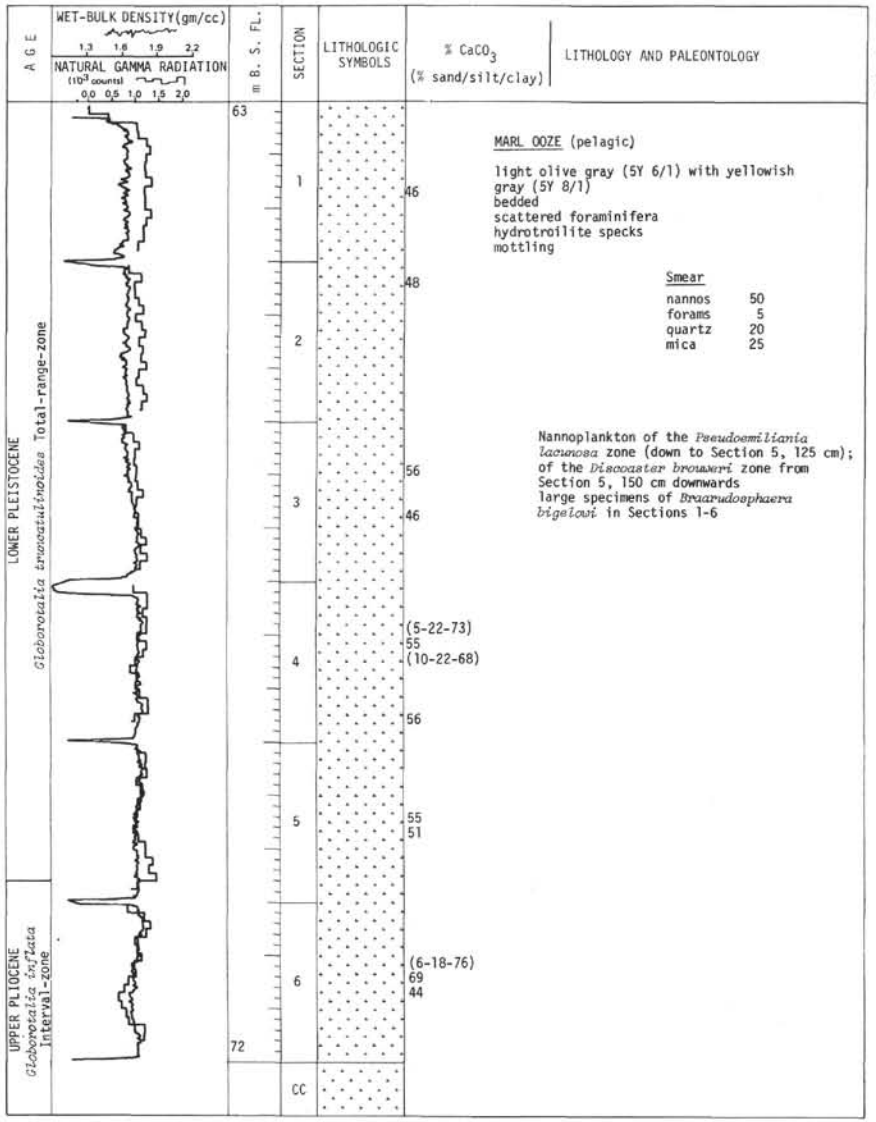

SITE 132 CORE 9 Cored Interval 72-81 m

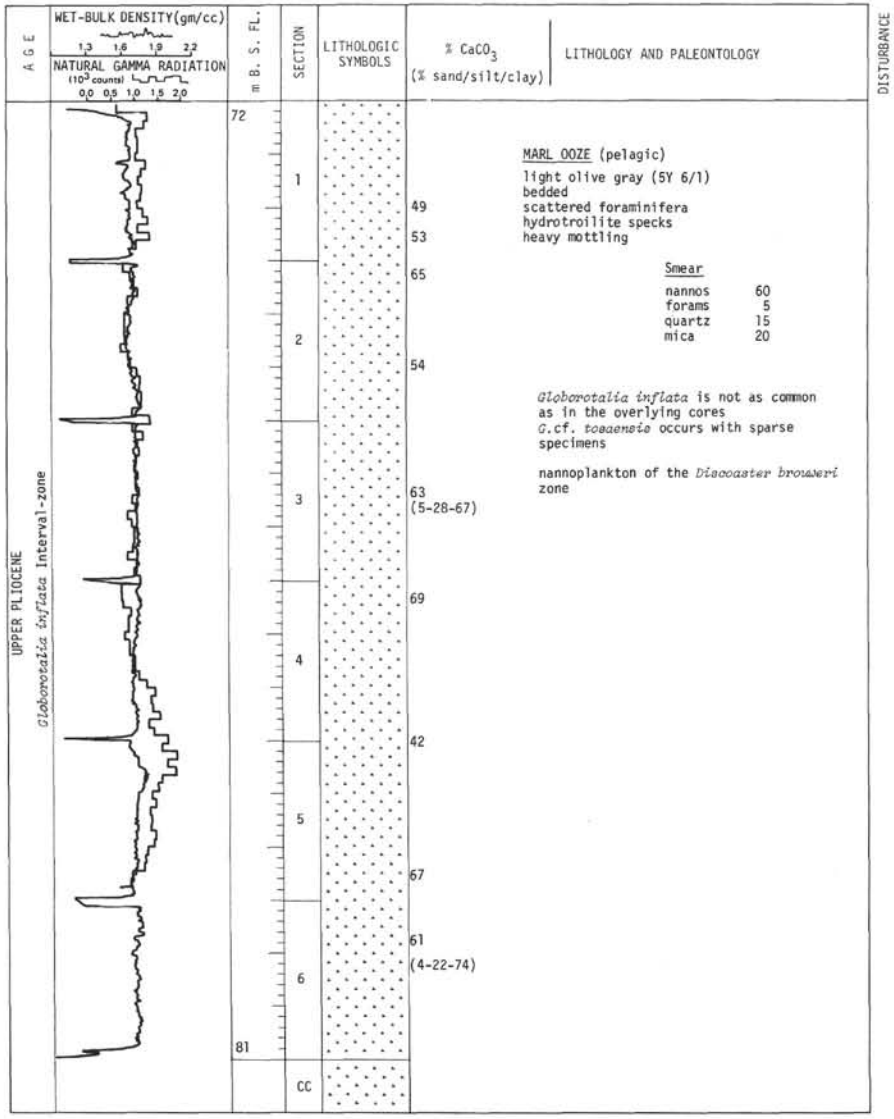

SITE 132 CORE 10 Cored Interval 81-90 m

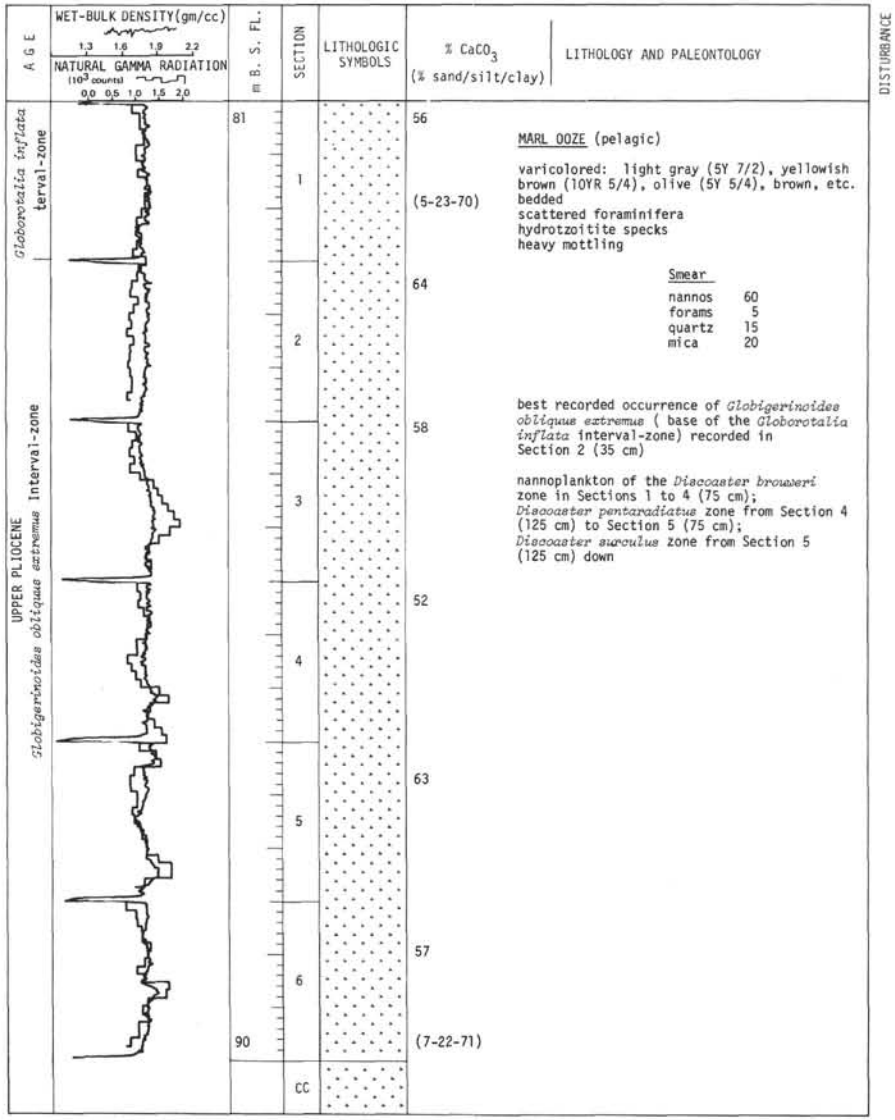

SITE 132 CORE 11 Cored Interval 90-99 m

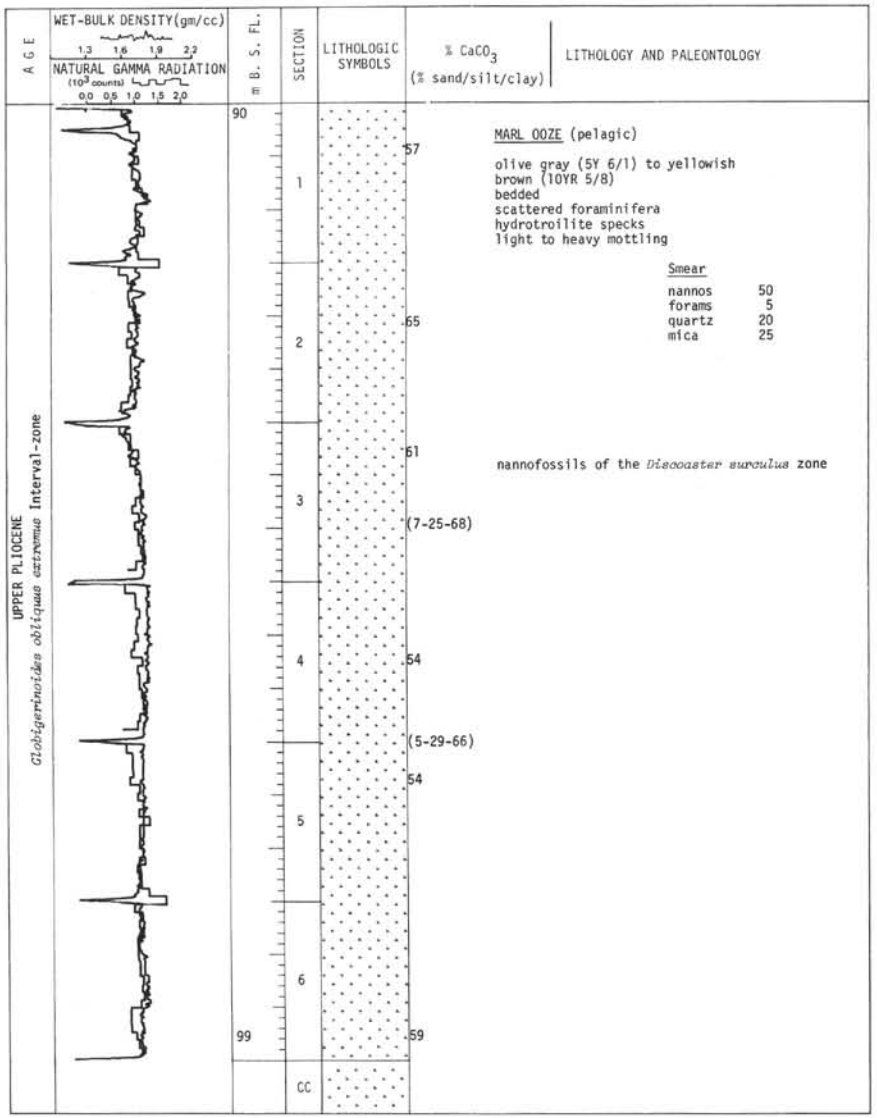

SITE 132 CORE 12 Cored Interval 99-108 m

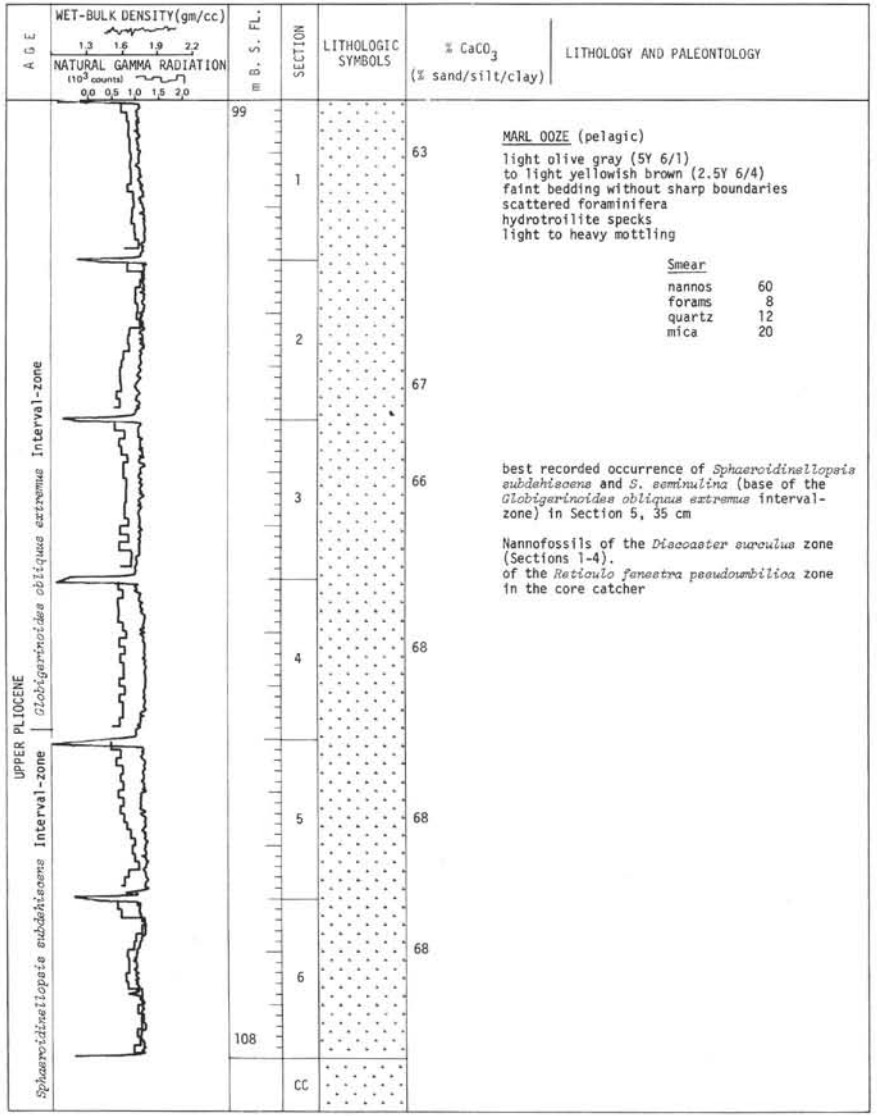

SITE 132 CORE 13 Cored Interval 108-117 m

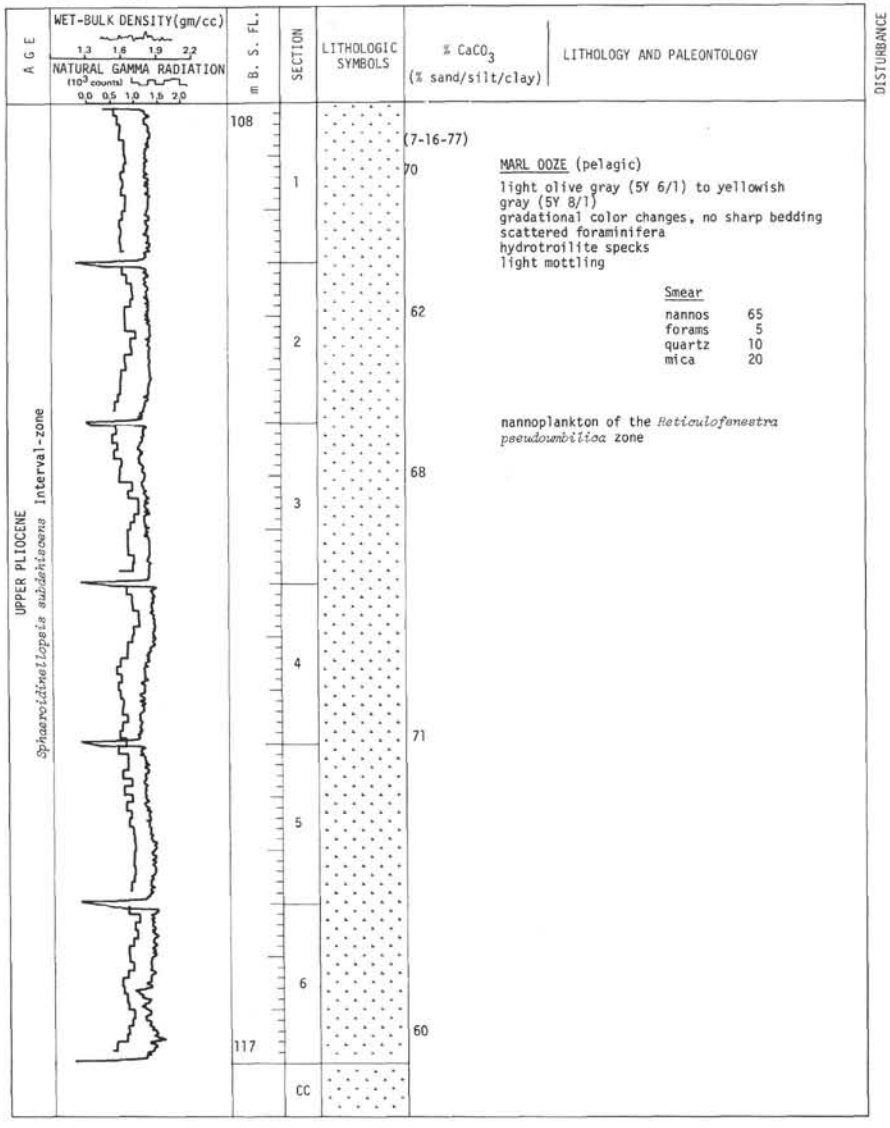

SITE 132 CORE 14 Cored Interval 117-126 m

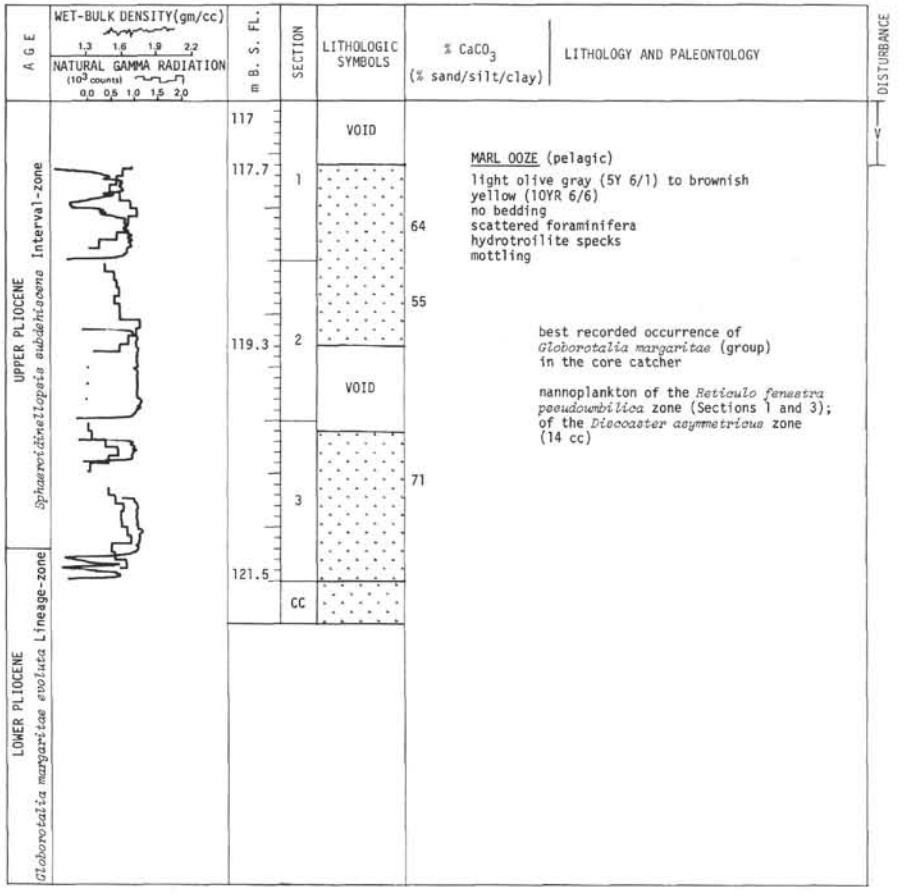

SITE 132 CORE 15 Cored Interval 126-135 m

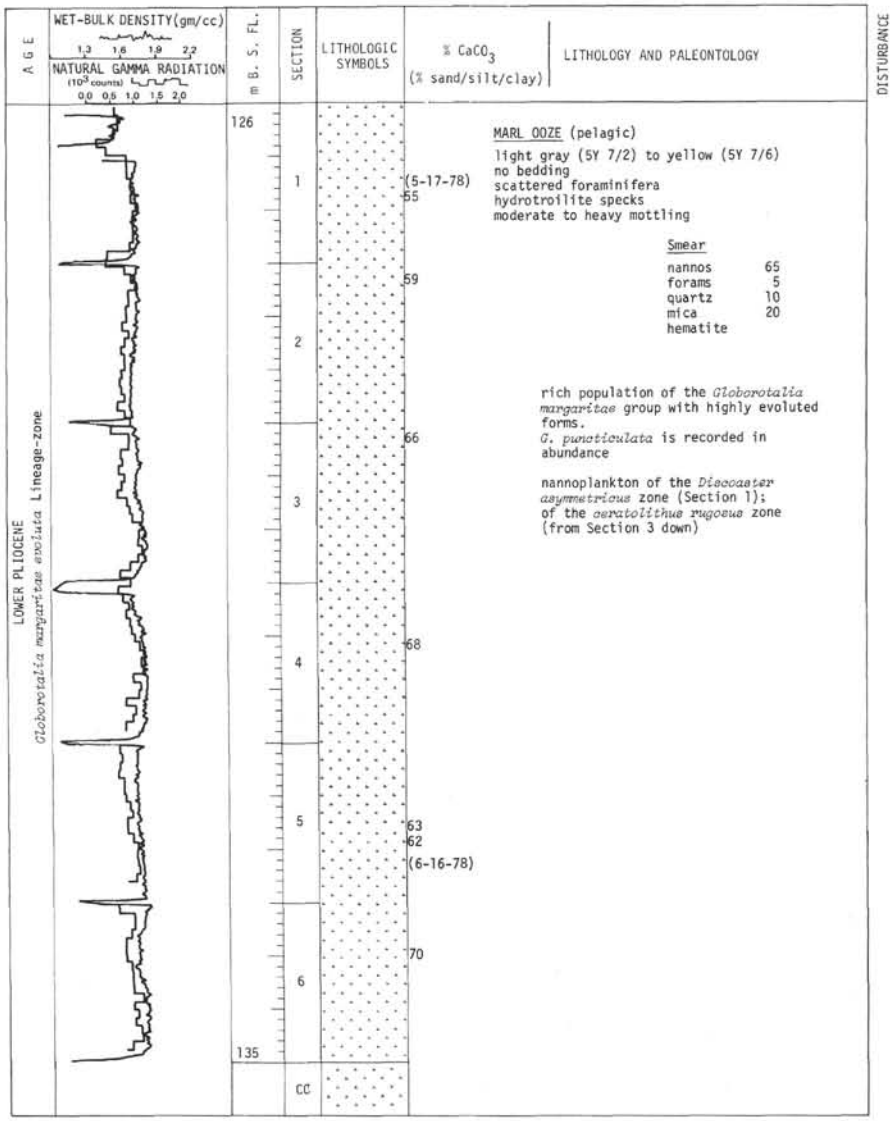

SITE 132 CORE 16 Cored Interval 135-144 m

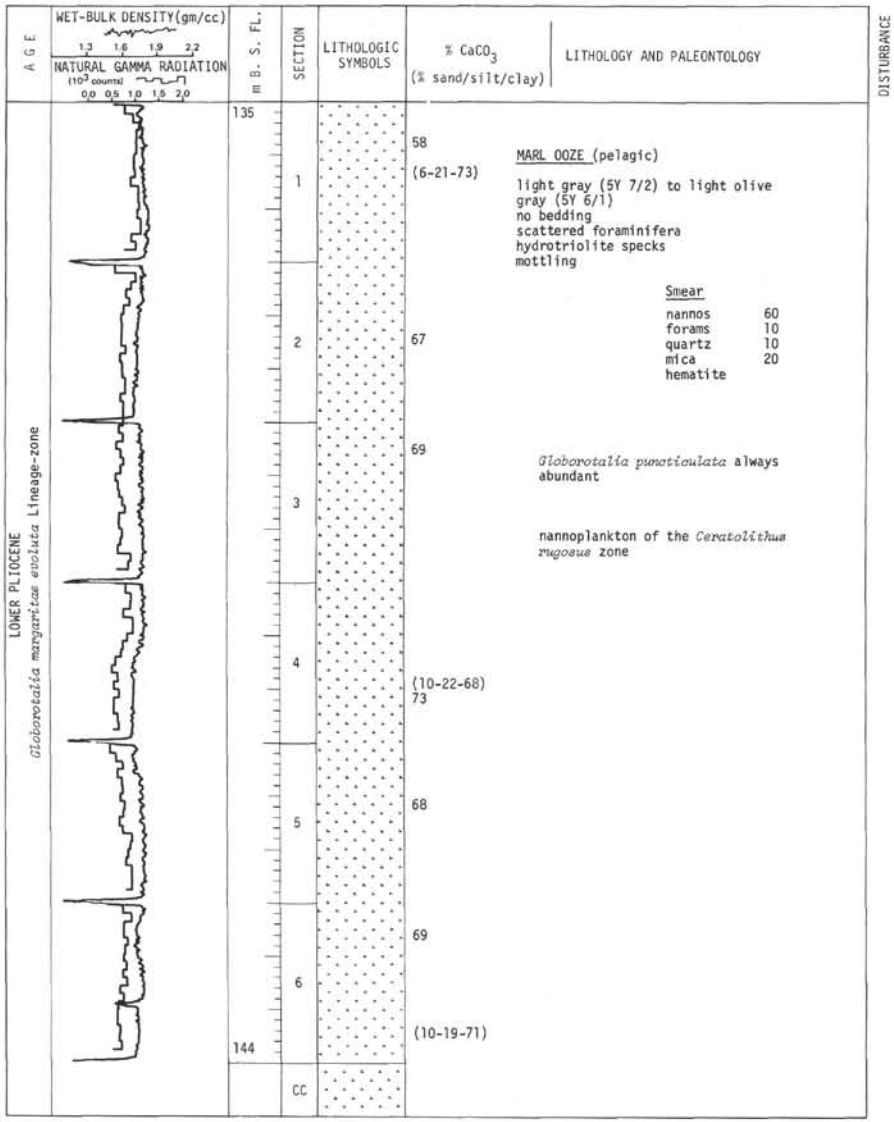

SITE 132 CORE 17 Cored Interval 144-153 m

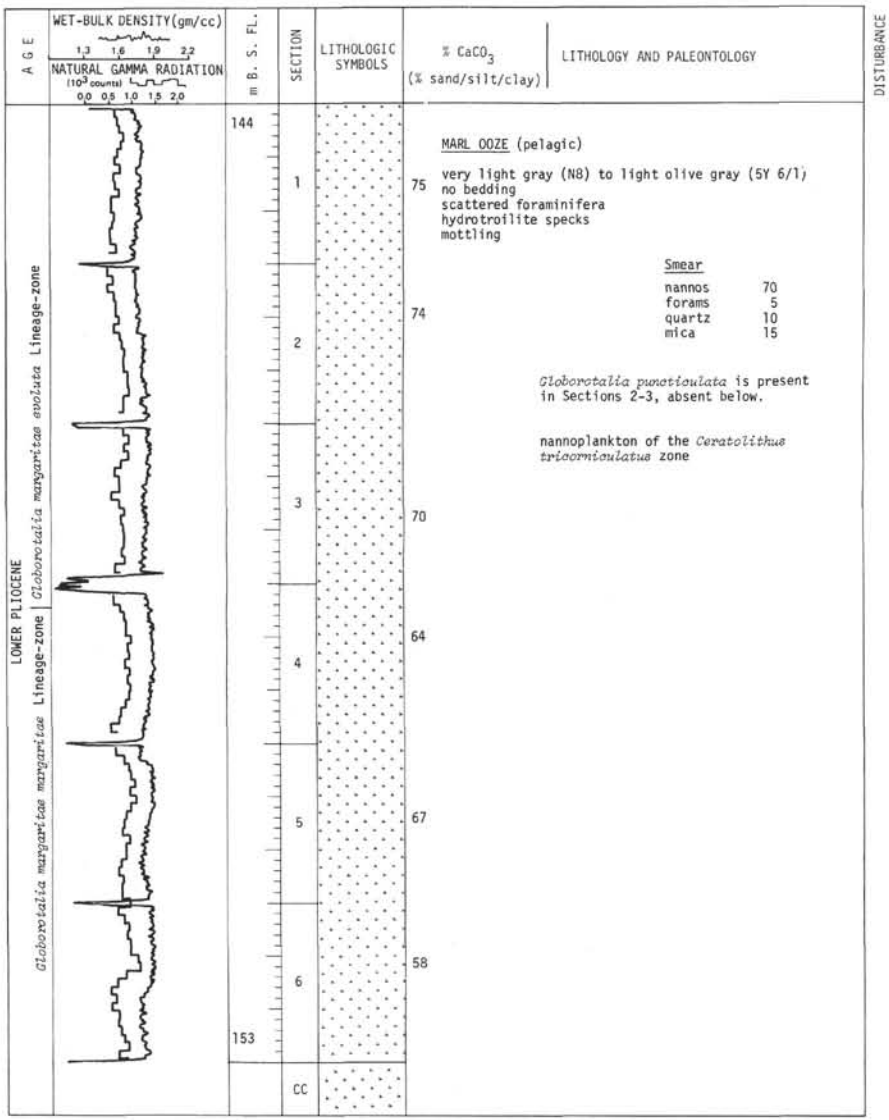

SITE 132 CORE 18 Cored Interval 153-162 m

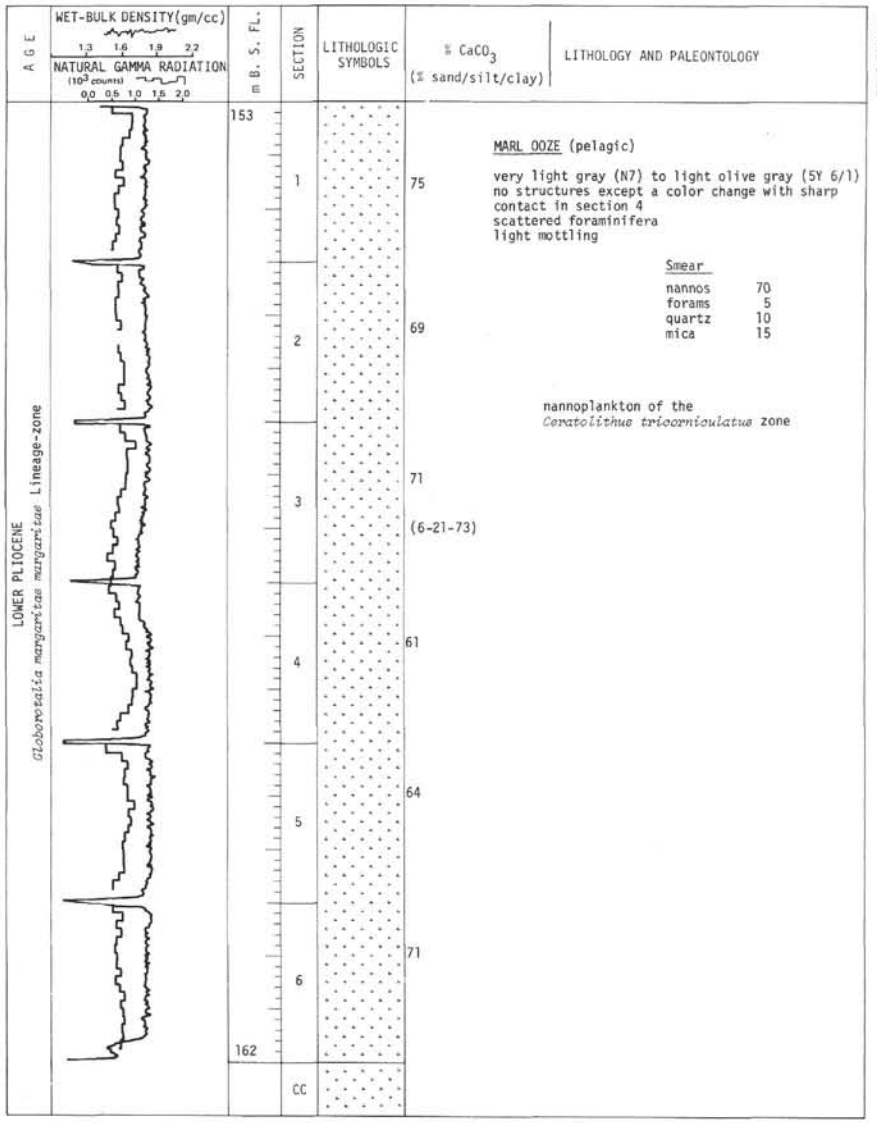

SITE 132 CORE 19 Cored Interval 162-171 m

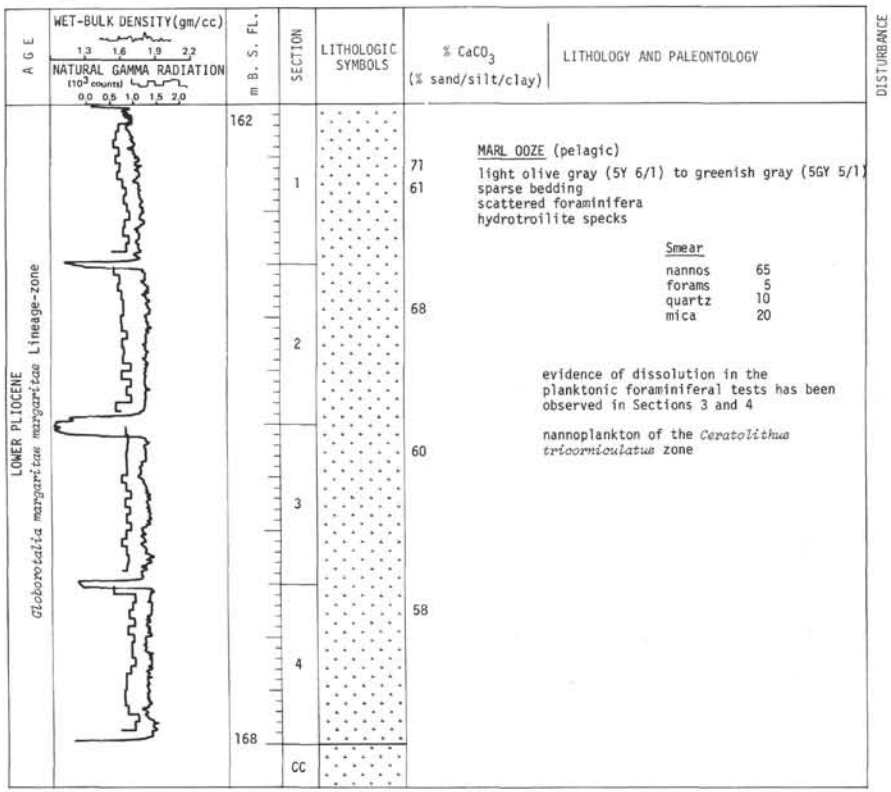

SITE 132 CORE 20 Cored Interval 171-180 m

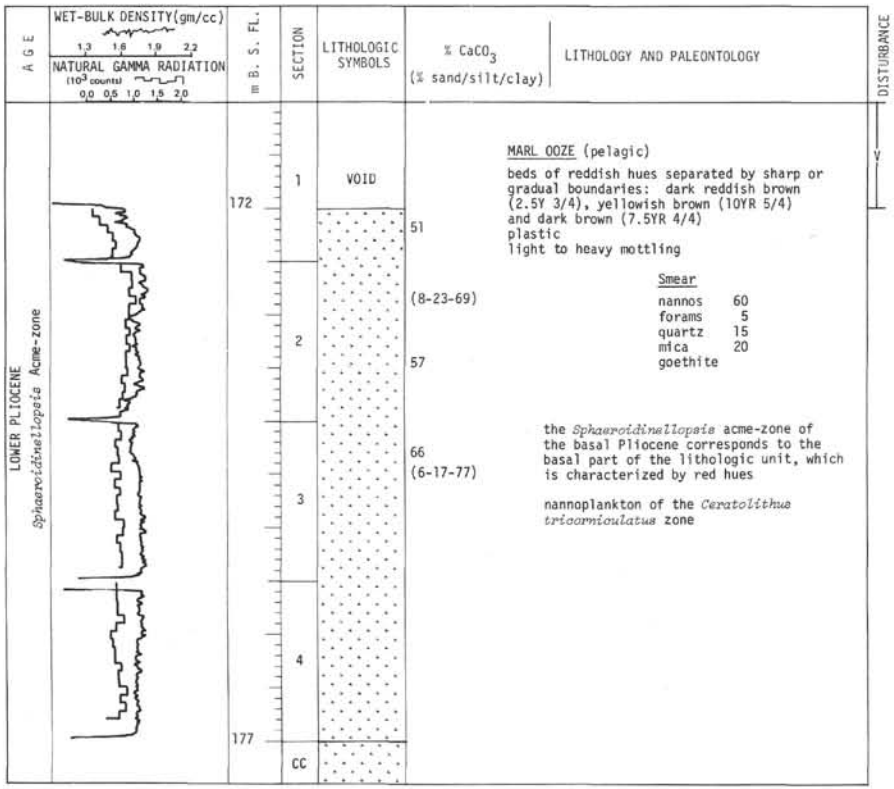

SITE 132 CORE 21 Cored Interval 180-189 m

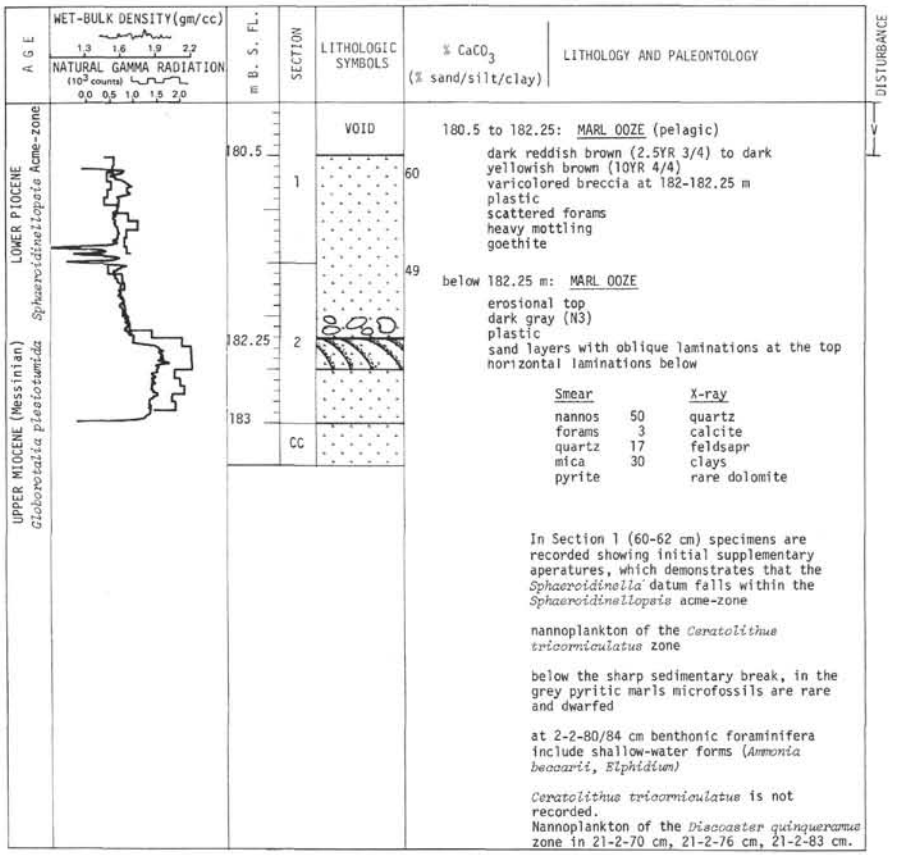

SITE 132 CORE 22 Cored Interval 189-191 m

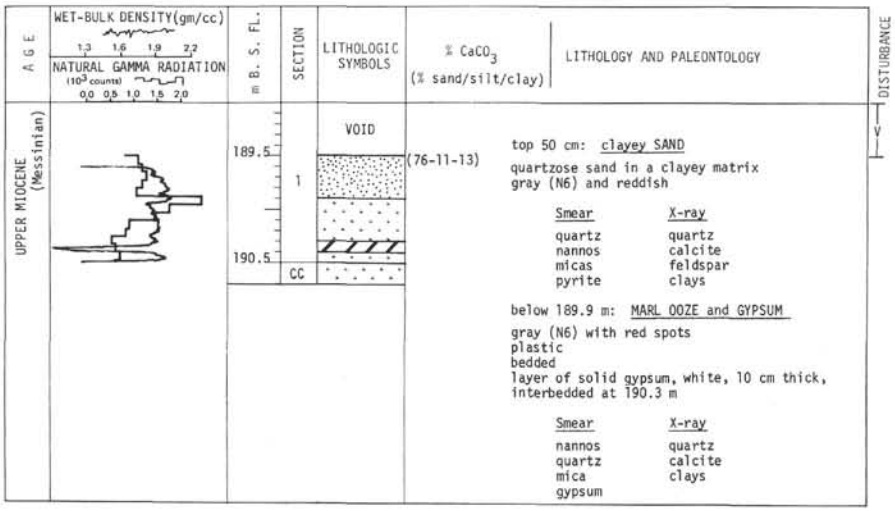

SITE 132 CORE 23 Cored Interval 191-198 m

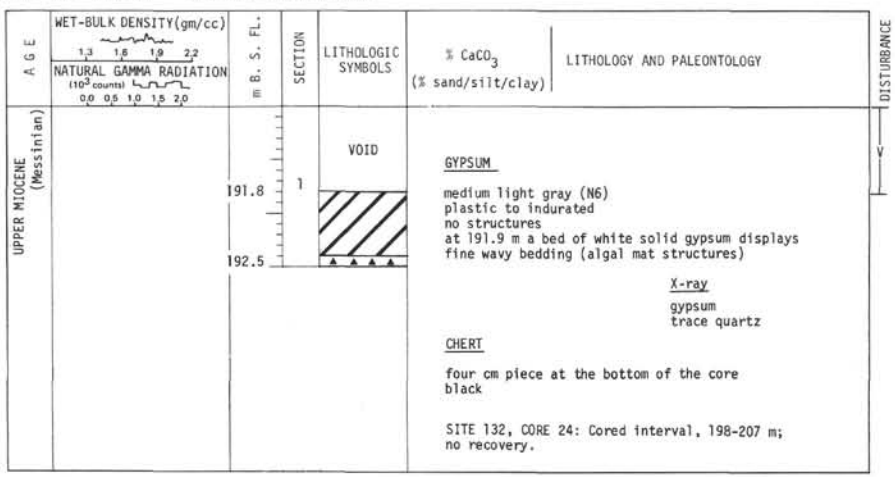

SITE 132 CORE 25 Cored Interval 207-214 m

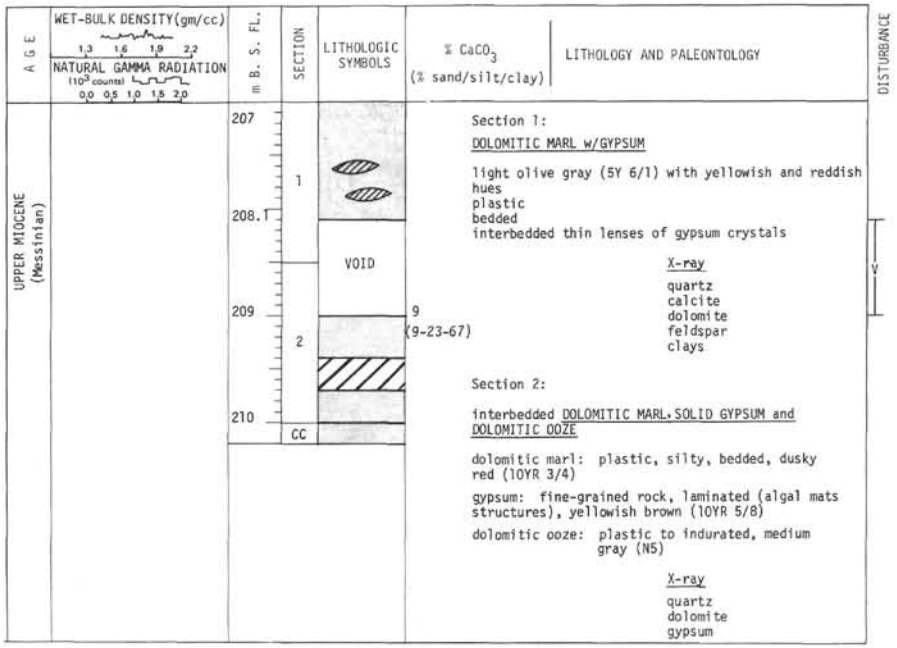

SITE 132 CORE 26 Cored Interval 214-220 m

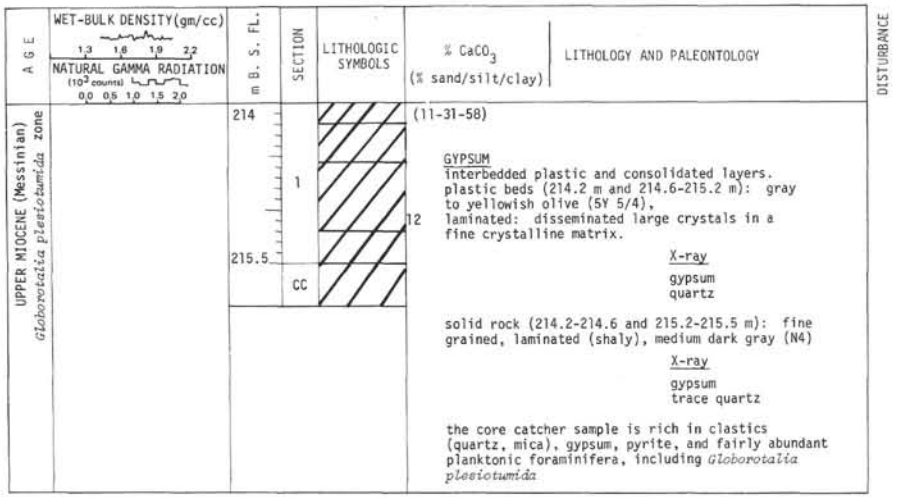

SITE 132 CORE 27 Cored Interval 220-223 m

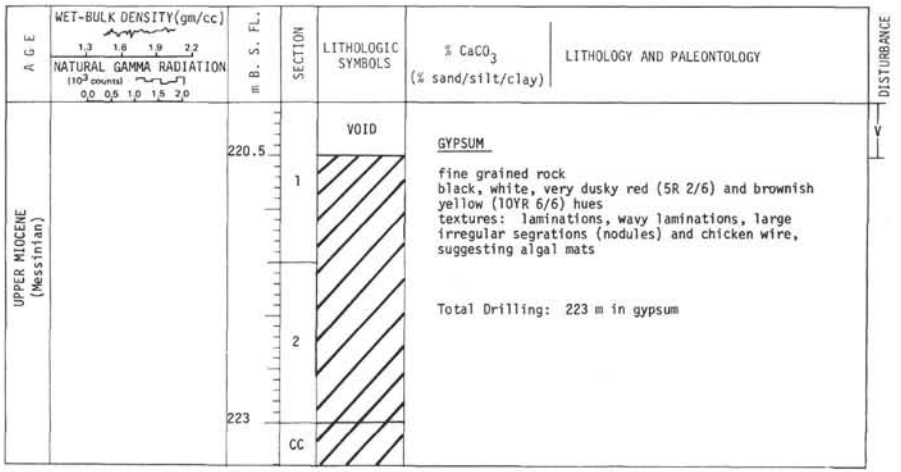

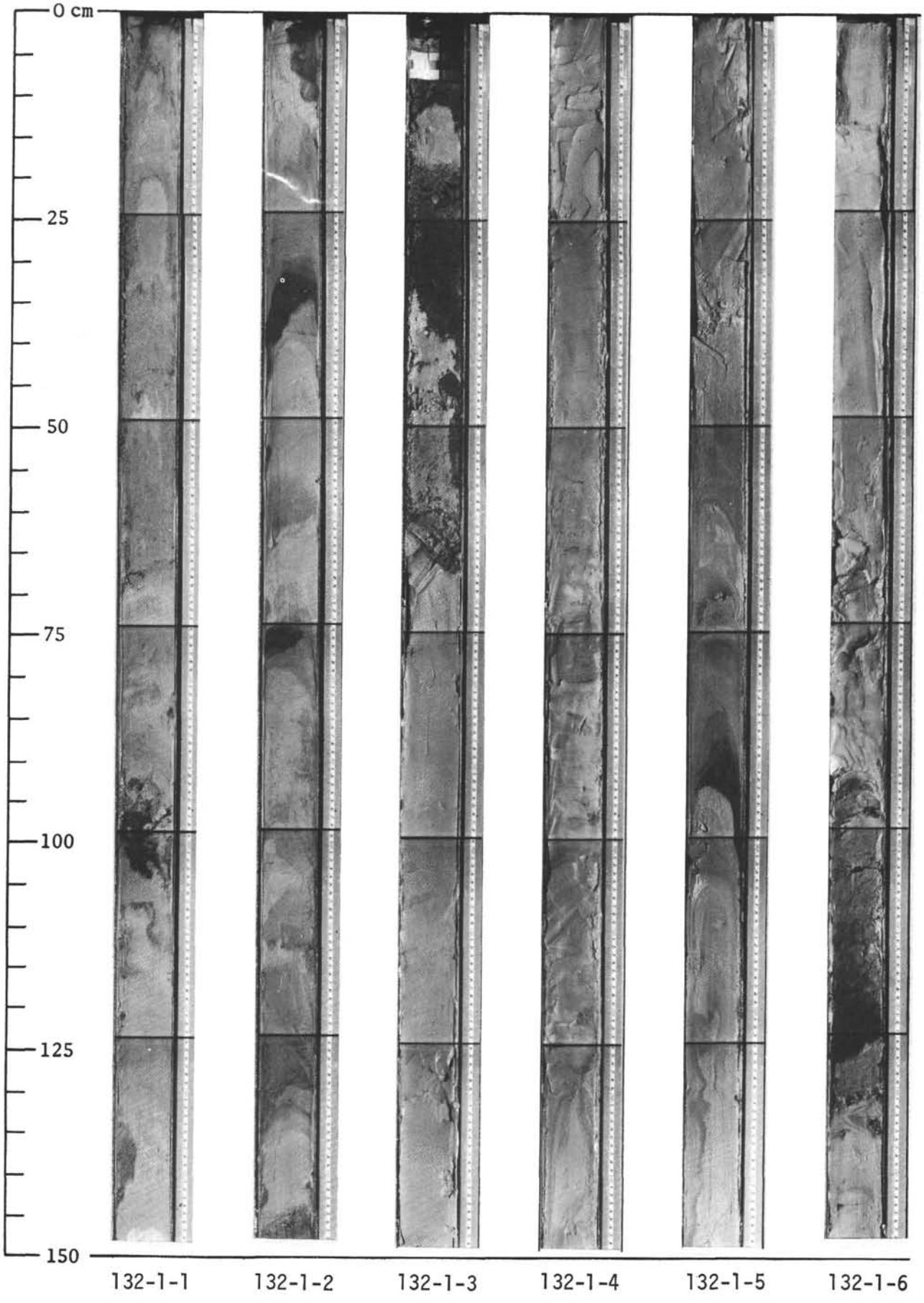
0 cm
25
50
75
100
125
150
132-1-1
132-1-2
132-1-3
132-1-4
132-1-5
132-1-6

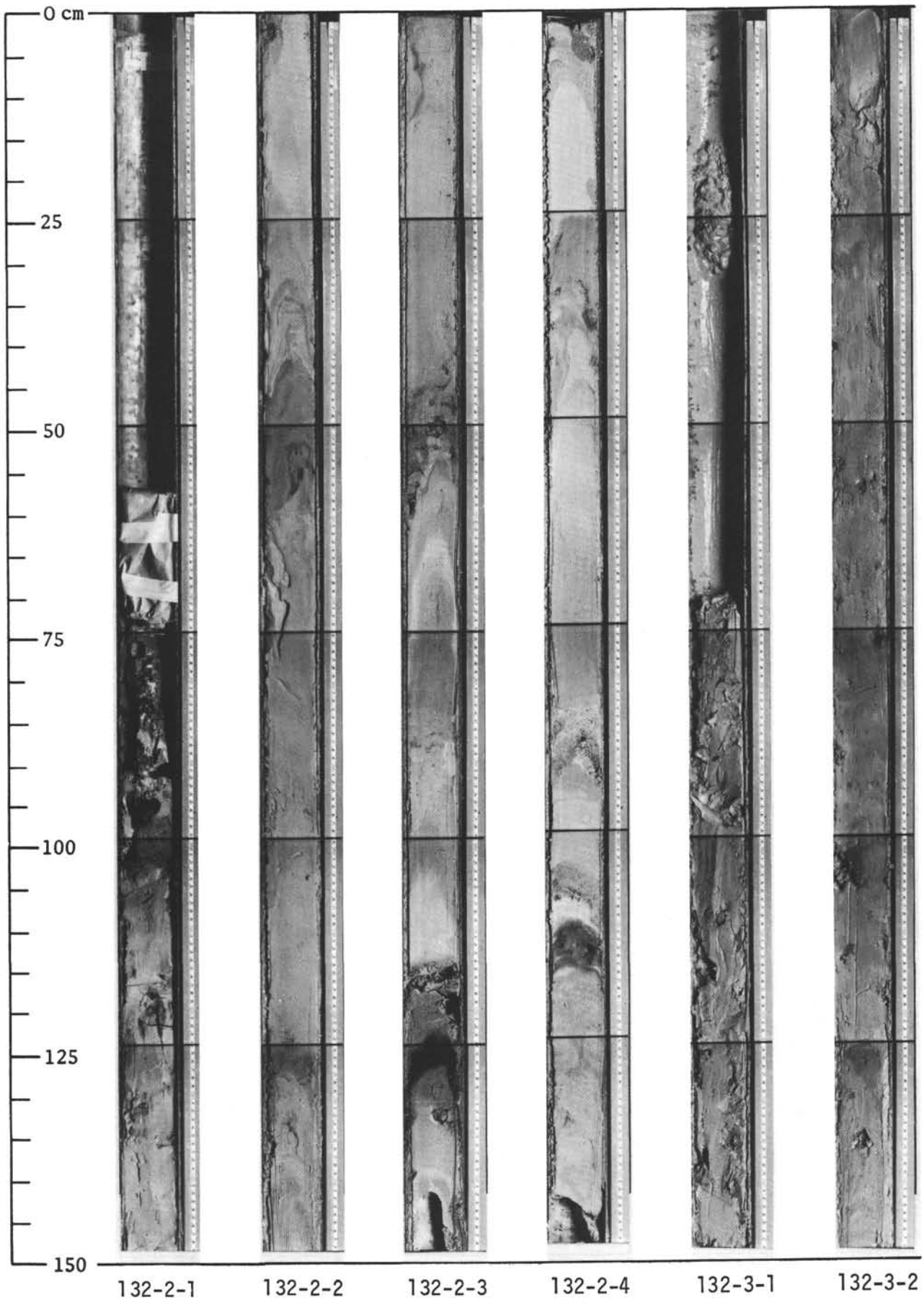
0 cm
25
50
75
100
125
150
132-2-1
132-2-2
132-2-3
132-2-4
132-3-1
132-3-2

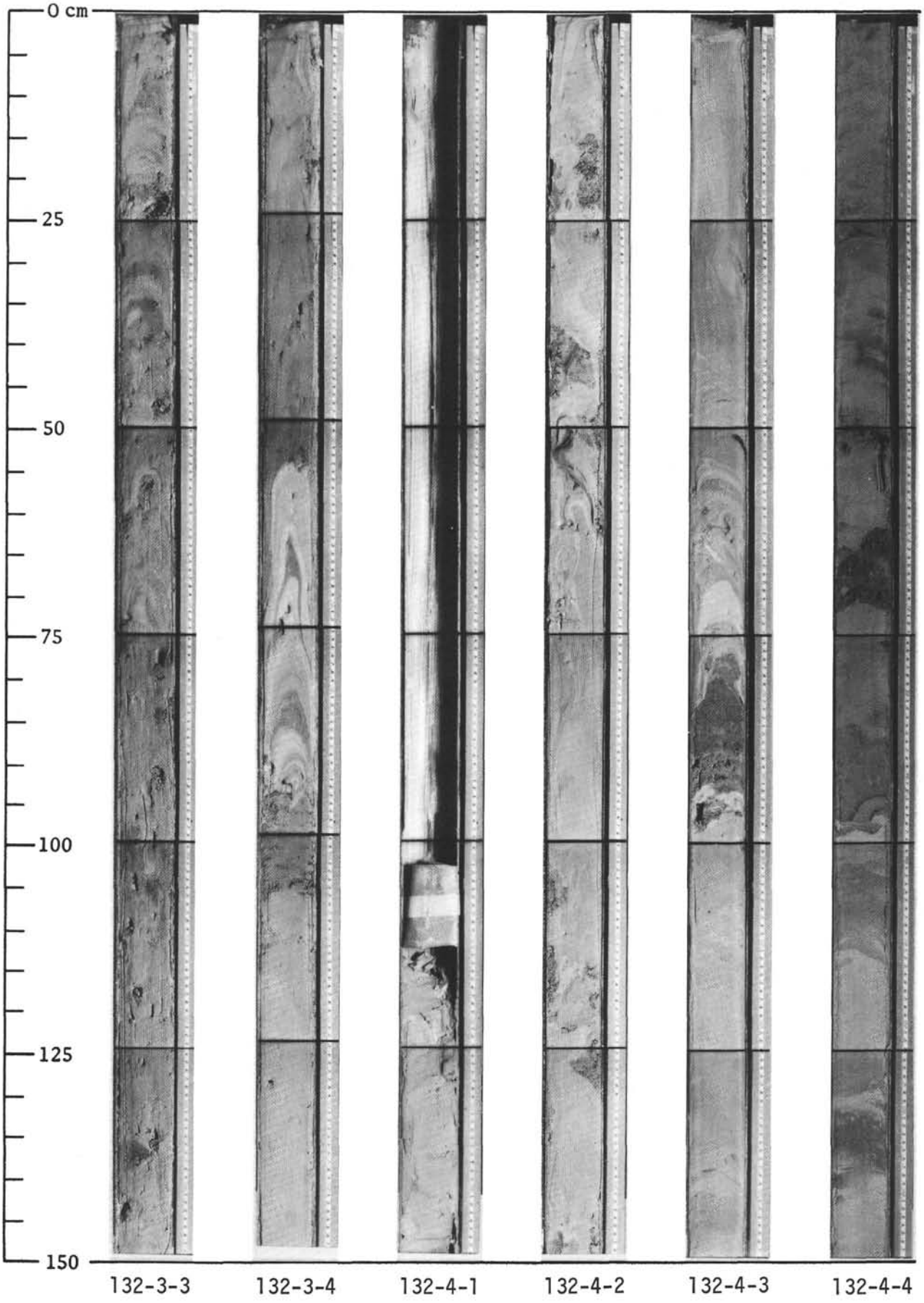
0 cm
25
50
75
100
125
150
132-3-3
132-3-4
132-4-1
132-4-2
132-4-3
132-4-4

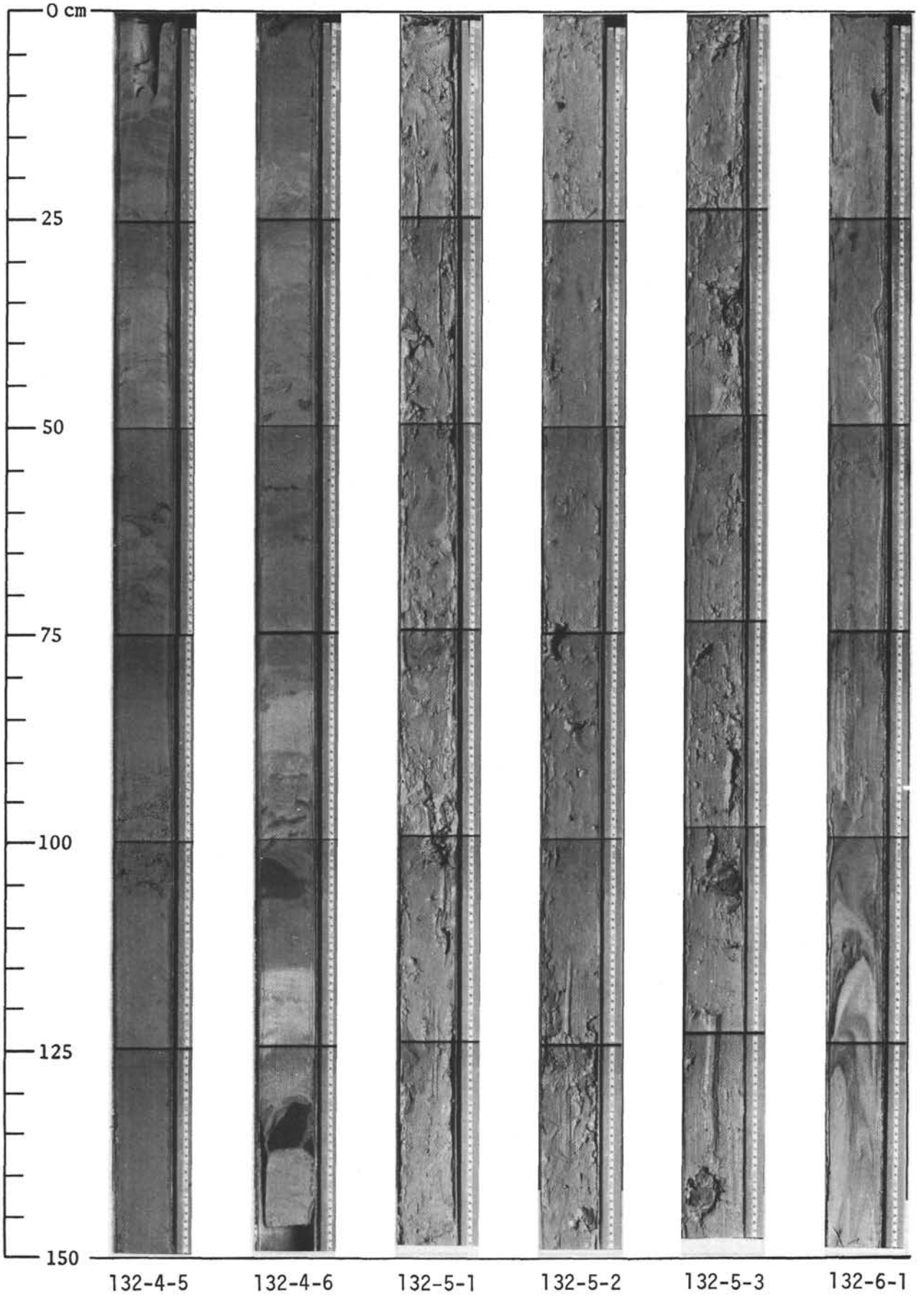
0 cm
25
50
75
100
125
150
132-4-5
132-4-6
132-5-1
132-5-2
132-5-3
132-6-1

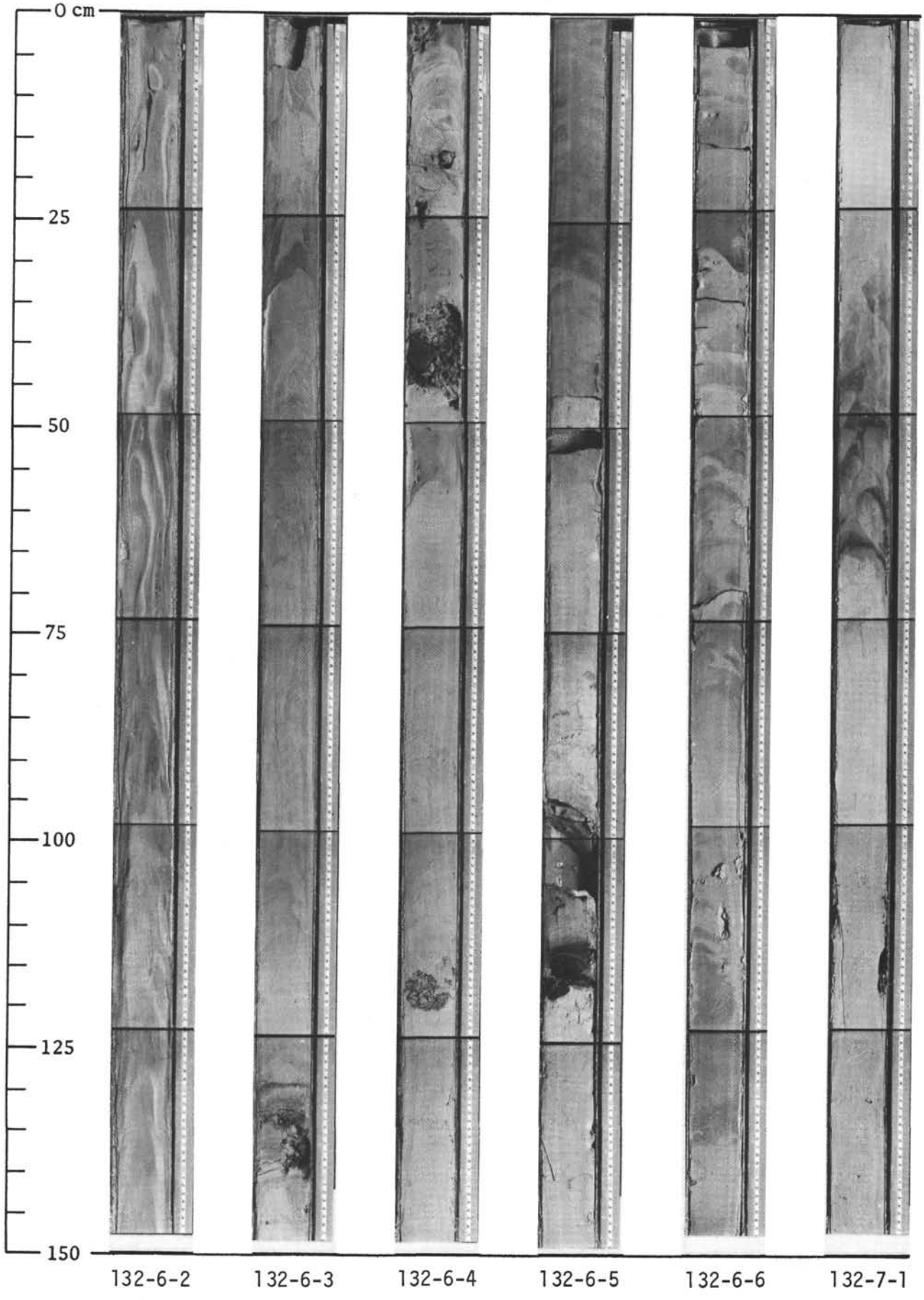
0 cm
25
50
75
100
125
150
132-6-2
132-6-3
132-6-4
132-6-5
132-6-6
132-7-1

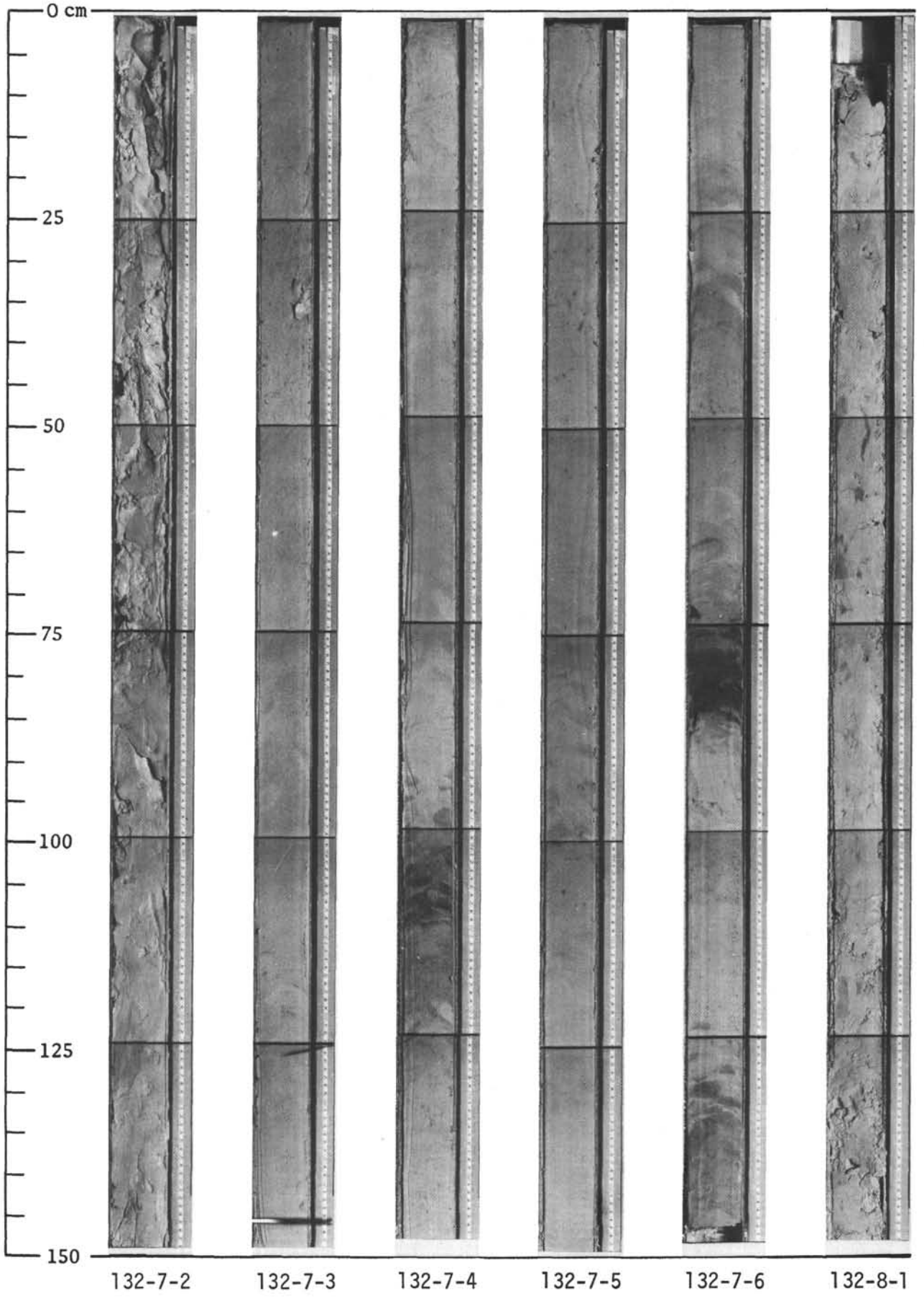
0 cm
25
50
75
100
125
150
132-7-2
132-7-3
132-7-4
132-7-5
132-7-6
132-8-1

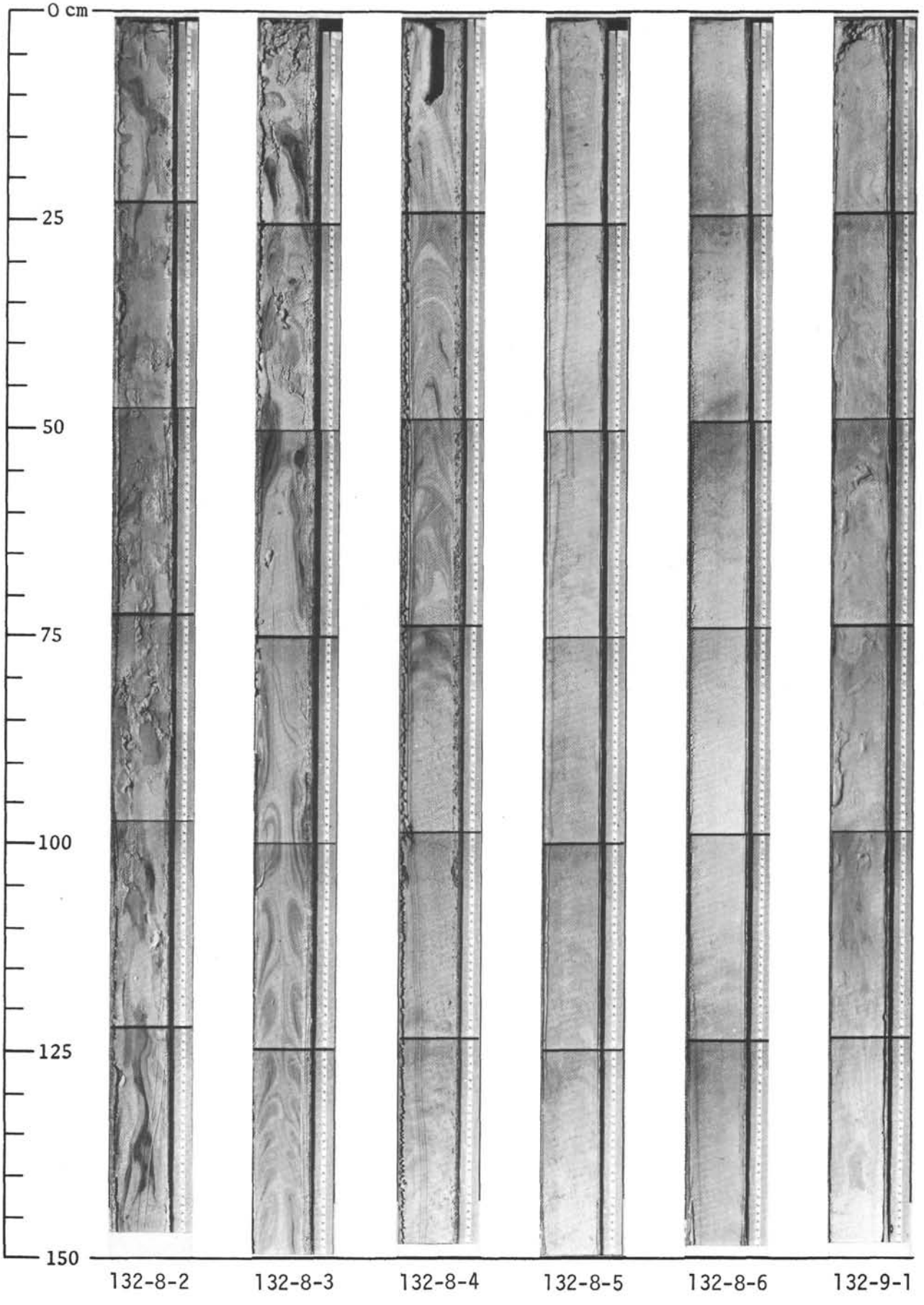
0 cm
25
50
75
100
125
150
132-8-2
132-8-3
132-8-4
132-8-5
132-8-6
132-9-1

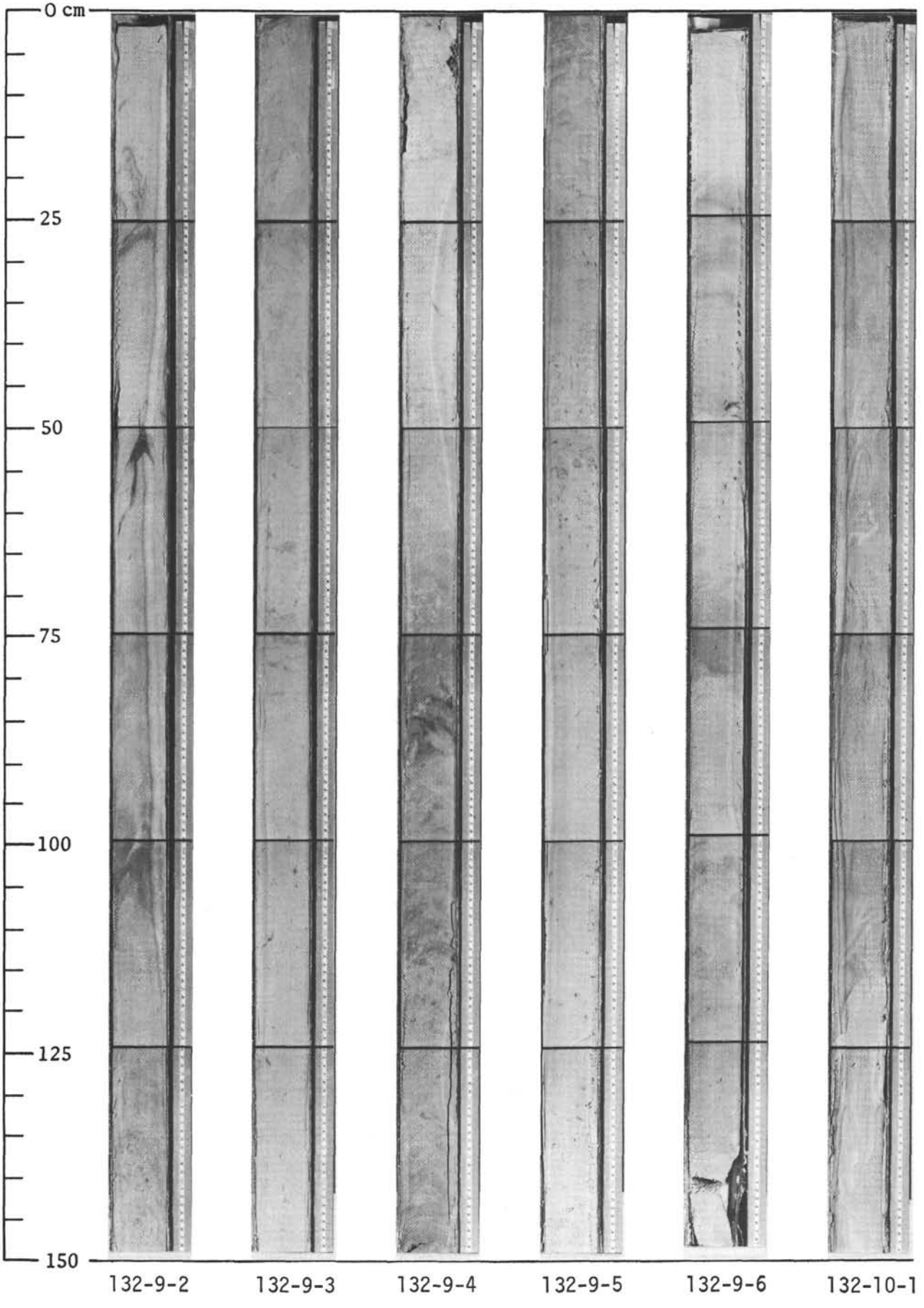
0 cm
25
50
75
100
125
150
132-9-2
132-9-3
132-9-4
132-9-5
132-9-6
132-10-1

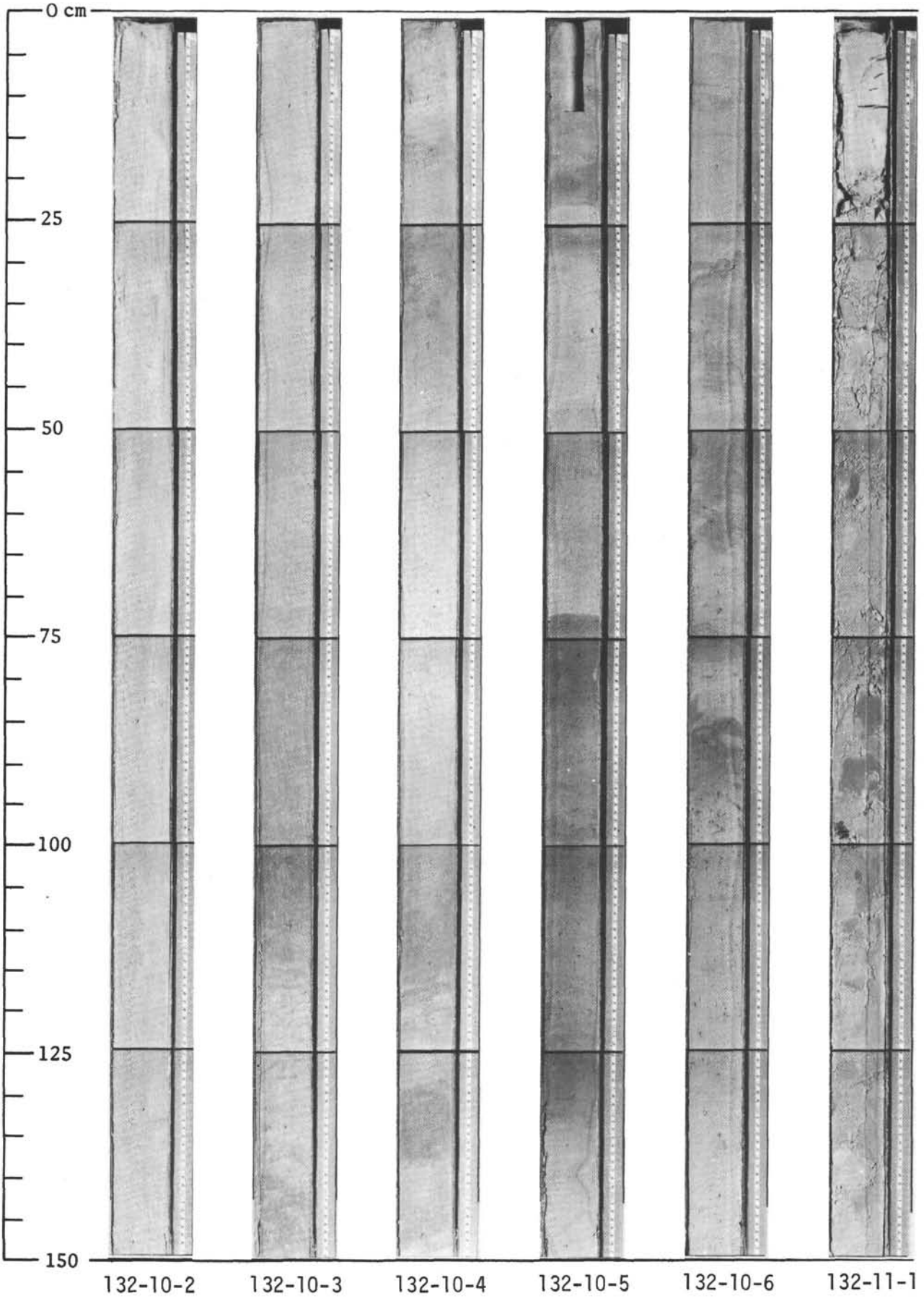
0 cm
25
50
75
100
125
150
132-10-2
132-10-3
132-10-4
132-10-5
132-10-6
132-11-1

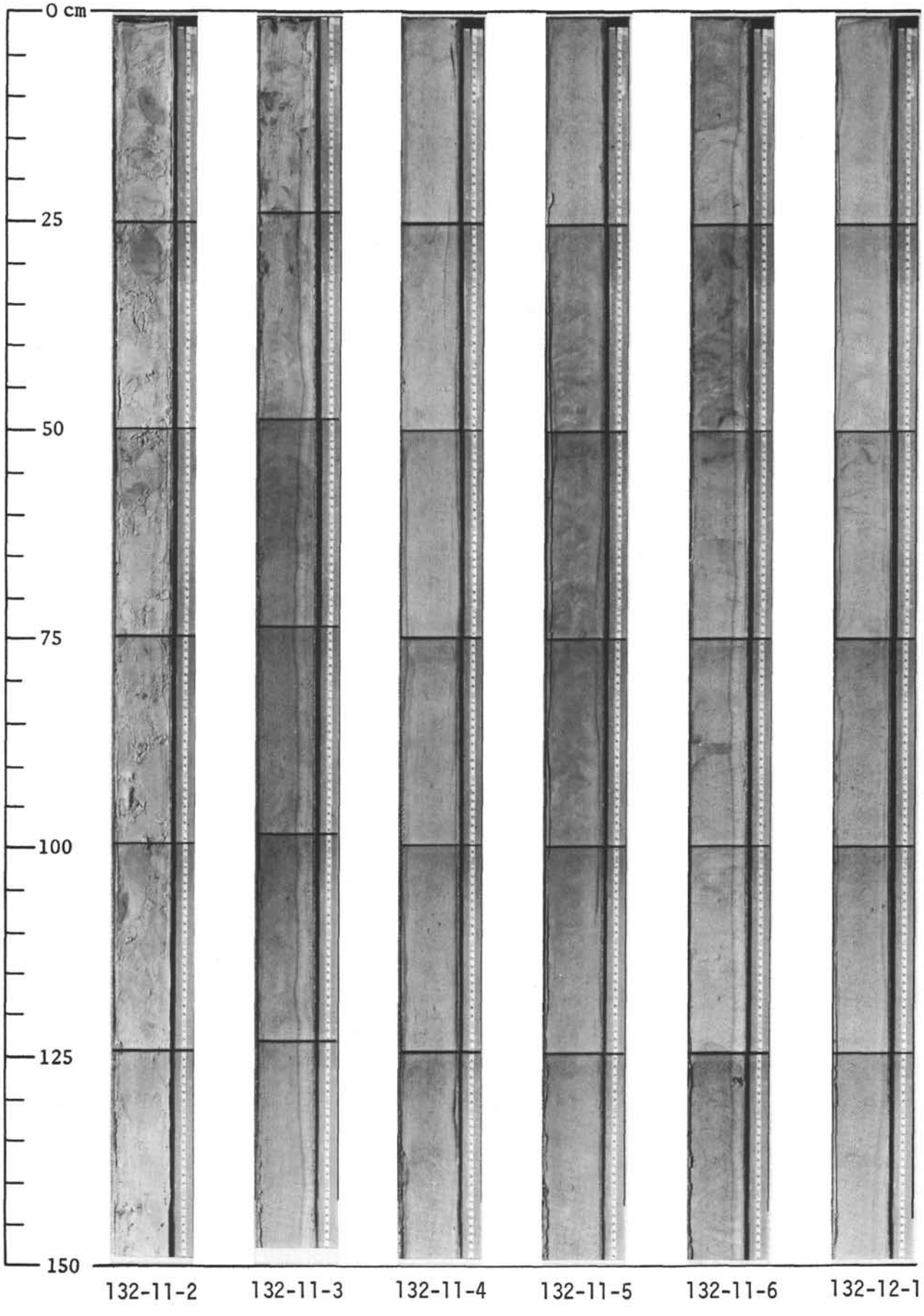
0 cm
25
50
75
100
125
150
132-11-2
132-11-3
132-11-4
132-11-5
132-11-6
132-12-1

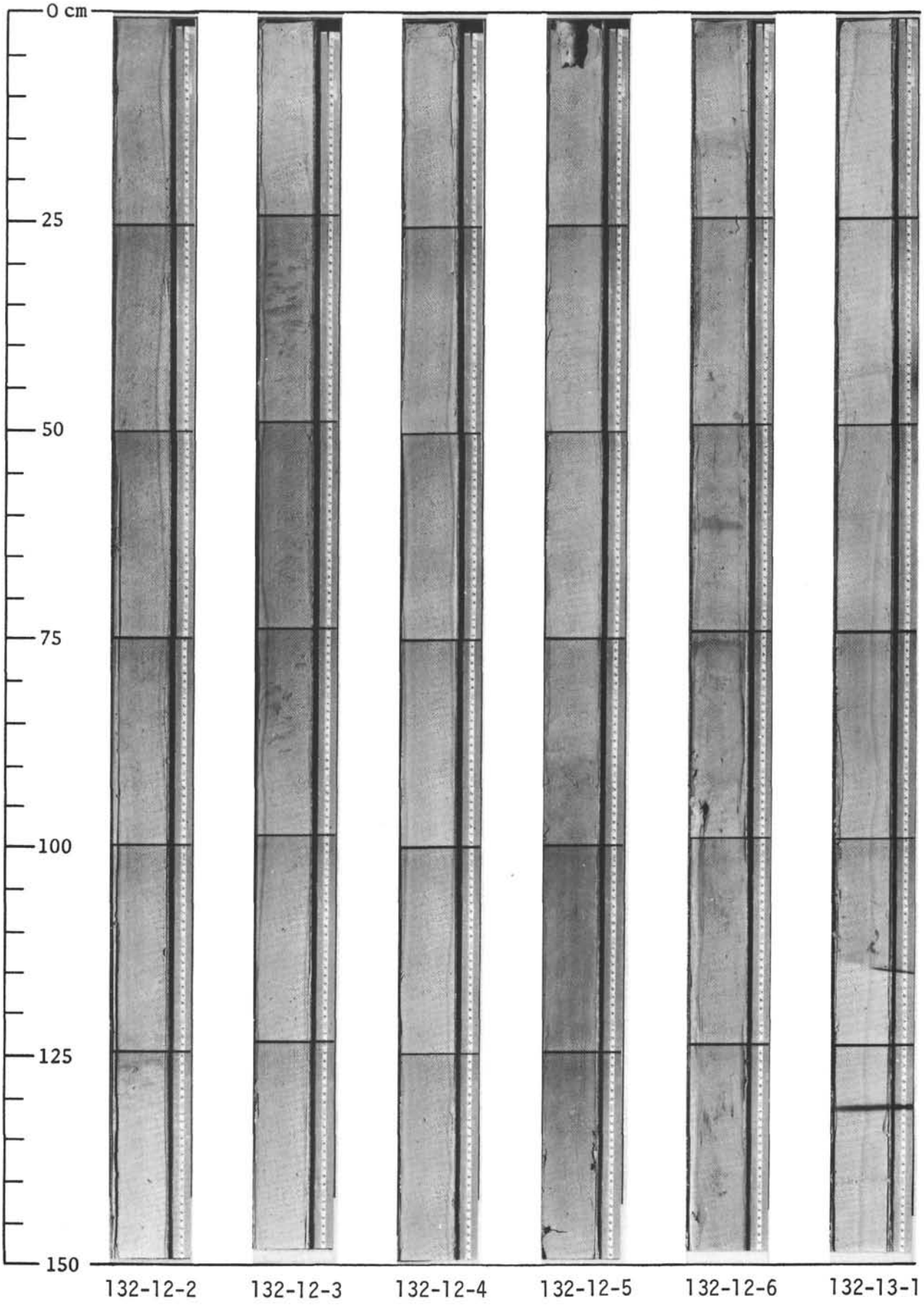
0 cm
25
50
75
100
125
150
132-12-2
132-12-3
132-12-4
132-12-5
132-12-6
132-13-1

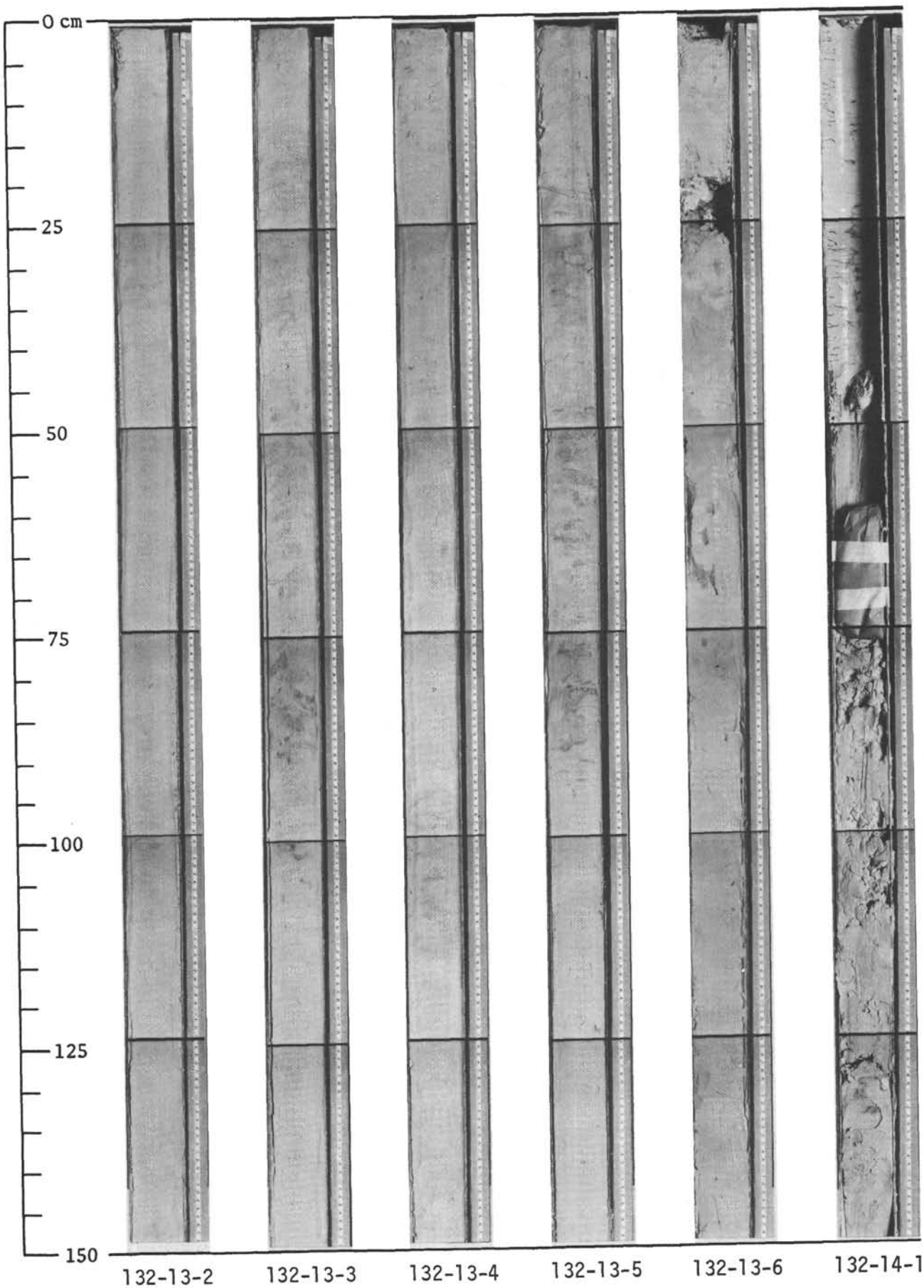
0 cm
25
50
75
100
125
150
132-13-2
132-13-3
132-13-4
132-13-5
132-13-6
132-14-1

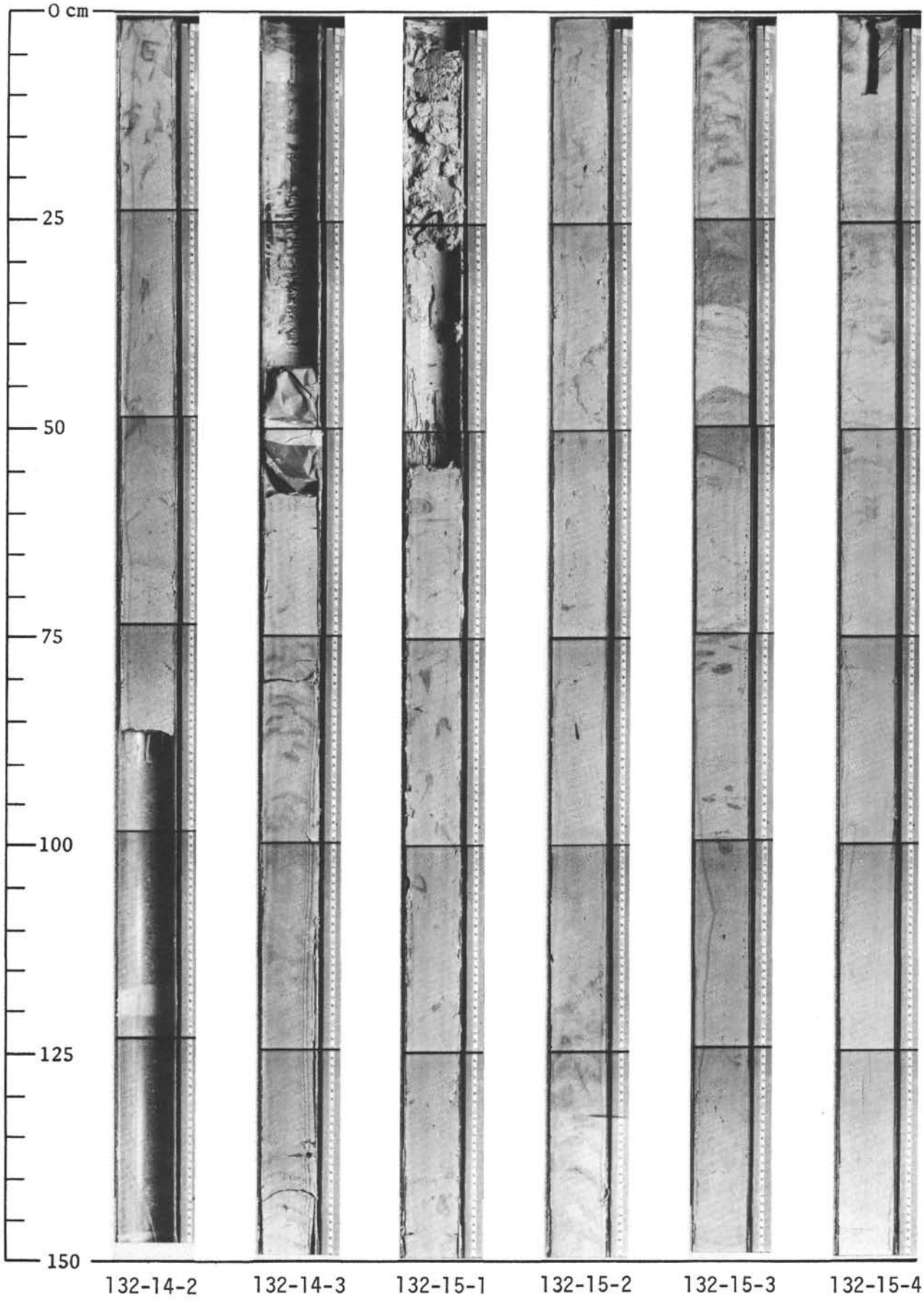
0 cm
25
50
75
100
125
150
132-14-2
132-14-3
132-15-1
132-15-2
132-15-3
132-15-4

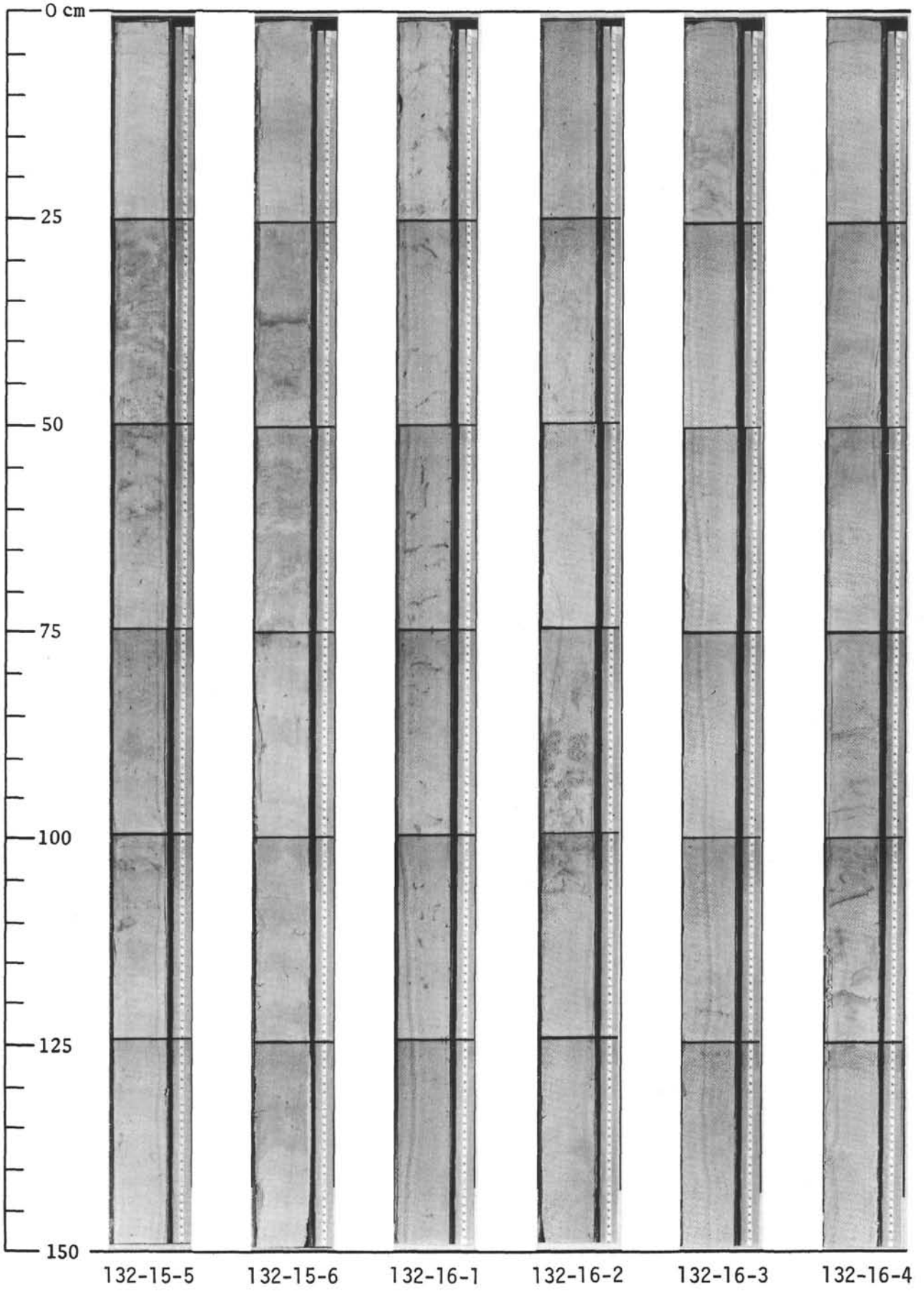
0 cm
25
50
75
100
125
150
132-15-5
132-15-6
132-16-1
132-16-2
132-16-3
132-16-4

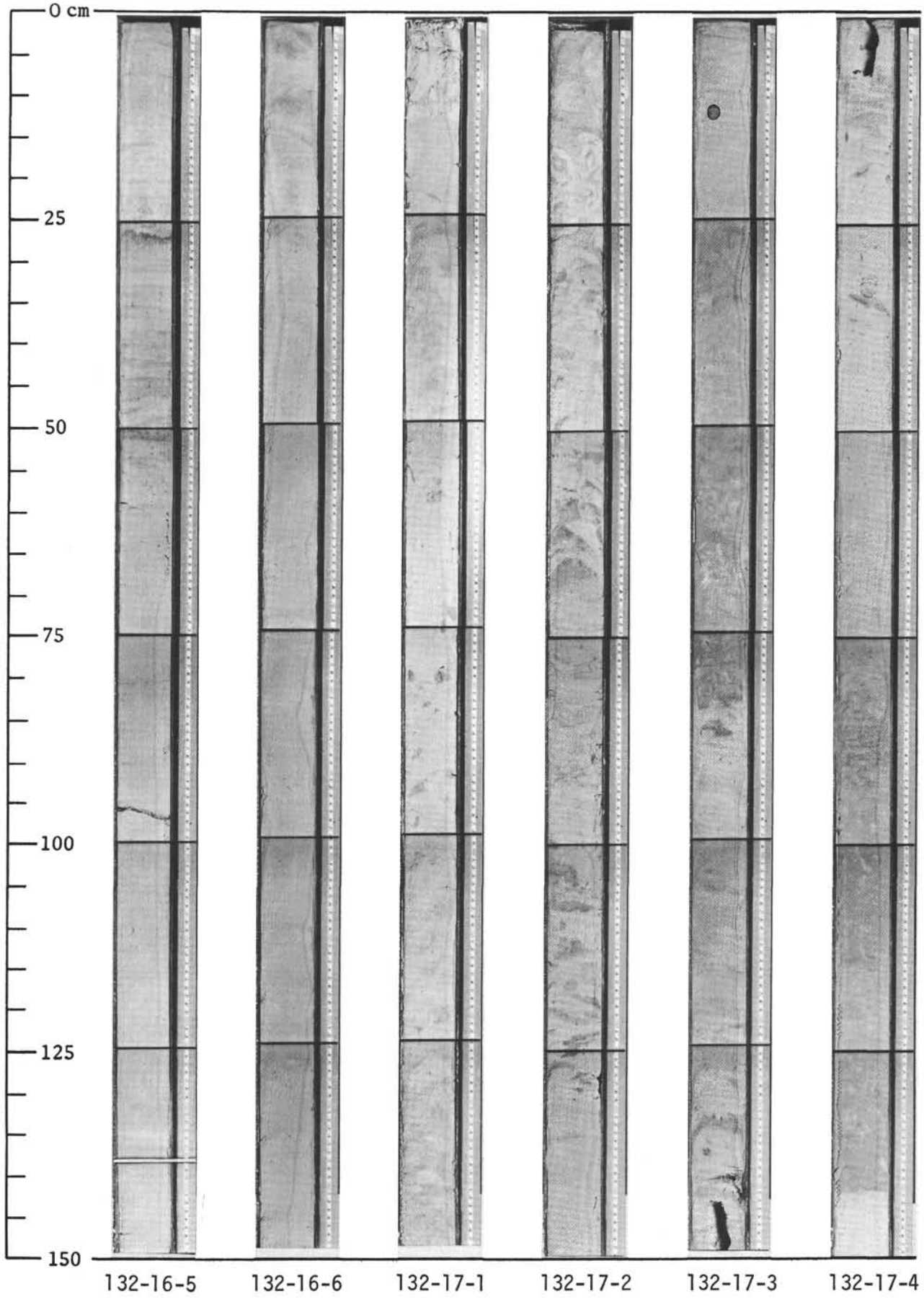
0 cm
25
50
75
100
125
150
132-16-5
132-16-6
132-17-1
132-17-2
132-17-3
132-17-4

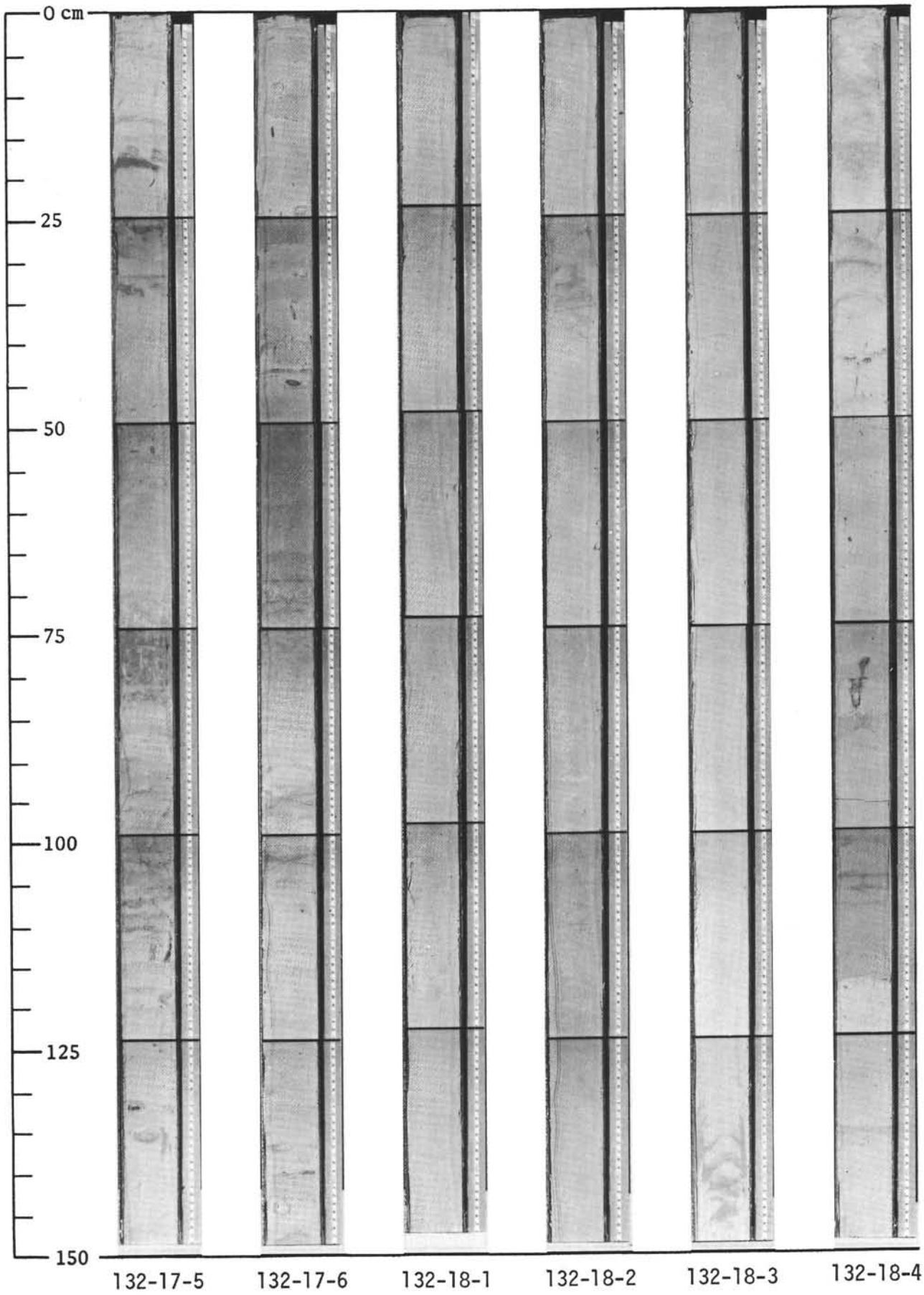
0 cm
25
50
75
100
125
150
132-17-5
132-17-6
132-18-1
132-18-2
132-18-3
132-18-4

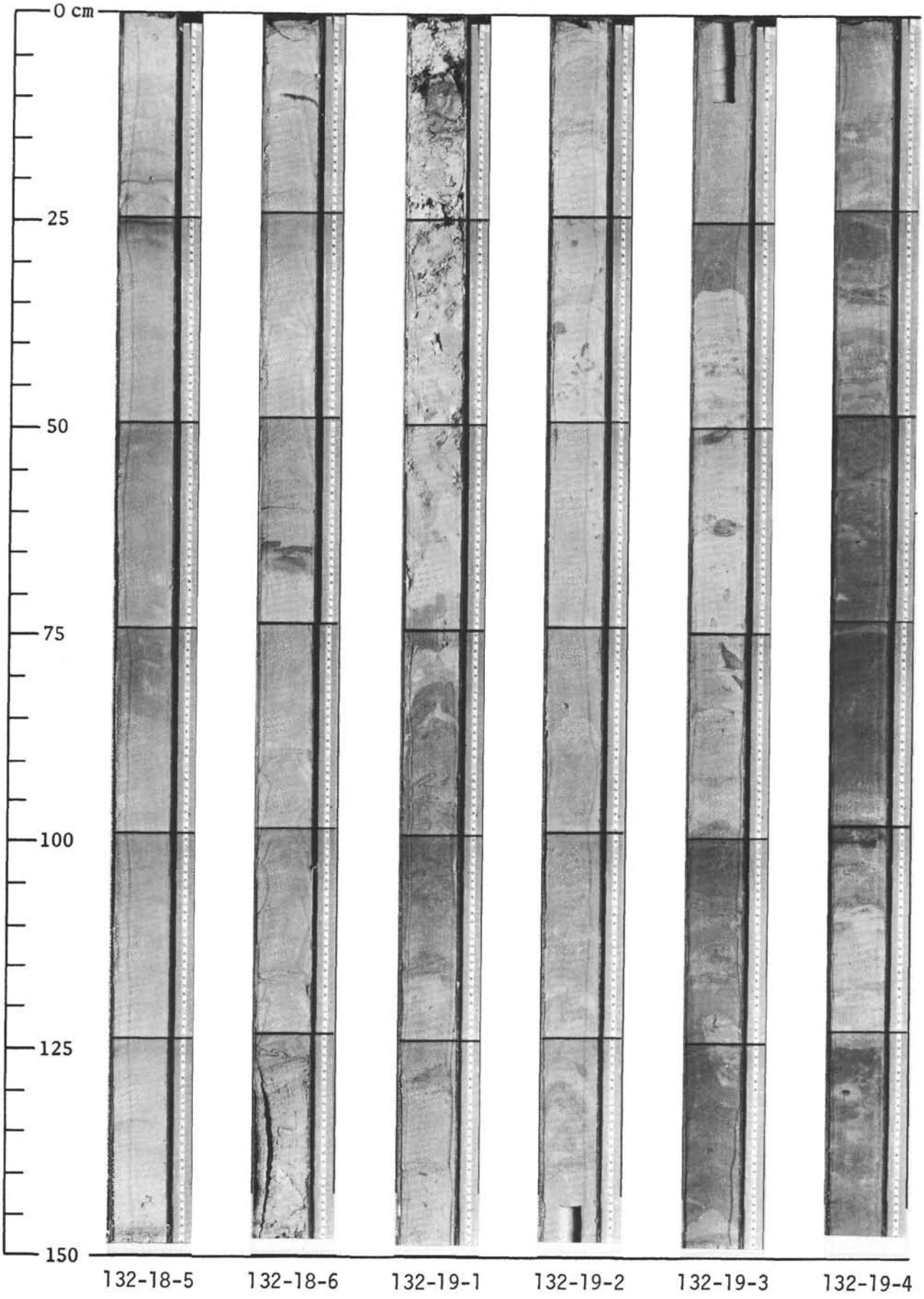
0 cm
25
50
75
100
125
150
132-18-5
132-18-6
132-19-1
132-19-2
132-19-3
132-19-4

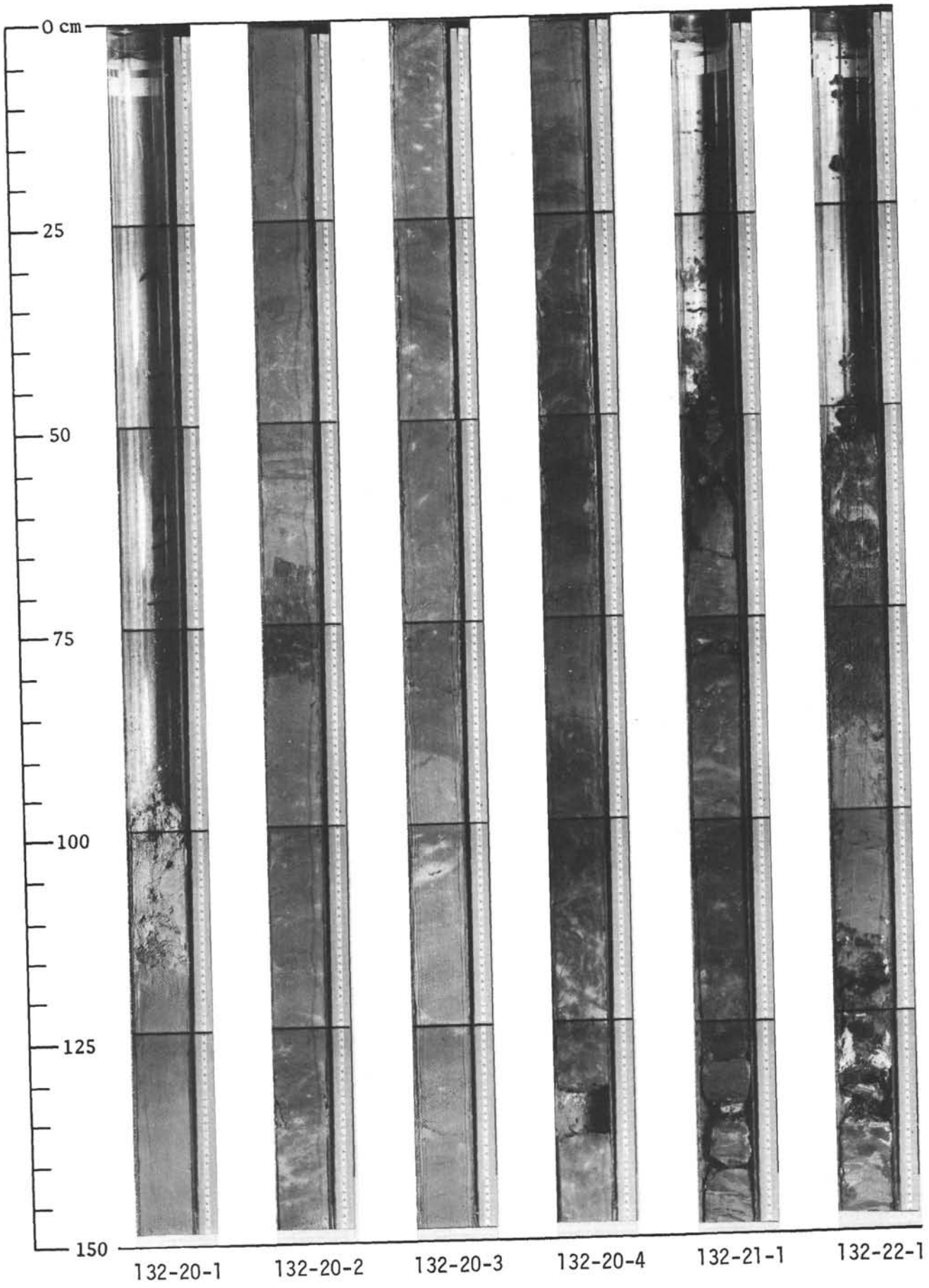
0 cm
25
50
75
100
125
150
132-20-1
132-20-2
132-20-3
132-20-4
132-21-1
132-22-1

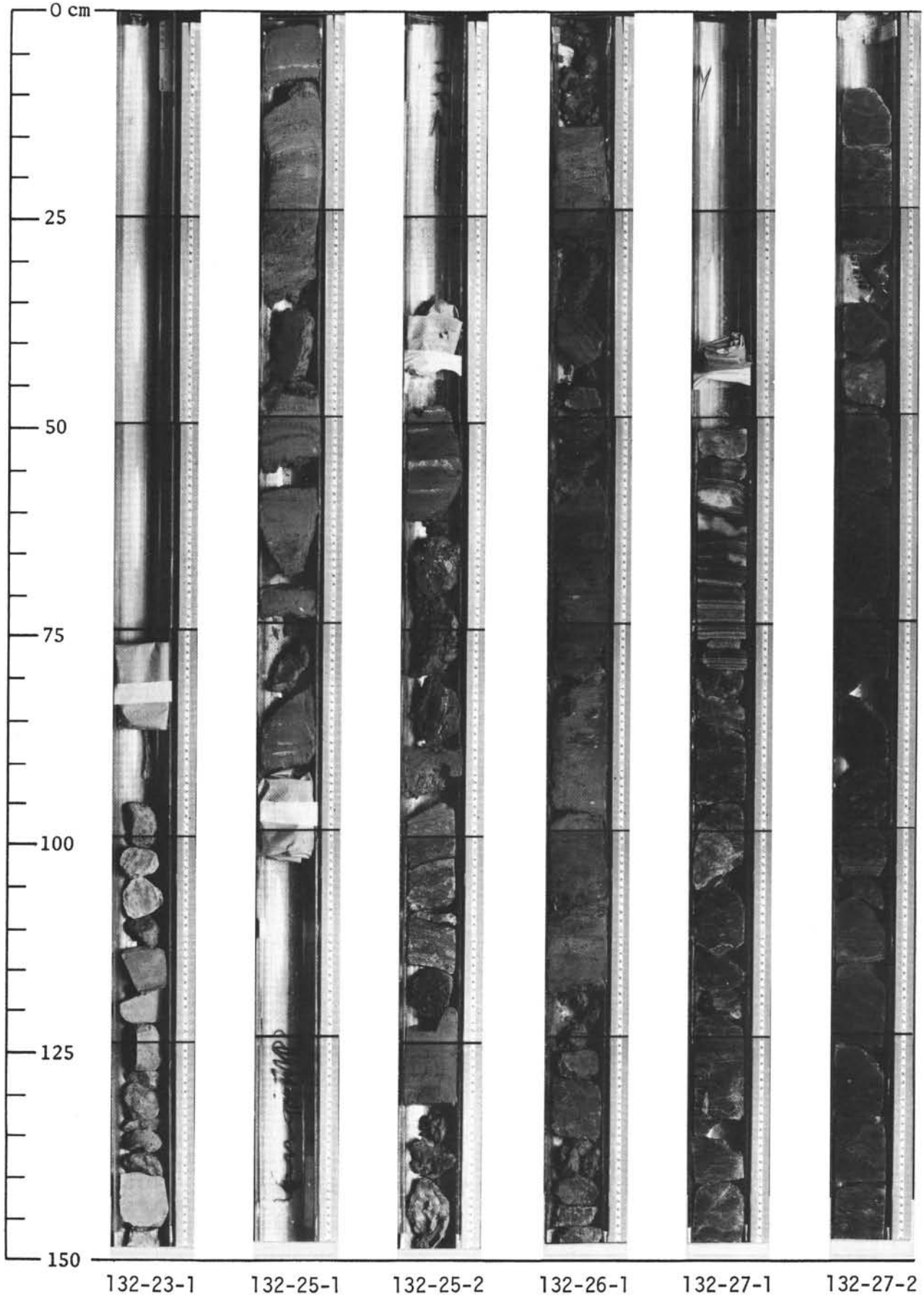
0 cm
25
50
75
100
125
150
132-23-1
132-25-1
132-25-2
132-26-1
132-27-1
132-27-2